Master Thesis in Geosciences

The tectonomagmatic evolution of Svalbards North-Western Terrane.

U/Pb-ages for Proterozoic crust and Caledonian magmatic evolution in Spitsbergen.

Per Inge Myhre

UNIVERSITY OF OSLO

FACULTY OF MATHEMATICS AND NATURAL SCIENCES

The tectonomagmatic evolution of Svalbards North-Western Terrane.

U/Pb-ages for Proterozoic crust and Caledonian magmatic evolution in Spitsbergen.

Per Inge Myhre

Master Thesis in Geosciences

Discipline: Tectonics, Petrology and Geochemistry
Department of Geosciences
Faculty of Mathematics and Natural Sciences

UNIVERSITY OF OSLO

[December 15, 2005]

Tutor(s): Professor Arild Andresen, Professor Fernando Corfu

This work is published digitally through DUO – Digitale Utgivelser ved UiO

http://www.duo.uio.no

It is also catalogued in BIBSYS (http://www.bibsys.no/english)

Cover photo: The Hornemantoppen nunatak, 1097 m.a.s.l., north-west Spitsbergen. Bjørnfjorden and the Smeerenburgbreen glacier in the foreground, view towards south-east.

Acknowledgements

Professor Arild Andresen was the main supervisor for this thesis. I have greatly appreciated his enthusiasm in *everything* he does; field geology, teaching, thesis supervision, social events… I thank Arild for providing me with this thesis, and for having faith in me.

Professor Fernando Corfu supervised the geochronology-part of the thesis, and patiently thought me most of what I know about "the business". Fernando has been genuinely interested in my thesis all the way, and spent a lot of his time in helping me out. Additionally, he is generally a great guy!

The field season 2005 would not have been possible without the help of Hans Amundsen and the AMASE-expedition. They were headed to north-western Spitsbergen with the MS Polarsyssel, and Hans thought he might as well pick us up and bring us to Smeerenburgfjorden and back again. Thanks!

Professor Alexander Tebenkov of the Russian PMGRE-expediton is acknowledged for his great attitude and for taking me to the localities when we were in the field together in the 2004 field season.

Endre Bergfjord was field assistant in 2005. He endured fog and rain, carried rocks and hauled zodiac for 10 days, always with a smile not far away.

Stig Nesbø stepped in on short notice as field assistant in 2004. It was great getting to know this lad from the west.

Gunborg Bye Fjeld is thanked for helping out in the mineral-separation-lab.

The Norwegian Polar Institute supported the project financially in 2004 & 2005.

Last, but not least, a big salute goes to all the friends that I made in the University of Bergen (2000-2003), the University Courses in Svalbard, UNIS (2002-2003) and finally, here in the department of Geosciences, University of Oslo (2004-2005). Hopefully I will get to spend time with many of you in the future.

Chapter 1: Introduction 11
1.1:Purpose of study 11
1.1:Geological setting 11
1.1: Study area and analytical methods 11
Chapter 2: Regional geological setting 13
2.1: Basement 14
The Western terranes 14
The Eastern terranes 23
2.2: Old Red Sandstone 27
The Haakonian phase 27
The Monacobreen phase 28
The Svalbardian phase 28
Chapter 3: Geology of the study area. 29
3.1: The Kongsfjorden area 31
Structure of the Kongsfjorden area 32
Smeerenburgfjorden Complex 36
Krossfjorden Group 38
3.2: The Krossfjorden area 42
The Kollerfjorden section 42
3.3: The Smeerenburgfjorden area 49
Introduction 49
Gneiss complex 50
The Bjørnfjorden section 53
Caledonian granitoid rocks 56
Chapter 4: U/Pb-chronology; results and interpretation of data 59
4.1: Analytical procedure 59
4:2: Results 61
4.2.1: Granodioritic hornblende gneiss (pim04-38) 61
4.2.2: Gneissic granitic xenolith (pim04-46) in Silurian granitoid (pim04-80) 63
4.2.3: Newtontoppen granitoid. 65
4.2.4: Grey two-mica granitoid, Bjørnfjorden (pimsm-22-05) 67
4.2.5: Grey migmatitic granitoid, inner Kongsfjorden (pim04-72) 69
4.2.6: Foliated granitoid leucosome, inner Kongsfjorden (pim04-75) 72
4.2.7: Hornemantoppen granitoid (pimsm19-05) 74
4.2.8: Two-mica leucosome of migmatite, Kollerfjorden (pim04-80) 76
4.3: Comment on monazite results 81
Chapter 5: Discussion 83
5.1: Introduction: 83
Pre-Caledonian evolution of the North-Western Block 83
Caledonian magmatic evolution 83
5.2: Laurentian affinities of the Western Terranes 85
A transcurrent transport and amalgamation regime 88
5.3: Conclusions: 91
References 92

Chapter 1: Introduction

1.1:Purpose of study

The Caledonian and pre-Caledonian basement of Svalbard is generally considered to represent a fragment of the Laurentian plate (e.g. Gee & Tebenkov, 2004; Johansson et al., 2005), and some areas (i.e. the eastern parts) of Svalbard are well correlateable with Laurentian areas in terms of tectonic evolution. The evolution of other areas, especially the north-west part of the archipelago, is not as well understood. The aim of this study is to reach a more detailed understanding of the tectonic evolution of this part of the archipelago based on field-observations and isotopic datings of the igneous and metamorphic rocks.

1.1:Geological setting

Today Svalbard constitutes the north-westernmost part of the passive continental margin of the Eurasian plate. The archipelago comprises pre-Caledonian and Caledonian basement overlain by Carboniferous to Neogene unmetamorphosed sedimentary rocks. The rocks record at least 3 tectonic events: the late Mesoproterozoic to early Neoproterozoic Grenvillian, the Ordovician to Devonian Caledonian and the Tertiary West Spitsbergen orogenic events. The Grenvillian record consists mostly of granitoid gneisses, whereas the Caledonian rocks are widely distributed and variedly deformed metamorphic and igneous rocks. The Tertiary thick-skinned fold and thrust belt involved basement and Carboniferous-Paleogene sedimentary rocks, but no thermal record is recorded from this event.

This thesis focuses on the Paleozoic Caledonian orogeny when Baltica collided with Laurentia to form part of the supercontinent Pangea (e.g. Torsvik et al. 1996). It is believed that during this collision, Baltica was subducted westwards underneath the Laurentian margin (e.g. Andersen & Jamtveit 1990; Andersen et al. 1991). As a consequence of this subduction, we find high-pressure metamorphic rocks in western Norway. The Laurentian crust was subject to extensive migmatization and intrusion of numerous granitoids during the collision (c. 430-410 Ma), (e.g. Hartz et al. 2000, 2001; Strachan et al. 2001; Gillotti et al. 2005) and high-pressure metamorphism (Gilotti & Krogh 2002, Gilotti et al. 2004). In both the Norwegian and the North East Greenland Caledonides we find allochtonous nappes. The various terranes of the Svalbard archipelago originated during the Caledonian orogeny, and is thought that they were assembled through large-scale transcurrent on north-south-trending faults in the aftermath or during the collision (Harland and Wright, 1979).

1.1: Study area and analytical methods

The archipelago of Svalbard is located between 76-82°N and 9-30°W (also the isolated island of Bjørnøya at c. 74°N and 19°W is considered a part of the archipelago). The study area for this thesis comprises the north-western part of the main island of Spitsbergen (figure 1.1). Fieldwork was conducted during two summer seasons, July-August 2004 and August 2005. The 2004-fieldwork was in cooperation with the Russian Polar Marine Geological Research Expedition (PMGRE) and Stockholm University. As means of transportation in the field, helicopter (2004), the MS Polarsyssel (2005) and an inflatable boat was facilitated. In the field, rock descriptions and structural data were recorded and samples were collected. For the subsequent analytical work, the ID-TIMS U/Pb technique of dating was applied to a number of samples.

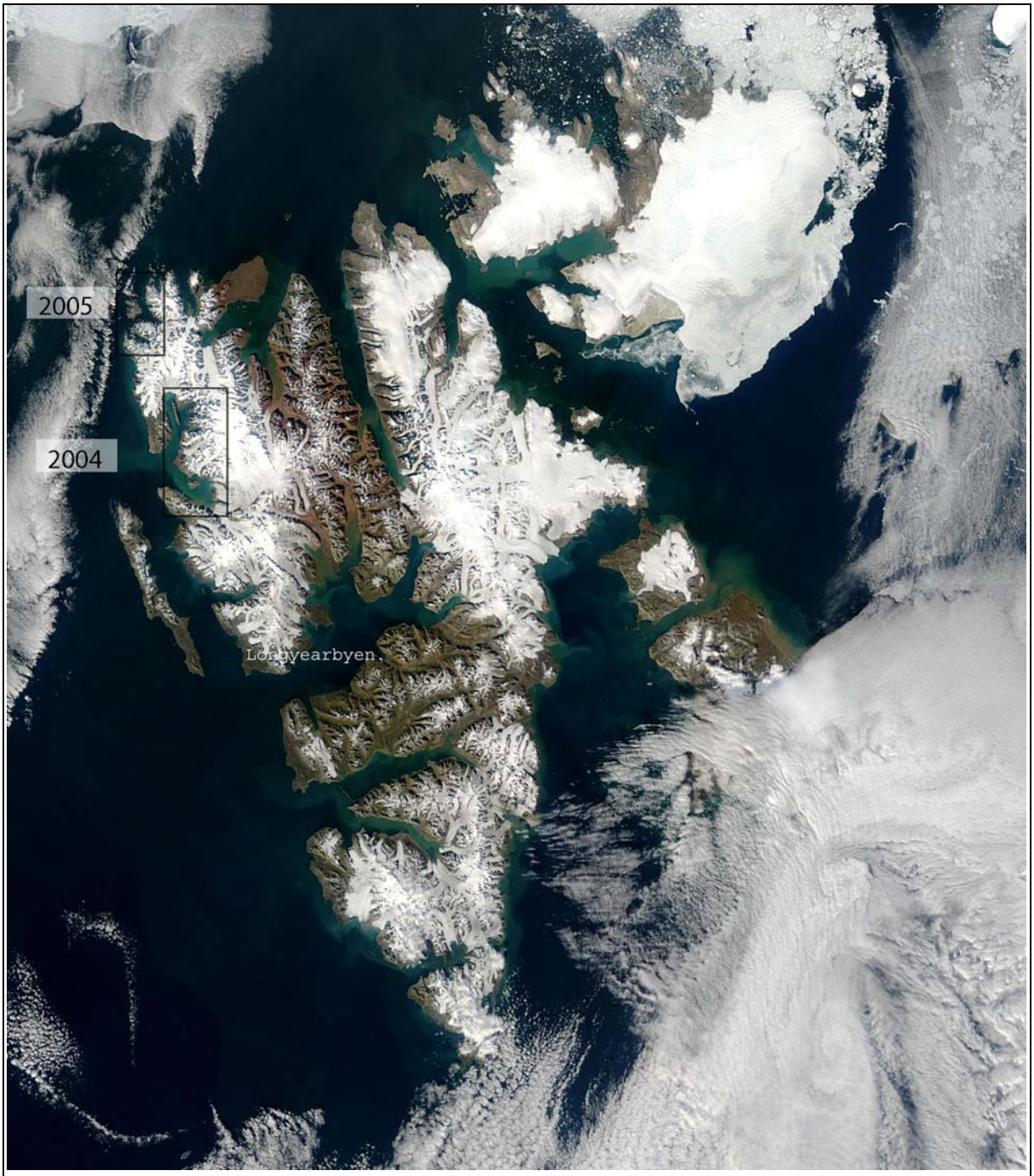

Figure 1.1: Satellite image of Svalbard. The study areas 2004 and 2005 are indicated as well as the administrative centre of the archipelago; Longyearbyen. Image courtesy of MODIS Rapid Response Project at NASA/GSFC.

Chapter 2: Regional geological setting

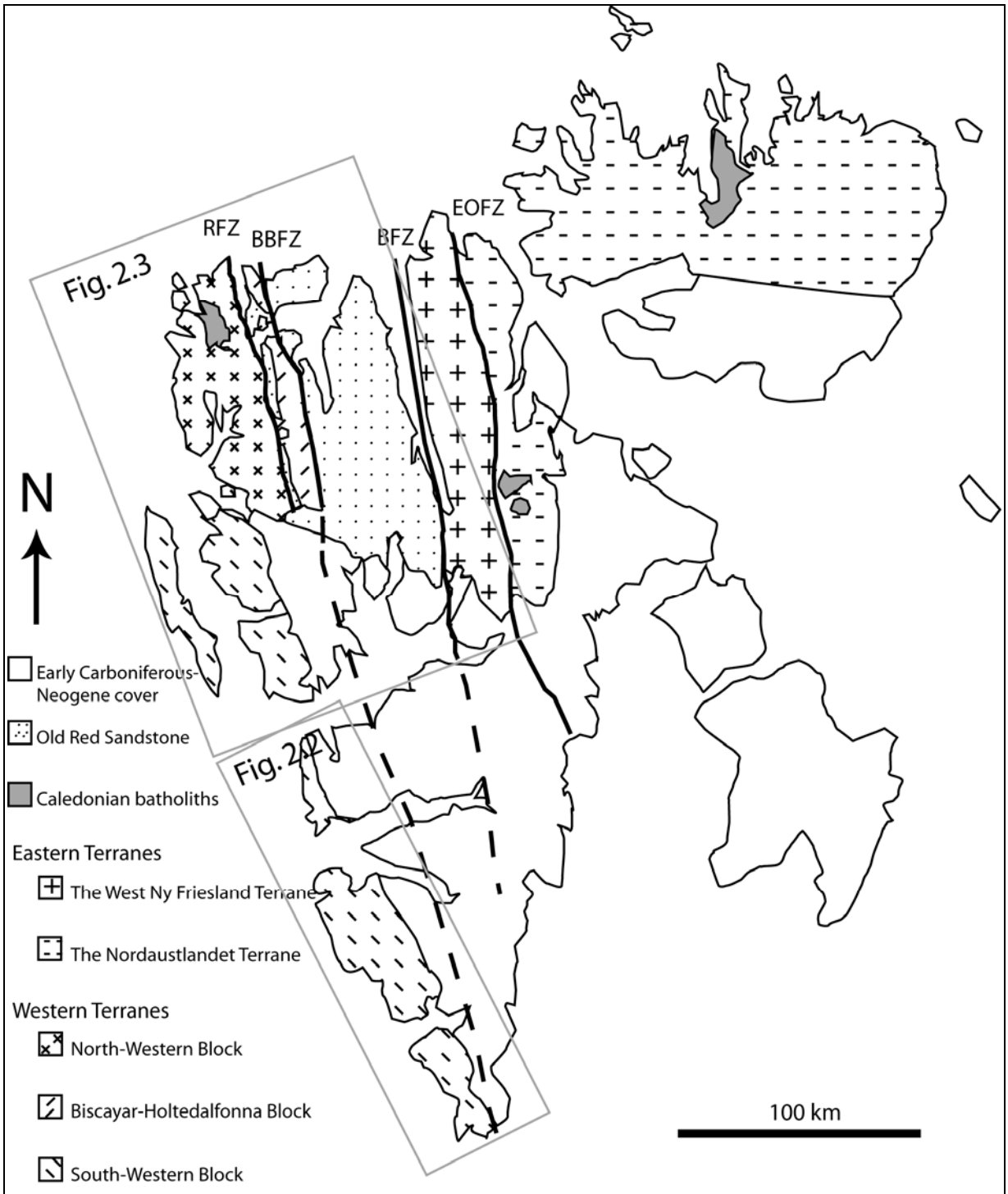

Figure 2.1: Simplified bedrock map of Svalbard. Major fault lines are indicated as referred to in the text, and detailed maps are indicated with grey squares. Abbreviations: RFZ: Raudfjorden Fault Zone, BBFZ: Breibogen-Bockfjorden Fault Zone, BFZ: Billefjorden Fault Zone, EOFZ: Eolsletta Fault Zone.

2.1: Basement

Svalbard's pre-Devonian basement consists of several blocks with contrasting geology separated by major north-south-trending fault zones, summarized by Gee and Tebenkov, (2004); Johansson et al.,(2005). The major blocks are the Western Terranes and the Eastern Terranes, located west and east of the Billefjorden fault zone (figure 2.1), respectively, but further subdivisions can be made.

The Western terranes

The western terrane encompasses the rocks along the west coast of Spitsbergen. In the north, the eastern bounding fault is the Breibogen-Bockfjorden fault zone (BBFZ) (figure 2.1). South of Kongsfjorden the basement and the Devonian Old Red Sandstone is covered by Early Carboniferous-Tertiary deposits, and the eastern terrane boundary disappears, but presumably continues underneath the cover and into the Barents Sea (Andresen, 2004; Harland, 1985).

The northern segment of the western terrane can be further subdivided into 2 blocks, the Biscayar-Holtedalfonna block and the North-Western block (Gee and Tebenkov, 2004). The bounding fault between the two blocks is the Raudfjorden Fault zone (figure 2.1, 2.2).

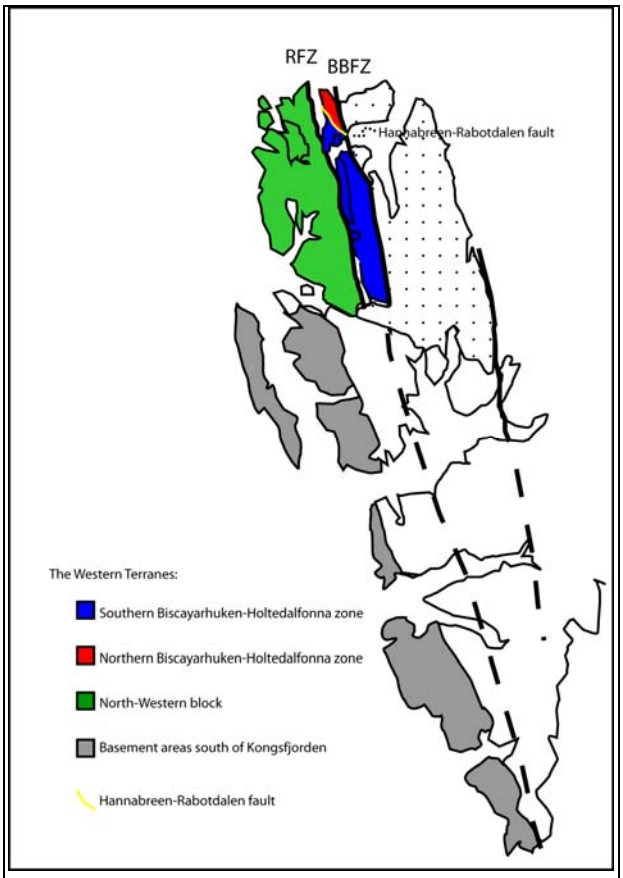

Figure 2.2: Appearance of the Western Terranes. BBFZ: Breibogen-Bockfjorden fault, RFZ: Raudfjorden fault.

North-Western block

The basement rocks north of Kongsfjorden and west of the Raudfjorden fault zone (RFZ) (figure 2.1, 2.2) belong to the North-Western block. The area consist of 3 main lithological units (Dallmann et al., 2002), a metasedimentary sequence (the Krossfjorden Group), a gneiss and migmatite complex (the Smeerenburgfjorden Complex) and a Caledonian granitoid batholith (the Hornemantoppen batholith, (Hjelle, 1979)). The southern part of the area is dominated by rocks of the Krossfjorden Group, whereas the northern part is dominated by rocks of the Smeerenburgfjorden Complex. The Krossfjorden Group is absent north of Magdalenafjorden

The Krossfjorden Group is further subdivided into 3 units; the ~2 km thick Generalfjella unit dominated by marbles, the 2-2,5 km thick Signehamna unit dominated by pelitic rocks with

minor quartzites and the 3 km thick Nissenfjella unit consisting of pelitic schist (Gee and Hjelle, 1966). The stratigraphic relationships, especially between the Signehamna and Nissenfjella units are not always clear, and a more informal stratigraphic subdivision is preferred by Ohta et al., (2002). The entire Krossfjorden Group is deformed by large-amplitude (2-3 km) west-vergent isoclinal folds with slightly south-plunging fold axes (Hjelle, 1979). Except for one locality at Mitrahalvøya, (Gee and Hjelle, 1966), little sedimentary structures are present in the Krossfjorden Group due to intense folding and metamorphism. Fossils are also absent, and the age of deposition of the metasediments is uncertain. Present geochronology data and field evidence indicate that the sediments are either Neoproterozoic or Mesoproterozoic in age. The youngest detrital zircon crystal, from a quartzite in eastern Krossfjorden, has a Pb/Pb age of c. 1,8 Ga (Ohta et al., 2002). See table 2.1 for a compilation of published age data.

The Smeerenburgfjorden Complex refers to the migmatitic and gneissic rocks in northwest Spitsbergen (Dallmann et al., 2002). These higher grade rocks are mainly exposed north of the Krossfjorden Group metasediments, except for a north-south-trending horst in the east (inner Kongsfjorden, figure 2.4). This horst is bounded in the east by the southern extension of the east-dipping Raudfjorden fault and in the west by a west-dipping fault (Dallmann et al., 2002). 3 main rock types make up the Smeerenburgfjorden Complex: migmatites, gneisses and grey granites (Hjelle, 1974; Ohta et al., 2003; Ohta et al., 2002).

Migmatites

The leucosome of the migmatites is generally a 2-mica fine to medium grained granitoid, e.g. (Ohta, 1974). Ohta et al., (2002) analyzed zircon from a leucosome in Vasahalvøya and the ages obtained range from c. 800 Ma -2922 Ma (table 2.1). The melanosome include biotite schist, felsic gneisses and marble. A felsic gneiss xenolith from Kollerfjorden gave crystallization ages in the range of c. 940-963 Ma (Ohta et al., 2002), using the Kober-method on zircon. Biotite Ar/Ar-data from the same sample yield 419 ± 1 Ma which was interpreted as an age of metamorphism. The melanosome is thought to correlate with the lower grade Kollerfjorden Group rocks, which is considered to be the protolith of the migmatites (Bucher-Nurminen, 1981; Gee and Hjelle, 1966; Ohta et al., 2002). The migmatite is interpreted to represent a lower crustal level. Because linear structures plunge gently to the north, this would be the expected situation.

Bucher-Nurminen, (1981) give P-T estimates for the metamorphic conditions of the northern part of the area using mineral assemblages from marble rocks. The temperature estimates is in the range of 600-680 ^{o} C at 4 Kbar, corresponding to a depth of c. 17 km with a geothermal gradient of 35 ^{O}C/km. Because of the spatial distribution of marble bands this P-T-estimate is valid for an area of c. 25 x 30 km.

Grey granitoids

Within the migmatite and gneiss area there are at least 5 grey granitoid bodies (Hjelle, 1979). The bodies are granitic to granodioritic in composition, and they have similar compositions to the leucosomes of the migmatites. The granitoids are thought to represent leucosome enrichment, and thus related in time and space to the migmatites. The contact relationship to the surrounding rocks is intrusive. Age data is available from 3 such granitoid bodies (Balasov et al., 1996a; Ohta et al., 2002). In these studies, the Kober Pb-evaporation method was applied to zircon:

- The Tinayrebukta granodiorite: 424 ± 4 Ma
- The Fuglefjorden granite-monzogranite: 423 ± 3 Ma
- Grey granite, Bjørnfjorden: 421 ± 34 Ma

The studies above also include older grains of zircon, but above the interpreted crystallization ages are referred. Two similar granitoid bodies occur in the Magdalenafjorden area (Hjelle 1979), but no age data are available for these.

Hornemantoppen granitoid

A large granitoid batholith, the Hornemantoppen granitoid (figure 2.2), named after Horneman (1906), occupies a part (~150 km^2) of the mountainous area south of Smeerenburgfjorden. Hjelle, (1979) and Balasov et al., (1996a) provide the most recent studies of this batholith, and they infer an intrusive relationship between the Hornemantoppen batholith and the migmatite/gneiss complex. Geochemical work indicates an S-type intrusion. Hjelle, (1979) obtained a whole-rock Rb/Sr isochron-age of 414 ± 10 Ma whereas Balasov et al., (1996) provides a crystallization age of 413 ± 4,8 Ma using the same method. Based on inclusions of grey granites and cross-cutting relationships the view is that the Hornemantoppen granitoid is a late orogenic batolith that intruded after the emplacement of the grey granites. This is supported by the Rb/Sr-data and the datings of the grey granites (references above).

Biscayarhuken-Holtedalfonna block

The Raudfjorden fault zone (RFZ) (Gee and Moody-Stuart, 1966; Gjelsvik, 1979), separates the Biscayarhuken-Holtedalfonna block from the North-Western block (figure 2.2). The most significant difference between the two terranes is the presence of eclogites and upper Silurian?-Devonian Old Red Sandstone in the Biscayarhuken-Holtedalfonna block. It constitutes a horst between the RFZ and the BBFZ, and is actually a composite terrane divided into a northern and southern part by the NW-SE-trending Hannabreen-Rabotdalen fault (figure 2.2). A migmatite complex, Caledonian granites and the Krossfjorden Group metasediments are found both east and west of the RFZ.

Northern Biscayar-Holtedalfonna block (NBH)

The basement rocks in the NBH have been divided into 3 tectonostratigraphic units (Ohta et al., 1996):

- Biscayarhuken unit: Garnet mica schist
- Mont Blanc unit: Mica schist, amphibolite and felsic gneiss
- Richardalen Group: Amphibolite/eclogite facies mafic and felsic rocks and marble.

Structure

The units are exposed in a large antiform with a north-trending axis (Ohta et al., 2003). The flanks of this structure are occupied by the Biscayarhuken unit, and the Richardalen complex crops out in the core of the anticline. The units are separated by thrust faults which are generally east-dipping, and constitute a west-verging thrust duplex structure throughout the NBH (Gee, 1972). In the east the basement rocks are in contact with the Devonian Andreè

Land Group along the down to the east Breibogen-Bockfjorden extensional fault. Inconformably overlaying the basement is the lowermost Devonian unit in Svalbard, the Siktefjellet group (Friend et al., 1997).

Lithologies

The Biscayarhuken unit consists of amphibolite facies metasedimentary garnet-bearing schist intruded by 961 ± 4 Ma now foliated granitic gneiss. Thus, the age of deposition of the metasediments is pre-Grenvillian (Ohta and Larionov, 1998). Structurally below the Biscayarhuken unit is the Mont Blanc unit composed of garnet-bearing amphibolites of unknown age, pelitic schist and felsic gneiss. Gromet et al., (1998) obtained a U/Pb-age of 430 ± 3 Ma from metamorphic titanite and apatite from the felsic gneiss (table 2.1).

The Richardalen unit consists of mafic and felsic rocks of upper amphibolite to eclogite grade. Eclogitic mineral assemblages show P-T conditions of formation of 680-700°C and 12-15 Kbar (Ohta et al., 1989), equivalent to a depth of c. 43-54 km and a geothermal gradient of 13-16 °C/km.

Grenvillian metagranites and gabbros occur within the thrust duplexes in the Richardalen unit as well as intrusives in the metasediments of the Biscayarfonna group. Peucat et al., (1989) dated a metagranite and a corona gabbro by the U/Pb method on zircon. The metagabbro have a well constrained upper intercept age of 955 ± 1 Ma. Discordant zircons from the metagranite plots close to a lower intercept of 965 ± 1 Ma on a discordia line with an upper intercept of c. 3234 Ma. Ohta et al., (2003) confirmed the presence of Grenvillian magmatic rocks within the Biscayarhuken-Holtedalfonna block (table 2.1).

Evidence of late Proterozoic rift related magmatism was presented by Peucat et al., (1989) and Gromet and Gee, (1998) who dated felsic and mafic upper amphibolite facies and eclogite facies rocks. The age of the magmatic protolith for the eclogites is c. 650 Ma (table 2.1), and Rb/Sr and Sm/Nd-data indicate a mantle influenced source. The age of metamorphism is 457 ± 8 & 459 ± 18 Ma based on metamorphic titanite from amphibolite and felsic gneiss (Gromet and Gee, 1998).

Southern Biscayar-Holtedalfonna block (SBH)

South of Liefdefjorden (figure 2.4) the pre-Devonian basement consist of 3 rock units (Dallmann et al., 2005):

- Generalfjella unit
- Signehamna unit
- Smeerenburgfjorden Complex

The western contact to the Devonian Red Bay Group is a thrust fault, and the sediments also occur as klippen in some areas. The eastern contact is an extensional fault (BBFZ).

Gee and Hjelle, (1966) and Gjelsvik, (1979) correlated these basement units with the basement east of the RFZ. Ohta et al., (2003) dated zircon from neosome of migmatite using the Kober-method and presented a Pb/Pb age of 942 ± 8 Ma (table 2.1). The migmatite/gneiss is intruded by granitoids that have not been dated. The rocks in the SBH is deformed in a large anticline with NNW/SSE-trending fold axis (Gjelsvik, 1979) which is cut by east-west-trending down-to-the north extensional faults that are related to the Monacobreen late Caledonian tectonic phase (McCann, 2000).

Basement areas south of Kongsfjorden

Rocks along the west coast of Spitsbergen south of Kongsfjorden are variably influenced by the Tertiary West Spitsbergen fold and thrust belt (Bergh and Andresen, 1990; Harland and Horsfield, 1974). The pre-Carboniferous rocks are made up of Meso- to Neoproterozoic supracrustals, Grenvillian igneous rocks and Caledonian metamorphic rocks, including the Vestgøtabreen (Motalafjella) blueschist complex.

Meso-Neoproterozoic supracrustals

The areas along the west coast of Spitsbergen are dominated by low-grade Neoproterozoic and Mesoproterozoic supracrustal rocks with a thickness of ~20 km (Bergh et al., 2003; Harland, 1997; Harland and Horsfield, 1974; Harland et al., 1979). The Vendian record generally consists of a basal conglomerate, limestone, pillow lavas and diamictoid rocks (Harland et al. 1993), whereas the pre-Vendian rocks consist of quartzites, micaschists, amphibolites and carbonates. Near Hornsund there is a Precambrian granite-gabbro complex (Balasov et al. 1996).

Bjørnerud, (1990); Bjørnerud et al., (1990) demonstrated the presence of a major unconformity below the Vendian succession in Wedel-Jarlsberg Land (figure 2.3). The sub-unconformity rocks are supracrustals with a different structural style reflecting a pre-Vendian tectonic event. The entire section was later affected by Caledonian contractional deformation and greenschist-facies metamorphism. The thrusting and folding was northeast-directed, and may be related to the early Ordovician metamorphism and (subsequent?) thrusting of the Vestgøtabreen Complex (Peucat et al., 1989). Bjørnerud, (1990) suggests that the Hornsund area was involved in an accretionary prism at a higher level in the same subduction-wedge. U/Pb and Rb/Sr data from Balasov et al., (1995); Balasov et al., (1996b); Gavrilenko et al., (1993) indicate a 1100-1200 Ma igneous event and 930 metamorphic event in Mesoproterozoic meta-eruptives of the Skålfjellet and The Vimsodden subgroups (figure 2.3, table 2.1).

Vestgøtabreen HP complex (with Motalafjella blueschists)

The metamorphic grade of the rocks south of Kongsfjorden differs from the areas further north. The supracrustals in the former area is generally of low metamorphic grade except for a tectonic sliver of HP-rocks; the Vestgøtabreen complex (Bernard et al., 1993). The complex is thrust upon Neoproterozoic and lower Carboniferous rocks, and is unconformably overlain by folded upper Ordovician fossiliferous carbonates (Armstrong et al., 1986). Hirajima et al., (1988) estimated the metamorphic conditions of formation at 575-645 °C and 17-24 Kbar, which corresponds to a depth of c. 61-86 km and a geothermal gradient between c. 7 and 11°C /km (with an average crustal density of 2,8 g/cm^3). Low subduction zone gradients are also documented by Agard et al., (2005), who estimated the P-T-conditions of the lower unit of the complex to 15-16 Kbar and 380-400 °C (c. 7 °C/km). Agard et al., (2005) also showed that the Vestgøtabreen complex comprises the oldest carpholite-bearing rocks in the world, and that low-T subduction gradients were present in the Paleozoic.

The complex is made up of meta-igneous and meta-sedimentary rocks of oceanic affinity (Bernard et al., 1993; Ohta, 1985). Late Ordovician metamorphic ages (c. 460-470 Ma) are provided by Bernard et al., (1993) and Dallmeyer et al., (1989), who used the zircon U/Pb and white mica-Ar/Ar and whole-rock-Rb/Sr-methods, respectively (Table 2.1). Sm/Nd model ages and a zircon upper intercept-age suggest that the age of the protolith of an eclogite is c. 2100 Ma. A protolith age for a blueschist unit within the complex is suggested between 475-1000 Ma by Sm/Nd-data (Bernard et al., 1993).

Age, Ma	Locality	Lithology	Method	Reference
2170 ± 50	Motalafjella, W Spitsbergen	eclogite, u. Vestgøtabr. unit	Sm/Nd model age	Bernard et al., (1993)
2300 (upper) 360(lower)	Hornsund, W Spitsbergen	mica schist Isbjørnhamna Gp.	4 zrc. discordia	Balasov et. al., (1996b)
2,06 ± 0,07, 2,13 ± 0,03, 2,14 ± 0,57 Ga	Motalafjella, W Spitsbergen	2 eclogitic metagabbros and eclogite, u. Vestgøtabr. unit	Sm/Nd model age	Bernard et al., (1993)
1834 ± 6 to 2865 ± 3	E Krossfjorden	quartzite Signehamna unit	8 single zrc. Pb evap. (Kober). (Kober)	Ohta et al., (2002)
1735 ± 4, 1736 ± 5 and 1739 ± 5	Siktefjellet, Biscayarhalvøya	Siktefj. Gp, ORS, kongl. igneous clast	3 clasts, 3 grs. single-zrc.Pb evap.	Hellman et al., (1998)
1278 ± 100	Hornsund, W Spitsbergen	granite-gabbros, Skålfjellet Gp.	Rb/Sr w.r., 8 pt isochron	Balasov et al., (1996b)
1200	Hornsund, W Spitsbergen	Pyroclastic conglomerate	U/Pb zrc.	Balasov et al., (1995)
1100-1200	Hornsund, W Spitsbergen	granite-gabbros, Skålfjellet Gp.	single zrc. Pb evap. (Kober).	Balasov et al., (1996b)
1154 ± 21	Hornsund, W Spitsbergen	gabbro, Skålfjellet Gp.	U/Pb zrc.	Balasov et al., (1996b)
0,97 ± 0,10, 1,07 ± 0,02, 1,10 ± 0,13 Ga	Motalafjella, W Spitsbergen	2 Blueschist and metaquartzite, u. Vestgøtabr. Unit	Sm/Nd model age	Bernard et al., (1993)
965 ± 1 (lower) 3234 + /- 43 (upper)	Biscayarhalvøya	metagranite, Richardalen unit	zrc.U/Pb	Peucat et al., (1989)
955 ± 1	Biscayarhalvøya	corona gabbro, Richardalen unit	zrc.U/Pb	Peucat et al., (1989)
937 ± 14 to 2539 ± 21	NBH	metagranite, Richardalen unit	9 grs.single zrc. Pb evap. (Kober).	Ohta et al., (2003)
938 ± 4 to 2669 ± 2	NBH	Grt 2-mica schist	26 single zrc. Pb evap. (Kober). (Kober).	Ohta et al., (2003)
930	Hornsund, W Spitsbergen	pyroclastic conglomerate	U/Pb zrc.	Balasov et al., (1995)
930	Hornsund, W Spitsbergen	Isbjørnhamna schist	Rb/Sr w.r.	Gavrilenko et al., (1993)
912 ±6 to 2922 ± 13	NØ Vasahalvøya	migmatite neosome	26 grs.single zrc. Pb evap. (Kober).	Ohta et al., (2002)
940 ± to 963 ± 13 (zrc.Pb) (419 ± 1 Ar/Ar)	Kollerbukta, E. Krossfjorden	granitic gneiss xenolith	4 grs.single zrc. Pb evap. (Kober). + bio.	Ohta et al., (2002)
942 ± 8 to 3604 ± 4	(SBH)	granitic neosome	20 grs.single zrc. Pb evap. (Kober).	Ohta et al., (2003)
661 ± 2	Biscayarhalvøya	felsic neosome	zrc.U/Pb 0=>620 Ma discordia (3 analyses)	Peucat et al., (1989)
655 ± 10 and 653 ± 9	Biscayarhalvøya	eclogite-facies garnet amphibolite, Richardalen	2 grs.single zrc. Pb-evap	Gromet & Gee (1998)
647 ± 4 and 667 ± 4	Biscayarhalvøya	eclogite-facies felsic gneiss, Richardalen unit	2 grs.single zrc. Pb evap. (Kober).	Gromet & Gee (1998)
625 ± 5	Biscayarhalvøya	eclogite	zrc.U/Pb 0=>620 Ma discordia (5 analyses)	Peucat et al., (1989)
615 ± 18	SE WJL, Hornsund (footwall)	mesoprot. Eimfjellet Gp.	hbl. Ar/Ar	Manecki et al., (1999)
584 ± 14	SE WJL, Hornsund (footwall)	mesoprot. Isbjørnhamna Gp.	mus. Ar/Ar	Manecki et al., (1999)
575 ± 15 mus. & 640 ± 6 bio.	SE WJL, Hornsund (footwall)	mesoprot. Isbjørnhamna Gp.	mus./ bio. Ar/Ar	Manecki et al., (1999)
504,7 to 552,6	Biscayarhalvøya (N-Spitsbergen)	Richardalen Complex (eclogite facies)	hbl.. Ar/Ar, 5 samples	Dallmeyer et al., (1990)
c 460-470 (± 0,9-2,4)	Motalafjella, W Spitsbergen	glaucophane mica schist, u. Vestgøtebr. unit	white mica Ar/Ar	Dallmeyer et al., (1990)

Age, Ma	Locality	Lithology	Method	Reference
c 460-470 (± 0,9-2,4)	Motalafjella, W Spitsbergen	glaucophane mica schist, u. Vestgøtebr. unit	white mica Ar/Ar	Dallmeyer et al., (1990)
484 ± 5	SE WJL, Hornsund (footwall)	mesoprot. Isbjørnhamna Gp.	bio. Ar/Ar	Manecki et al., (1999)
476 ± 30 & 2121 ± 50	Motalafjella, W Spitsbergen	eclogite, u. Vestgøtabr. unit	U/Pb discordia, 4 frac. zrc.	Bernard et al., (1993)
459 ± 18	Biscayarhalvøya	eclogite-facies garnet amphibolite, Richardalen	tit. U/Pb (6 grs.isochron)	Gromet & Gee (1998)
458 ± 9	SE WJL, Hornsund (footwall)	mesoprot. Eimfjellet Gp.	mus. Ar/Ar	Manecki et al., (1999)
458 ± 10	Motalafjella, W Spitsbergen	eclogite, u. Vestgøtabr. unit	white mica + W.R. Rb/Sr	Dallmeyer et al., (1990)
457 ±11 to 474 ±11	Motalafjella, W Spitsbergen	glaucophane schist, u. Vesgøtabr. unit	white mica + W.R. Rb/Sr	Dallmeyer et al., (1990)
457 ± 8	Biscayarhalvøya	eclogite-facies felsic gneiss, Richardalen unit	tit. U/Pb (4 grs.isochron)	Gromet & Gee (1998)
454,9 ± 0,7, 443,3 ± 0,6, 480,5 ± ,6	Biscayarhalvøya	Richardalen Complex (eclogite facies)	mus. Ar/Ar 3 samples	Dallmeyer et al., (1990)
440 ± 6 to 1370 ± 7	Raudfjorden graben	Red Bay Gp, ORS, tuffite	8 grs. single-zrc.Pb evap.	Hellman et al., (1998)
> 436	Bjørnfjorden/ Smeerenburgbreen	grey granites	Rb/Sr W.R., 2 pt. Isochron	Balasov et al., (1996 a)
432,5 ± 6.9	SW WJL, Hornsund(hanging wall)±	upper Neoprot. Sofiebogen Gp.	mus. Ar/Ar	Manecki et al., (1999)
432 ± 10	Southern Ny Friesland	Newtontoppen granitoids	Rb/Sr W.R., 7 samples	Tebenkov et al., (1996)
424 ±4 to 1251 ±29	Tinayrebukta, E Krossfjorden	granodioritt/ monzodioritt	4 grs.single zrc. Pb evap. (Kober).	Ohta et al., (2002)
423 ± 3 to 1725 ± 8	Fuglefj., NW Vasahalvøya	granite-monzogranite	10 grs.single zrc. Pb evap. (Kober).	Ohta et al., (2002)
421 ± 34 to 952 ± 20	Bjørnfjorden/ Smeerenburgbreen	grey granites	11 grs.zrc. Pb-evap.	Balasov et al., (1996 a)
420 ± 3 & 415 ± 4	Feiringfj., Kongsfjorden	mica schist	mus./ bio. Ar/Ar	Ohta et al., (2002)
c 420 ±5 (?) + 3 discordantees	Southern Ny Friesland	Newtontoppen granitoids	U/Pb ID-TIMS zrc.	Tebenkov et al., (1996)
418 ± 10 (Pb/Pb) and 445 ± 33 (206Pb/238U)	Innvika, central., Nordaustlandet	migmatite neosome (2 samples)	NORDSIM single zrc.U/Pb	Tebenkov et al., (2002)
412,7 ± 4,8	Bjørnfjorden/ Smeerenburgbreen	Hornemantoppen granitoids	Rb/Sr W.R., 5 pt. Isochron	Balasov et al., (1996 a)
407 ± 10 (bio.) & 433 ± 22 (mus.)	Biscayarhalvøya	Richardalen Complex (eclogite facies)	K - Ar, 2 samples	Gee et al., (1966)
397 ± 10 to 550 ± 24 Ma	Biscayarhalvøya	Richardalen Complex (eclogite facies)	hbl. K - Ar, 4 samples	Gee et al., (1966)
389 ± 12 (bio.) & 439 ± 20 (hbl.)	Biscayarhalvøya	Biscayarfonna complex, amphibolite facies	K - Ar, 2 samples	Gee et al., (1966)

Table 2.1: Published radiometric data from western Spitsbergen. Abbreviations: frac.: fraction, gr/grs.: grain (s), evap.:evaporation, ID-TIMS: Isotope Dilution Thermal Ionizing Mass Spectrometer W.R.: Whole Rock, hbl: hornblende, mus.: muscovite, bio.: biotite, tit.: titanite, zrc.: zircon WJL. :Wedel Jarlsberg Land, NBH/SBH.: Northern/Southern Biscayar-Holtedalfonna zone, ORS: Old Red Sandstone

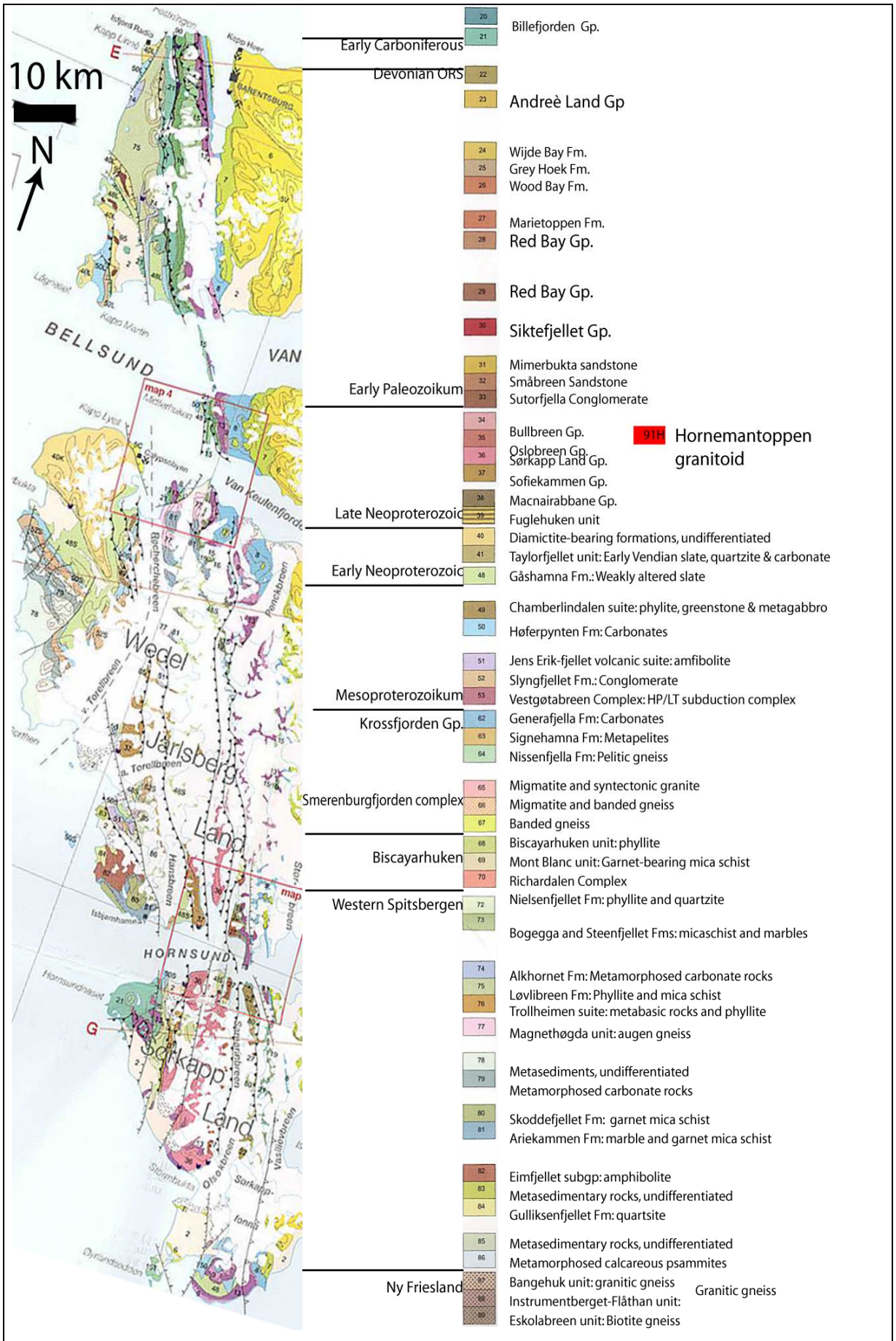

Figure 2.3: Geological map of south-western Spitsbergen . Simplified legend. From Dallmann et al. (2002).

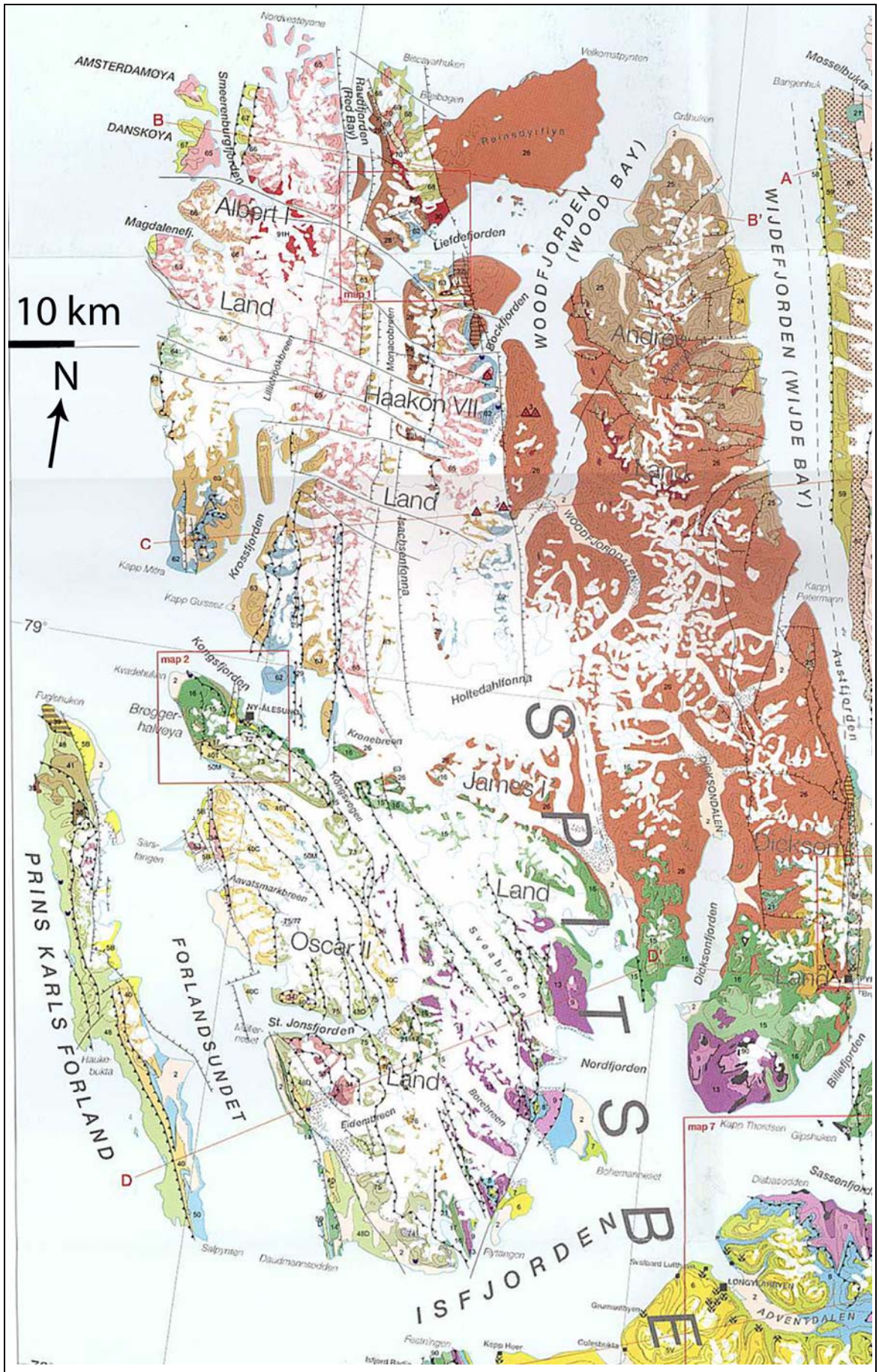

Figure 2.4: Bedrock map of western and north-western Spitsbergen. From Dallmann et al.(2002). Legend in figure 2.3.

The Eastern terranes

The tectonometamorphic evolution of the Eastern terranes is reasonably well understood because of extensive structural, isotopic and stratigraphic studies the last 15 years by Russian, Swedish and British geologists.

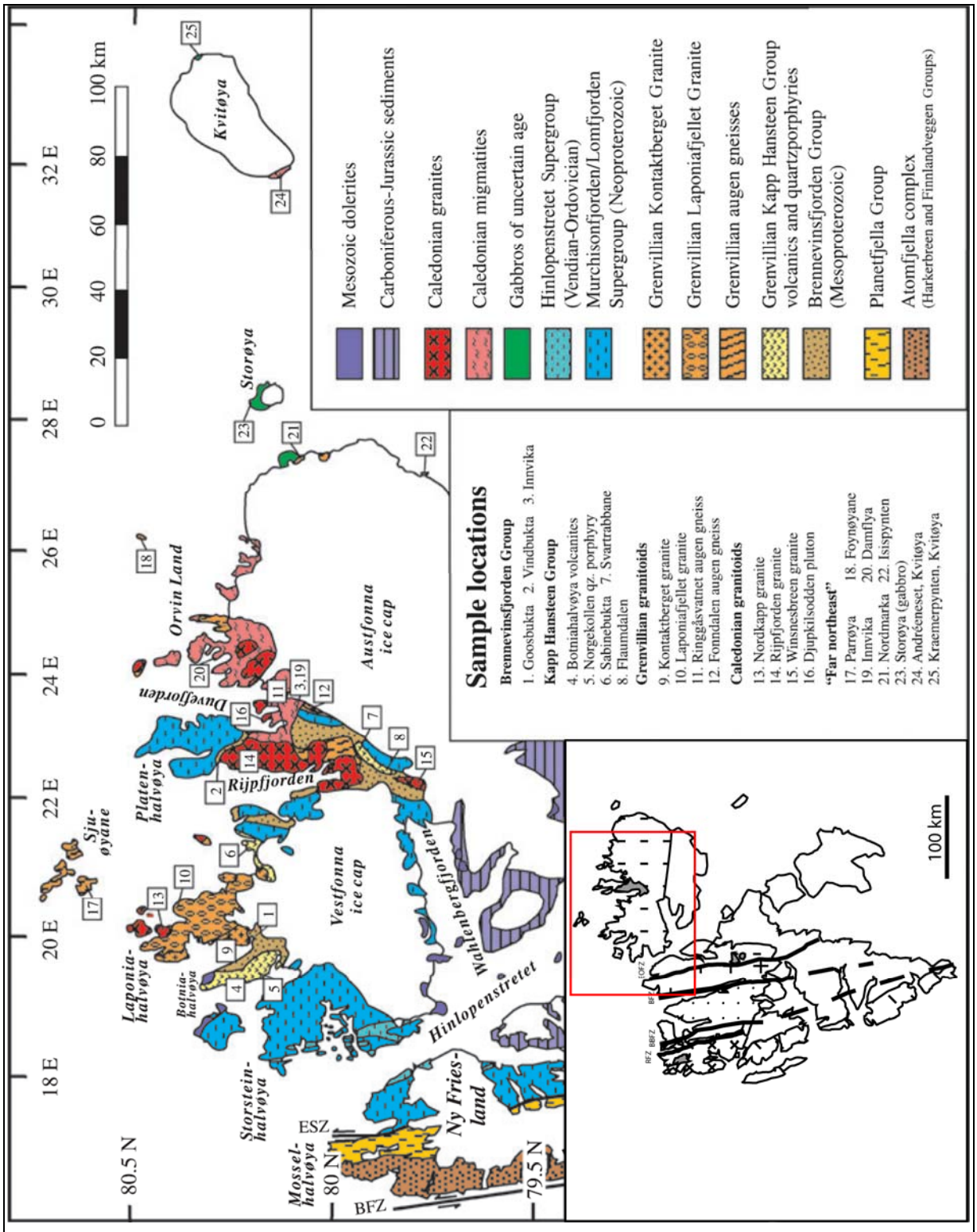

Figure 2.5: Geological map of northern Ny Friesland and Nordaustlandet. Modified from Johansson et al. (2005). Inset map (red frame) shows location of map and major fault lines discussed in the text. Sample lithologies refers to data in figure 2.7 Abbreviations: RFZ: Raudfjorden Fault zone, BBFZ: Breibogen-Bockfjorden Fault zone, BFZ: Billefjorden fault zone, LFZ: Lomfjorden fault zone.

The basement rocks of Ny Friesland and Nordaustlandet are assigned to the Eastern Terrane (Harland, 1985). They form a composite terrane divided along the Eolsletta fault (Lyberis and Manby, 1999), or the Mosselhalvøya thrust, (Gee et al., 2001) consisting of the West Ny Friesland Terrane and the Nordaustlandet Terrane.

West Ny Friesland terrane

This terrane is dominated by the 5 km wide and 150 km long Atomfjella Antiform (Witt-Nilsson, 1998). It consists of Paleoproterozoic gneisses and supracrustals in a Caledonian thrust stack consisting of 5 thrust sheets. This structure is bounded in the west by the Billefjorden fault zone (Harland et al., 1974; Witt-Nilsson 1998) and in the east by the Eolsletta fault (Lyberis and Manby, 1999). In the south it is unconformably overlain by Carboniferous strata. The protolith age for the orthogneisses is c. 1750 Ma (4 of the thrust units) (Johansson, 2001) and c. 2780 Ma (1 unit)(Witt-Nilsson, 1998). During the Caledonian orogeny the protoliths were metamorphosed under amfibolite facies conditions, and Gee and Page, (1994) dated this event by the Ar/Ar-method to c. 412-429 Ma.

The Nordaustlandet terrane

The structurally overlaying North-Eastern Terrane encompasses Nordaustlandet and the north-eastern part of Spitsbergen and consists largely of upright to west-verging folded Mesoproterozoic and Neoproterozoic supracrustals and Grenvillian and Caledonian granitoids (Dallmann et al., 2002).

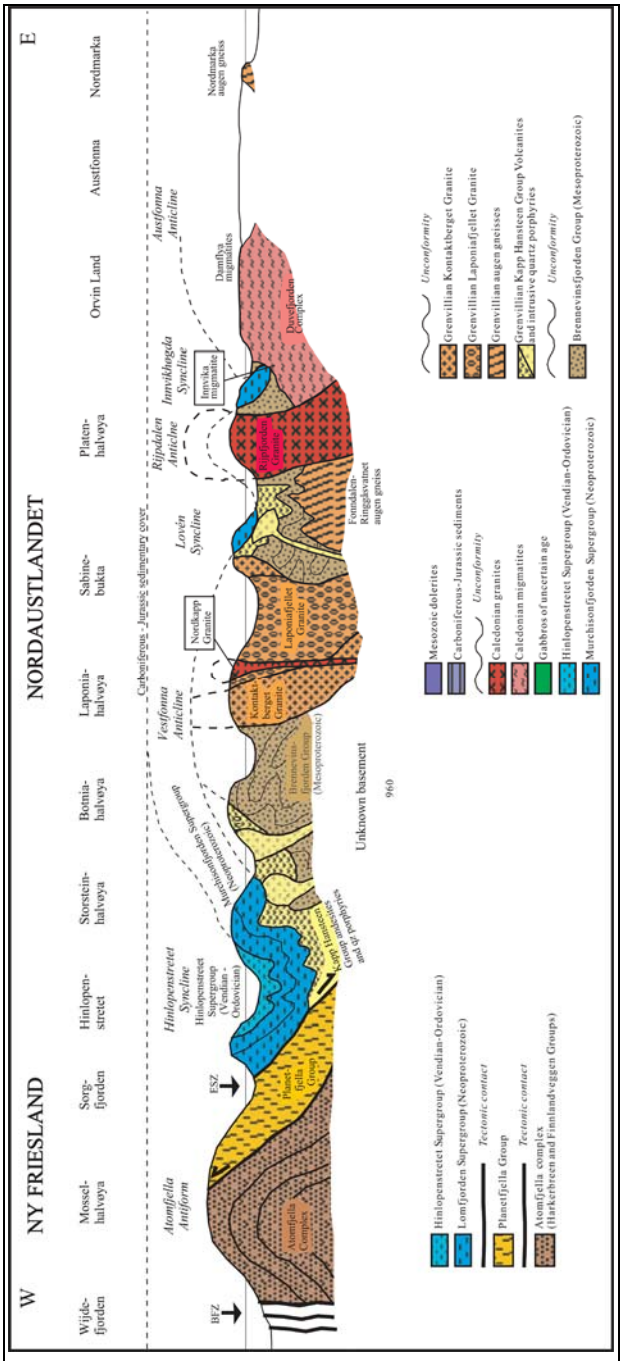

Figure 2.6: Schematic E-W-profile through northern Ny Friesland and Nordaustlandet. From Johansson et al., 2005

The Mesoproterozoic supracrustal sequence consists of phyllite, quartzites and tuff (Brennevinsfjorden Group) stratigraphically below a Grenvillian (Johansson et al., 2000) metavolcanic complex (Kapp Hansten volcanites), (Ohta, 1982). The volcanics are dated to c. 960 Ma (Johansson et al., 2000). The Brennevinsfjorden Group sediments contain detrital

zircon with ages from 1050-2700 Ma (Larionov in Johansson 2005). Intruding these rocks are Grenvillian gneissic granitoids. It is generally believed that they are partly result of migmatization of an old crust (Johansson et al., 2000). The overlying Neoproterozoic low-grade Murchisonfjorden Supergroup consist of a basal conglomerate, shales, sandstone and stromatolite-bearing carbonate rocks (Sandelin et al., 2001), whereas the Vendian-Ordovician Hinlopenstredet Supergroup consist of stromatolite-bearing carbonates, glacial diamictites and sandstones (Fairchild and Hambrey, 1995; Harland et al., 1993). This succession is correlated with the Neoproterozoic Eleonore Bay Supergroup and the Tillite Group of East Greenland (e.g. Fairchild and Hambrey, 1995; Johansson et al., 2005; Watt and Thrane, 2001). The metamorphic grade of the Neoproterozoic succession is generally greenschist facies, but in the central parts of Nordaustlandet they are migmatitic (Tebenkov et al., 2002) and intruded by granitoids. A large Caledonian batholith, the Newtontoppen granitoid, also intrudes the Neoproterozoic succession in southern Ny Friesland (Tebenkov et al., 1996). The Caledonian granitoids are considered to be S-type or transitional S-I-type (Johansson et al., 2004; Johansson et al., 2002; Tebenkov et al., 1996) based on their 2-mica mineralogy, peraluminous chemistry and initial Sm/Nd and $^{87}Sr/^{86}Sr$-ratios. The igneous evolution history is summarized in figure 2.7: In the Grenvillian, early volcanism was followed by 930-950 Ma plutonism. The Caledonian thermal record spans some 40 Ma, but the main event was probably around 420-435 Ma.

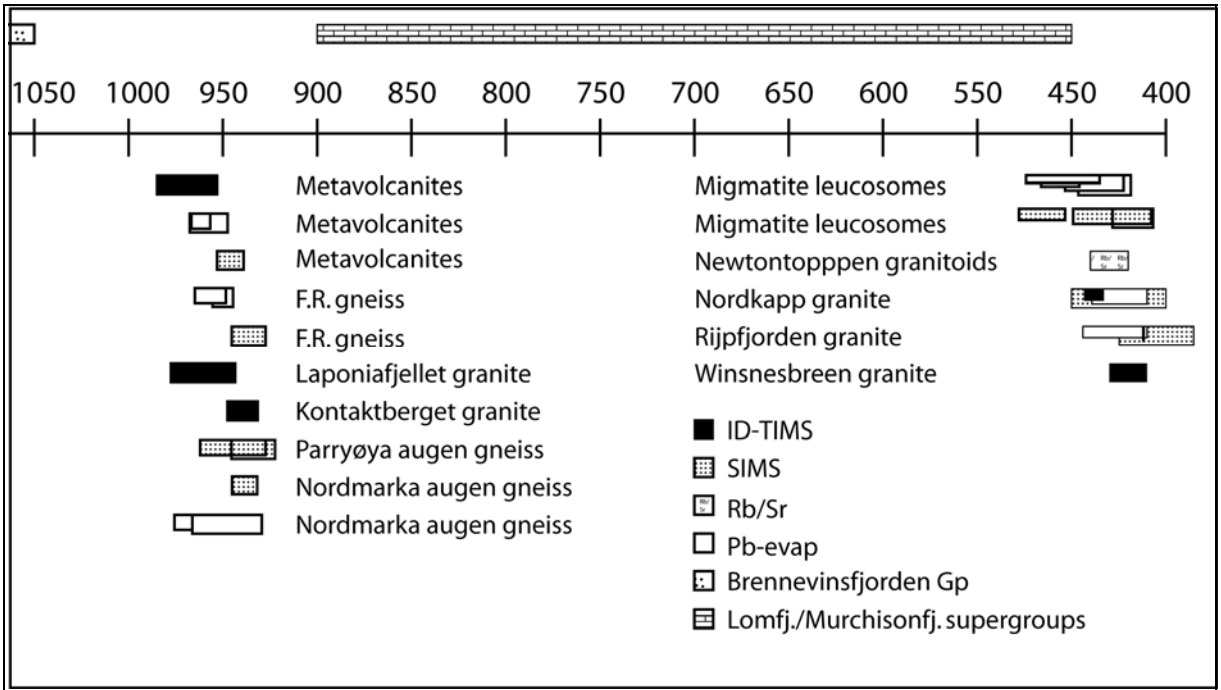

Figure 2.7: Timeline for the Nordaustlandet terrane. Time in Ma. Legend indicate analytical method. Based on Johansson et al. (2005) and others, references as in table 2.2. Age bars are given with analytical error, and ages with large errors are not plotted. F.R. gneiss: Fonndalen-Ringåsvatnet-gneiss.

Age (Ma)	Lithology	Method	Reference
2700, 1900-1050	Brennevinsfjorden Gp. quartzites	SIMS U/Pb zrc.	Larionov in Johansson et. al (2005)
2700, 1800-1100	Brennevinsfjorden Gp. quartzites	Pb-evap zrc.	Larionov in Johansson et. al (2005)
967 ± 15	Svartrabbane Fm. & Kapp Hansteen Gp. volcanics	ID-TIMS U/Pb zrc.	Johansson et al. (2004)
963 ± 5, 958 ± 10	Svartrabbane Fm. & Kapp Hansteen Gp. volcanics	Pb-evap zrc.	Johansson et al. (2000)
961 ± 17	Laponiafjellet granite	ID-TIMS U/Pb zrc.	Gee et al. 1995
957 +30/-18	Fonndalen-R. augen gneiss	ID-TIMS U/Pb mnz.	Johansson et al. (2000)
950 ± 10, 958 ± 4	Kapp Hansten complex qtz. porhyries	Pb-evap zrc.	Johansson et al. (2000)
949 ± 4, 956 ± 7	Fonndalen-R. augen gneiss	Pb-evap zrc.	Johansson et al. (2000)
947 ± 18, 959 ± 19	Nordmarka augen gneiss	Pb-evap zrc.	Johansson et al. (2004)
946 ± 7	Kapp Hansten volcanic complex	SIMS U/Pb zrc.	Johansson et al. (2000)
939 ± 8	Kontaktberget granite	ID-TIMS U/Pb zrc.	Gee et al. (1995)
939 ± 7	Nordmarka augen gneiss	SIMS U/Pb zrc.	Johansson et al. (2004)
937 ± 9	Fonndalen-R. augen gneiss	SIMS U/Pb zrc.	Johansson et al. (2000)
936 ± 12, 944 ± 17	Parryøya augen gneiss	SIMS U/Pb zrc.	Johansson et al. (2004)
446 ± 40	Normarka syenite	Pb-evap zrc.	Johansson et al. (2004)
445 ± 14	Aplite dyke, Kvitøya	Pb-evap zrc.	Johansson et al. (2004)
440 ± 3	Nordkapp granite	ID-TIMS U/Pb mnz.	Johansson et al. (2002)
440 ± 26	Foynøyane grey granite	Pb-evap zrc.	Johansson et al. (2004)
438 ± 16, 457 ± 9, 452 ± 19	Kvitøya migmatite	Pb-evap zrc.	Johansson et al. (2004)
437 ± 12	Foynøyane grey granite	SIMS U/Pb zrc.	Johansson et al. (2004)
434 ± 8	Normarka syenite	SIMS U/Pb zrc.	Johansson et al. (2004)
432 ± 7	Damflya migmatite	Pb-evap zrc.	Johansson et al. (2004)
432 ± 10	Newtontoppen granitoids	Rb/Sr W.R., 7 samples	Tebenkov et al. (1996)
431 ± 7	Aplite dyke, Kvitøya	SIMS U/Pb zrc.	Johansson et al. (2004)
430 ± 21, 465 ± 11	Kvitøya migmatite	SIMS U/Pb zrc.	Johansson et al. (2004)
Ri	Rijpfjorden granite	Pb-evap. mnz.	Johansson et al. (2002)
424 ± 14	Rijpfjorden granite	Pb-evap zrc.	Johansson et al. (2002)
423 ± 6	Rijpfjorden granite	Pb-evap zrc.	Johansson et al. (2002)
420 ± 54	Aplitic granite, Kvitøya	Pb-evap tit.	Johansson et al. (2004)
c. 420	Winsnesbreen granite	ID-TIMS U/Pb mnz.	Johansson et al. (2002)
418 ± 10 (Pb/Pb) and 445 ± 33 (206Pb/238U)	migmatite neosome (2 samples)	SIMS single zr. U/Pb (weighted avr)	Tebenkov et al (2002)
417 +18/-7	Djupkilsodden pluton	ID-TIMS U/Pb zrc.	Gee et al. (1999)
416 ± 37	Parryøya grey granite	Pb-evap mnz.	Johansson et al. (2004)
412,5 ± 0.5	Rijpfjorden granite	ID-TIMS U/Pb mnz.	Johansson et al. (2002)
410 ± 15	Rijpfjorden granite	SIMS U/Pb zrc.	Johansson et al. (2002)
c. 410	Djupkilsodden pluton	Pb-evap zrc.	Gee et al. (1999)
c. 400-450	Nordkapp granite	SIMS U/Pb zrc.	Johansson et al. (2002)
c. 400	Isispynten grey granite	SIMS U/Pb zrc.	Johansson et al. (2004)

Table 2.2: Published radiometric data from theNordaustlandet terrane (in chronological order). Data with large errors are generally left out. Abbreviations: mnz.: monazite, zrc.: zircon, Fm.: Formation, Gp.: Group, W.R.:Whole Rock. Methods: SIMS: Secondary Ionizing Mass Spectrometer/Ion probe, ID-TIMS: Isotope Dilution Thermal Ionizing Mass Spectrometer, Kober: Pb-evaporation-TIMS. From Johansson et al. (2005).

2.2: Old Red Sandstone

Upper Silurian-Devonian deposits cover a large area in central northern Spitsbergen (figure 2.8). The maximum total thickness of the deposits is around 8-10 kilometers (Harland, 1997) and they are divided into 3 groups; the Siktefjellet, the Red Bay and the Andreè Land Groups, respectively (figure 2.9). The lithologies are mainly fining upwards continental fluvial deposits. 3 tectonic phases accompanied the stratigraphic evolution, and the deformation structures within the deposits provide direct evidence of transpressive/ transtensive movements (e.g. Friend et al., 1997; McCann, 2000).

The Haakonian phase

The c. 4500 meters thick Siktefjellet Group is exposed in the northern part of Biscayarhalvøya and constitutes the lowermost post-Caledonian stratigraphic unit, and rests unconformably on Caledonian basement. Biscayarhalvøya is separated into a northern and southern part (abbreviated here NBH and SBH, receptively) by the Rabotdalen-Hannabbreen fault (figure 2.2). This fault is considered to be a splay fault from the Breibogen-Bockfjorden fault (McCann, 2000). Movement occurred as left-lateral strike-slip prior to the deposition of the Red Bay Group (McCann, 2000), and lead to the juxtaposition of the two basement blocks. Friend et al., (1997) introduced the Siktefjellet strike-slip zone between the Breibogen-Bockfjorden and Raudfjorden fault. The zone was active prior to, during and after the deposition of the Siktefjellet Group, and the rocks experienced different strike-slip regimes events that included; tectonic transport (and exhumation?) of the basement; strike-slip basin formation and basin inversion.

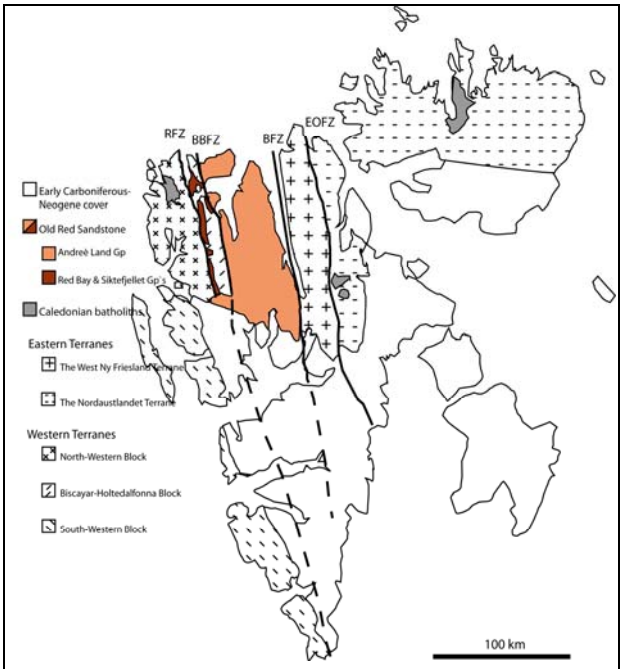

Figure 2.8: The main Old Red Sandstone basins of Svalbard. Minor deposits also occur in the Kongsfjorden area west of RFZ and in the Hornsund area in southwest Spitsbergen, but are not indicated on map. Abbreviations: RFZ: Raudfjorden Fault Zone, BBFZ: Breibogen-Bockfjorden Fault Zone, BFZ: Billefjorden Fault Zone, LFZ: Lomfjorden Fault Zone

The clast composition of the Siktefjellet Group differs from the overlaying Red Bay Group, and Helman et al., (1998) showed that quartz porphyry clasts from the Liljeborgfjellet Formation crystallized at c. 1740 Ma, thus ruling out any known basement rocks in western Svalbard as the source for the deposits. The nearest provenance for the clasts is found in Ny Friesland, around 55 km to the east, but an alternative source for the clasts may be the unexposed basement below the Andreè Land Group deposits east of the BBFZ (Helman et al., 1998; Gee and Page, 1994). The upper time bracket of the Haakonian phase (Gee, 1972) is given by the overlaying Lochkovian Red Bay Group, which apparently is not affected by this phase.

The Monacobreen phase

Unconformably above is the Red Bay Group that comprises c. 3,5 km of fluvial sediments. It rests partly on Siktefjellet Group sediments and partly on basement (marbles, pelites and migmatitic rocks). The unit was subjected to c. 30 km of north-south extension during the Monacobreen phase (McCann, 2000). Presently the formation constitutes several north-tilted fault blocks. These structures are related to left-lateral strike-slip movement between the RFZ and a now hidden fault to the east (McCann 2000). Following the extensional event, the Red Bay Group was subjected to basin inversion and folding, an event also affecting the underlying Siktefjellet Group.

The Svalbardian phase

The uppermost ORS unit, the Andreè Land Group, is exposed in a large basin now bounded by the Billefjorden fault zone in the east and the Breibogen-Bockfjorden fault zone in the west (figure 2.8). The Breibogen-Bockfjorden fault is not exposed south of Holtedalfonna (approximately where the solid line ends in figure 2.8). South of here the Andreè Land Group is unconformably overlaying crystalline basement rocks (Andresen, pers. comm). The total thickness of the deposits reach 4-5 km (Friend and Moody-Stuart, 1972). After deposition the basin was subjected to a deformation event named the Svalbardian (Vogt, 1938), which inverted the entire ORS basin. The upper limit of this deformation is given by the age of the lowermost post-deformation deposits which are Lower Carboniferous (Tournisian to Visean) in age and belong to the Billefjorden Group (Piepjohn et al., 2000a,b). The deformation is related to movements on the Billefjorden fault which juxtaposes ORS-rocks with Precambrian rocks of the Ny Friesland terrane and Piepjohn, (2000a,b) also infers Svalbardian deformation in the basement rocks in north-western Spitsbergen, outside of the ORS basin (and west of the BBFZ).

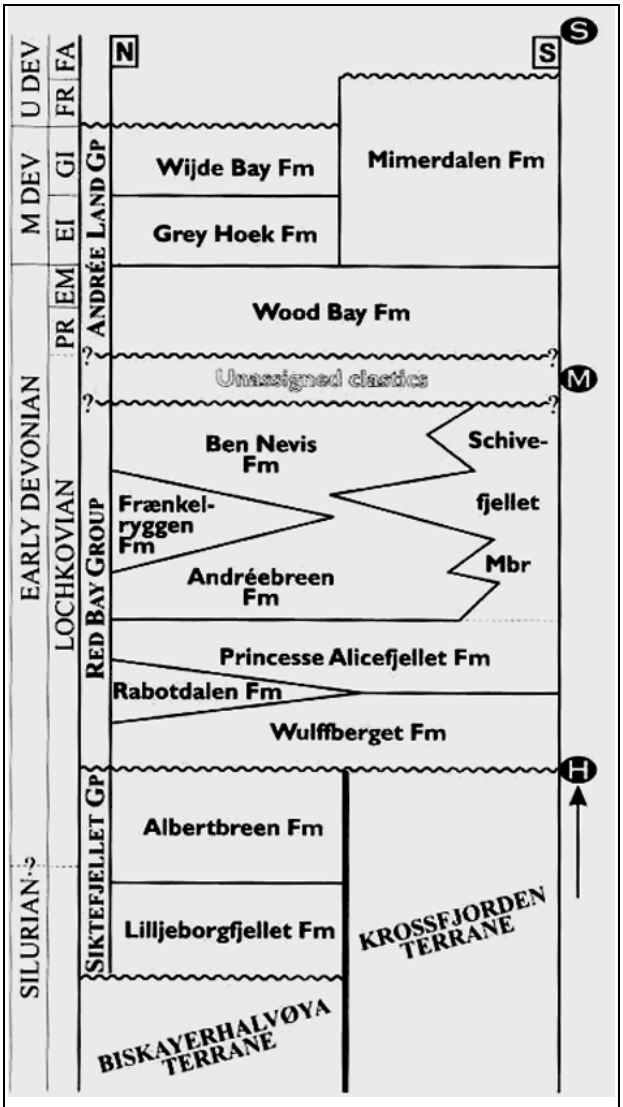

Figure 2.9 Stratigraphic scheme for the Old Red Sandstone of Spitsbergen: H=Haakonian, M= Monacobreen, S=Svalbardian deformation phases. From McCann,(2000).

Chapter 3: Geology of the study area.

This study encompasses the metamorphic rocks north of Kongsfjorden in Western Spitsbergen, which make up the North-Western Block of Svalbards Western Terrane (chapter 2). The study area spans some 100 km north-south and 30-40 km east-west, and fieldwork and sampling was concentrated in 3 main areas: The Kongsfjorden and Krossfjorden areas in the south and Smeerenburgfjorden area in the north. In the two southern areas the dominating lithologies are Proterozoic metasediments, migmatites and Caledonian grey granitoids. Further north, the lower-grade metasediments are absent and the Smeerenburgfjorden area is dominated by high-temperature metamorphic, partially migmatitic lithologies, Caledonian grey granitoids and a major Caledonian batholith, the Hornemantoppen batholith.

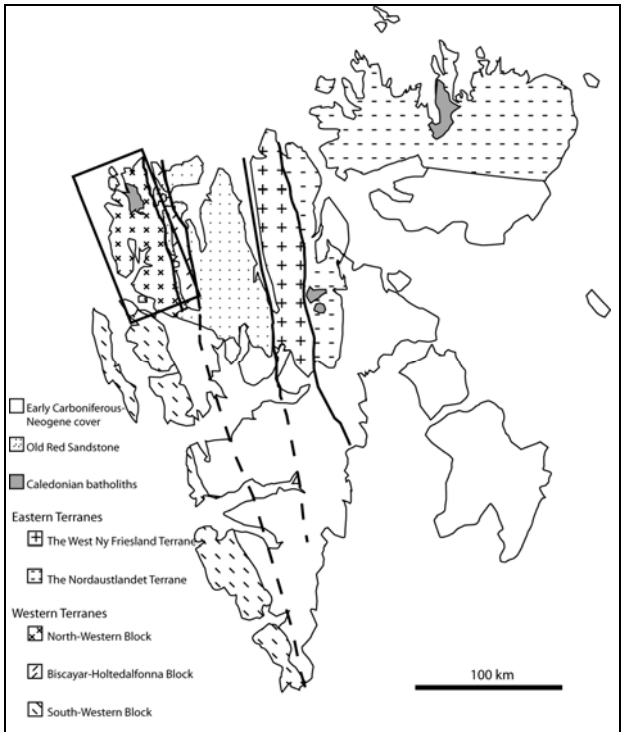

Figure 3.1: Location of the study area marked by black frame.

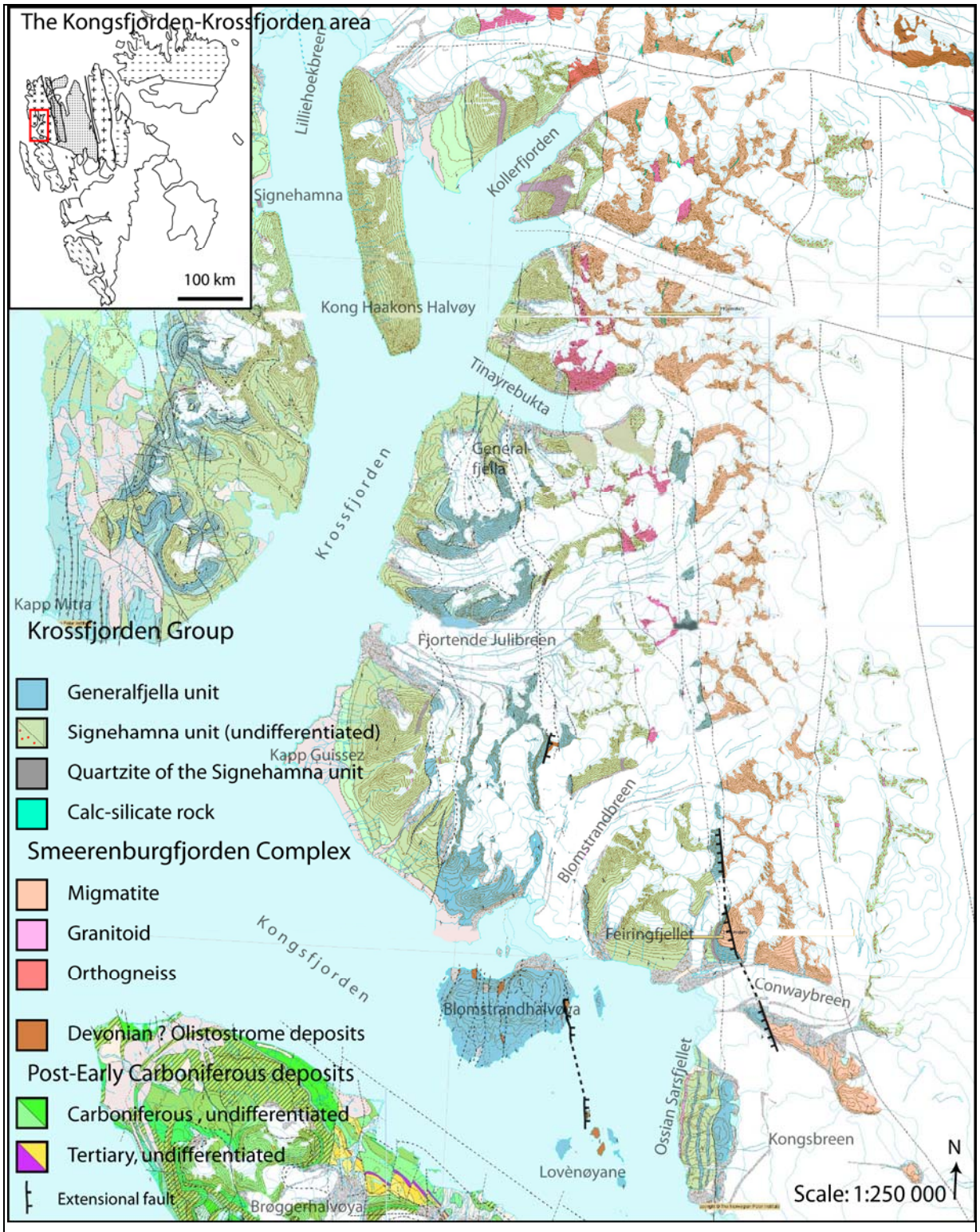

Figure 3.2: Geological map of the southern part of the study area; Kongsfjorden and Krossfjorden areas. Modified from the Norwegian Polar Institute (http://npolar.no).

3.1: The Kongsfjorden area

Near perpendicular to the strike, the north shore of Kongsfjorden constitutes a c. 20 km long cross section (figure 3.3, 3.4) comprising metasedimentary rocks of the Signehamna and Generalfjella units and undifferentiated migmatites of the Smeerenburgfjorden Complex (chapter 2).

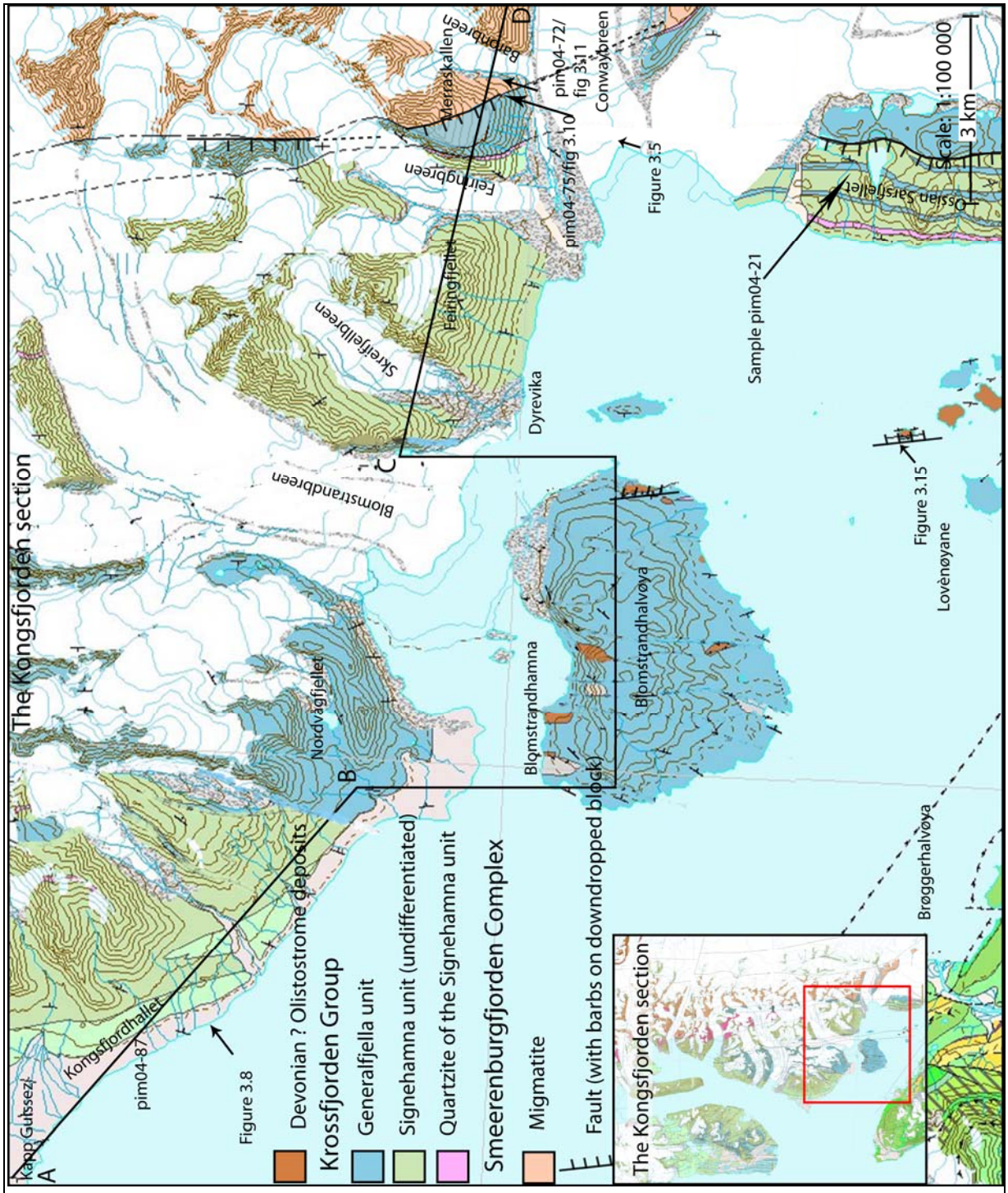

Figure 3.3: Geological map of the Kongsfjorden area. Inset map shows location of main map Sample localities are indicated as well as bearing and locality of photos. Trace of cross section (figure 3.4) is indicated by solid line. Verified faults are marked. Modified from the Norwegian Polar Institute (http://npolar.no)

Structure of the Kongsfjorden area

Two structural elements dominate the outcrop pattern in the Kongsfjorden area: Large-scale west vergent folding and the Merraskallen and related faults.

The large-scale folding style is illustrated in figures 3.4 and 3.5. It affects the Kollerfjorden Group rocks but not the Smeerenburgfjorden Complex migmatites, which are largely unfolded except for the melanosomes/xenoliths. The dominating fabric in the pelites is S_1 axial plane cleavage (trending upper left to lower right in figure 3.7) associated with the D_1 phase. The S_0 compositional banding is subparallel to S1 in most cases (illustrated in figures 3.4 and 3.8). The thin section in figure 3.7 is a case where the S_1 and S_o are not parallel (S_0 trends horizontally from left to right). An S_2 crenulation cleavage is present in some localities.

The Generalfjella marble and the rest of the Krossfjorden Group sits in the hanging wall of the extensional Merraskallen fault (figures 3.4, 3.5). The rocks in the footwall are migmatitic and have a Caledonian age of metamorphism of c. 420 Ma based on monazite (chapter 4). The faulted nature of the contact between marbles and migmatite is evident from brecciation in the marbles in the hanging wall (figure 3.6) and an east-dipping fabric in the migmatitic Smeerenburgfjorden Complex in the foot wall (figure 3.10). The Smeerenburgfjorden Complex rocks are intensively oxidized near the fault, probably as a result of fluids penetrating the permeable fault zone. A few kilometres to the south, on Ossian Sarsfjellet (figure 3.3) the shear zone continues in the marble which is brecciated and have a west-dipping fabric due to drag. The fabric indicates a down-to-the west relative motion. These faults are subparallel and along the strike of the Tertiary Pretender fault further to the south, which is an west-dipping extensional fault that displaces Devonian and Carboniferous rocks unconformably overlaying basement rocks similar to the Smeerenburgfjorden Complex (Welbon and Andresen 1992).

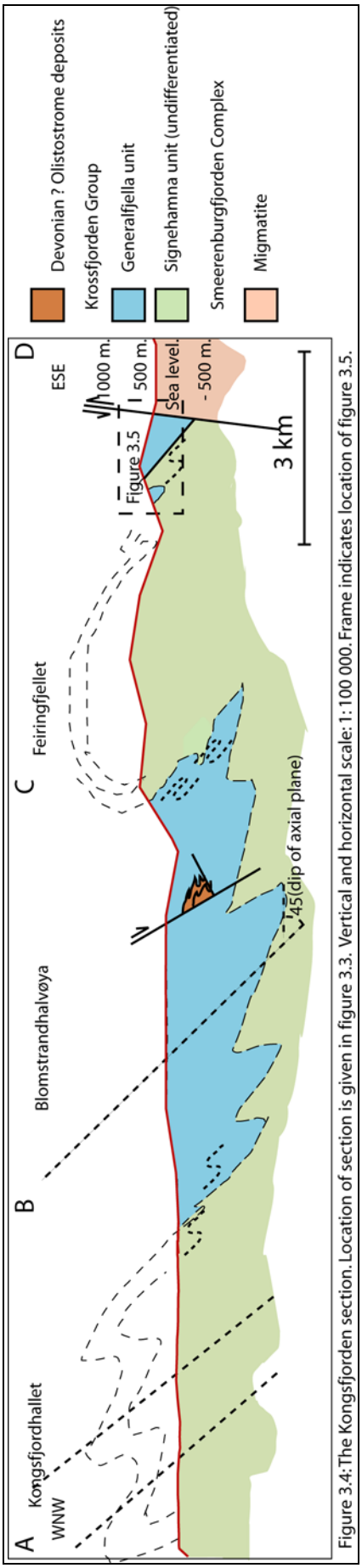

Figure 3.4: The Kongsfjorden section. Location of section is given in figure 3.3. Vertical and horizontal scale: 1:100 000. Frame indicates location of figure 3.5.

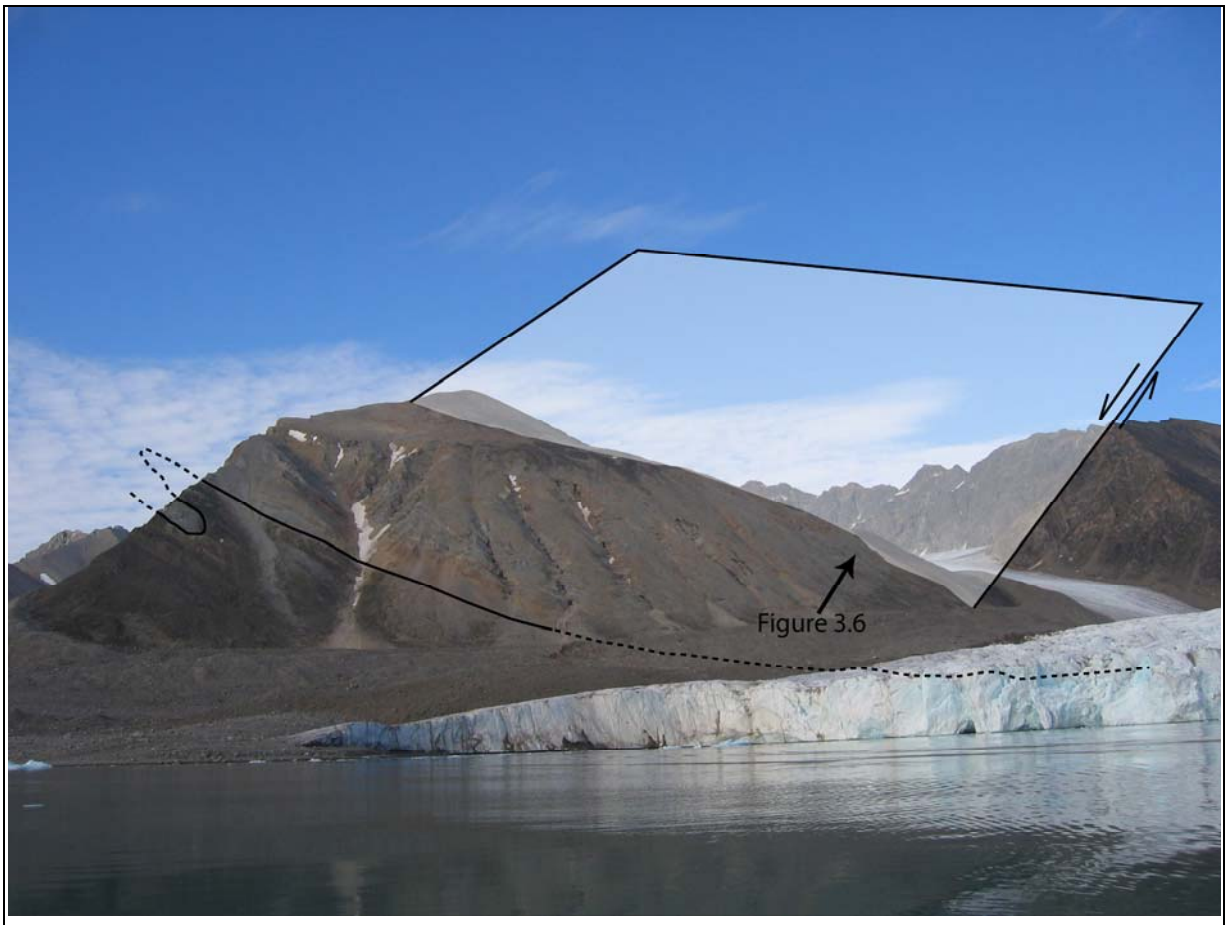

Figure 3.5 The mountain Merraskallen in the inner parts of Kongsfjorden. The glacier running into the fjord is Conwaybreen. Location of photo is indicated in figure 3.4. The folding style and the orientation of the Merraskallen fault are illustrated. View towards north-east. Lithologies are from left to right: Signehamna unit pelitic schist (dark foliated rock), Generalfjella unit marble (light grey) and Smeerenburgfjorden Complex migmatite (dark, massive rock). Arrow indicates location of brecciated marble (photo below).

Figure 3.6: Marble breccia near the Merraskallen fault. Note red colour caused by oxidation. C. 5 cm wide compass for scale. Location is indicated on figure 3.5 (above).

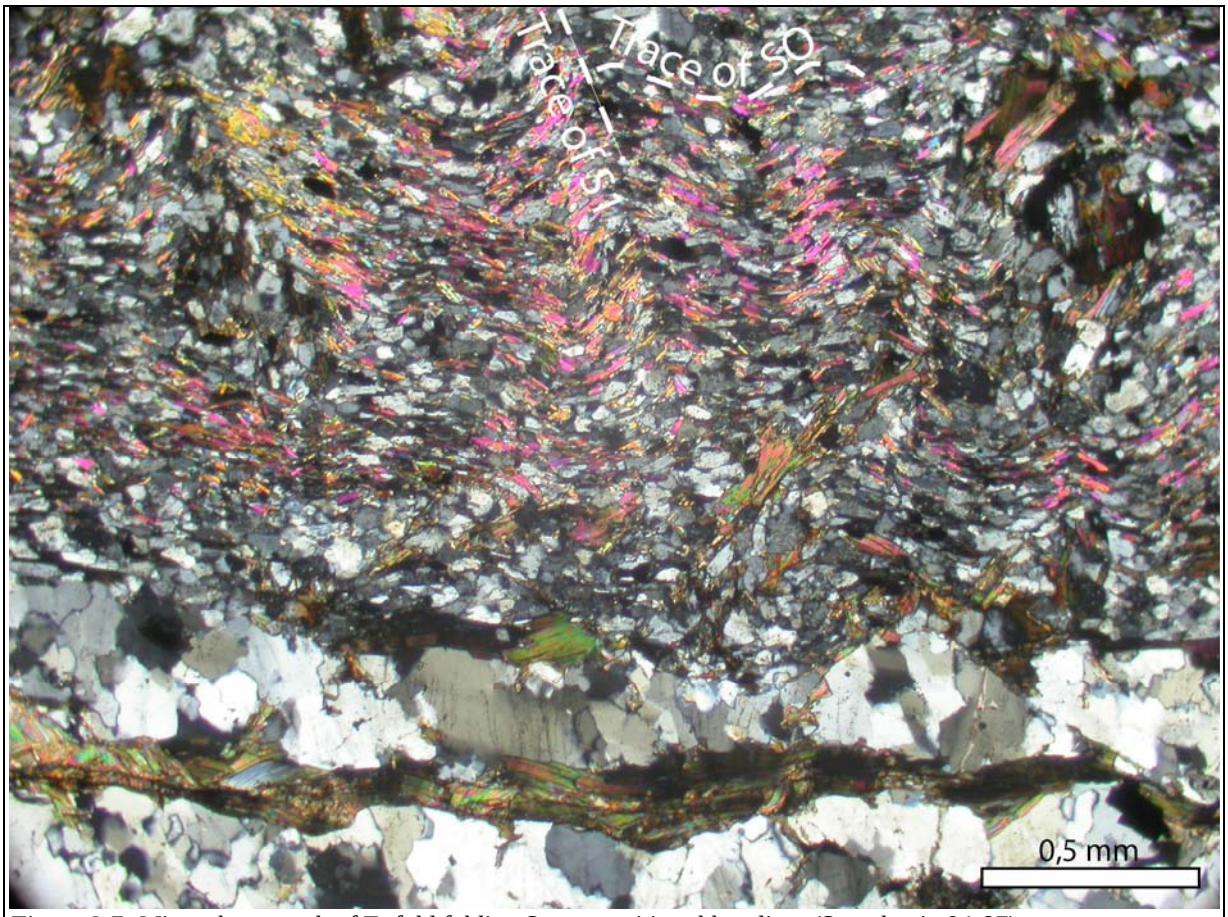

Figure 3.7: Microphotograph of F_1 fold folding S_0 compositional banding. (Sample pim04-87)

Figure 3.8: F_1 ptygmatic fold folding a quartz band in pelitic schist. Axial plane is parallel to S_0 and dips east c. 50° at this locality (Kapp Guissez). 5 cm wide compass for scale.

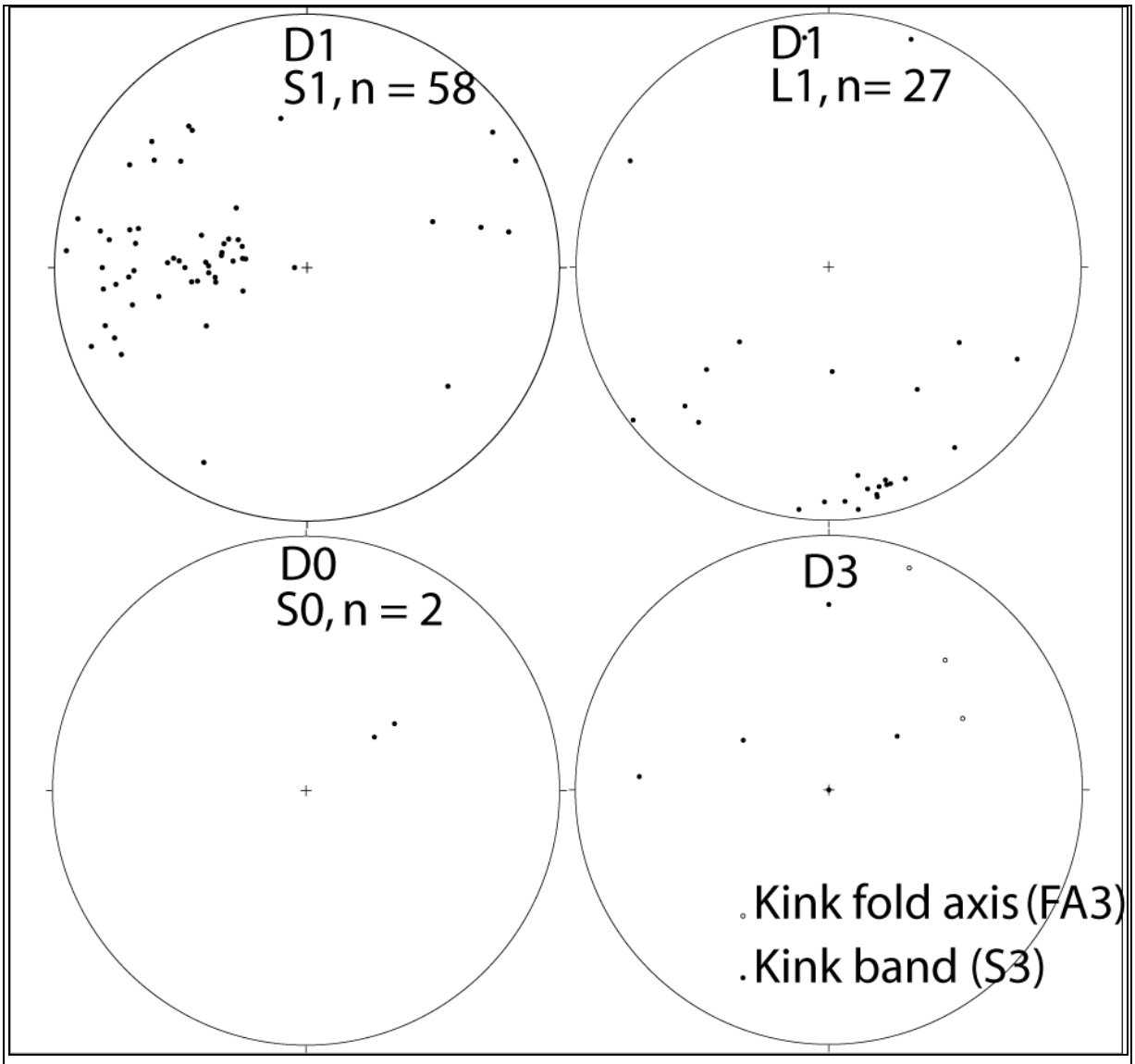

Figure 3.9: Structural elements, Kongsfjorden area.

Smeerenburgfjorden Complex

Field descriptions

In the inner part of Kongsfjorden crystalline rocks of the Smeerenburgfjorden Complex (Dallmann et al., 2002) are in fault contact with the meta-supracrustal Generalfjella marbles in the west (Dallmann et al., 2002). There are different interpretations of the nature of this fault (Dallmann et al., 2002; Hjelle et al., 1999), but here it is interpreted to be a west-dipping top to the west extensional fault (figure 3.5). The eastern margin of the Smeerenburgfjorden Complex is defined by the Raudfjorden fault, which is an east dipping extensional fault that sets the complex in contact with rocks of Signehamna unit (Dallmann et al., 2002).

Near the contact to the marble the gneiss has a distinct, east-dipping foliation. The characteristic red colour is due to intensive limonitization (figure 3.10). Paralleling the foliation are lenses of quartz/feldspar in between layers of micas, often green chlorite. The lenses are up to 10 cm long, and are often elongated parallel to the foliation (fig 3.10).

Figure 3.10: Limonitized gneiss from the inner part of Kongsfjorden. View towards north-east, 10 cm long compass for scale.

Further to the north-east the rock is migmatitic, with a distinct, little deformed granitic leucosome mixed with melanosome of quartzofeltspatic and biotite-rich nature. By appearance these enclaves may resemble either igneous gneiss or folded metasedimentary lithologies. The leucosome to melanosome ratio varies throughout the area, and in some localities the rock is dominated by granitic leucosome with minor mafic schlieren (figure 3.11) and in other localities the leucosome is only seen as thin bands paralleling or crossing the compositional banding of the melanosome.

Figure 3.11: Granitoid leucosome with biotite-rich schlieren. Photo from the inner part of Kongsfjorden, c. 200 meters east of the Merraskallen fault. View towards east. Compass for scale.

Krossfjorden Group

The metasedimentary rocks north of Kongsfjorden are assigned to the Krossfjorden Group by (Dallmann et al., 2002). The 2 major units are Signehamna unit (mainly schists) and Generalfjella unit (mainly marbles).

Pelitic schist

The pelitic schist was assigned to the Signehamna unit by Gee and Hjelle, (1966). It occurs both interlayered with marble and as homogenous units covering large areas. The schist often contains quartz lenses that occur parallel to the foliation and is part of the compositional banding. In the western part of the Kongsfjorden section, towards the core of an antiform, the mica schist is garnet bearing. The garnet porphyroblasts are 2,5- 5 mm across, and often rimmed by calcite. The garnet mica schist contain around 50 % quartz that occur in 2 settings: as folded ribbons 0,5 - 2.5 mm thick consisting of pure quartz and in the mica-dominated very fine-grained matrix. Micas constitute c. 25 % of the rock of which biotite is c. 10 % and muscovite c. 15 %. Calcite, chlorite, feldspar and zircon occur in minor amounts. The compositional banding is folded in tight folds on the centimetre scale (figure 3.8, 3.7). A later phase of deformation caused a crenulation cleavage to develop (fig 3.12).

Figure 3.12: Field appearance of pelitic garnetiferous schist of the Signehamna unit. Note the S_1 axial plane cleavage (subparalell S_0 compositional bedding) trending from upper left to lower right and the near-vertical S_3 crenulation cleavage. View towards north. Location: Kongsfjordhallet. 10 cm long compass for scale.

Marbles

The marbles within the Krossfjorden Group are broadly assigned to the Generalfjella unit and are overlaying the pelitic Signehamna unit. The units are folded in west vergent assymetric folds with wavelengths 2-3 km, and the marbles generally occur in the synform areas (figure 3.4). The largest continuous outcrop of marble is from Blomstrandhalvøya and northwards along strike to Tinayrebukta (figure 3.2). They also occur in the eastern limb of the Feiringfjellet-Ossian Sars antiform in eastern Kongsfjorden (figure 3.2, 3.3, 3.4) and on Mitrahalvøya in the west (figure 3.2).

In the inner parts of Kongsfjorden marbles occur as beds 5 m to more than 50 m thick interlayered with pelitic rocks. The bedding is commonly defined by bands of impurities of silicate phases. The modal content of silicates is between 5-30 %.

Merraskallen:

One medium grained sample from near the contact between the Generalfjella marbles and the migmatitic gneiss of the Smeerenburgfjorden Complex (figure 3.3) contains 5-10 modal-% silicates. These fragments occur in 0.1-1 mm large aggregates consisting of clay minerals and quartz. Quartz often occurs in bands parallel to the foliation, which is E-dipping.

Ossian Sarsfjellet

Ossian Sarsfjellet lies in the innermost part of Kongsfjorden, isolated from the other outcrop areas by glaciers and sea (figure 3.3). Beds of marble and pelitic schist alternate, with thicknesses from 5 to more than 50 m. The beds form the eastern limb of a west-vergent anticline and are generally east-dipping. One sample contains c. 20 modal-% silicates , and the phases present are calcite (20-50 %), dolomite (20-50 %), tremolite (20 %) quartz (<1 %) and fine-grained clay minerals. The 1-2 cm long silicate aggregates parallel the foliation. Tremolite occur as porphyroblastic, 0,5 - 0,4 mm long subhedral grains in the fine grained carbonate matrix (figure 3.13).

Blomstrandhalvøya marbles

The Blomstrandhalvøya marbles form a homogenous body of marble covering several km^2 generally with little impurities.

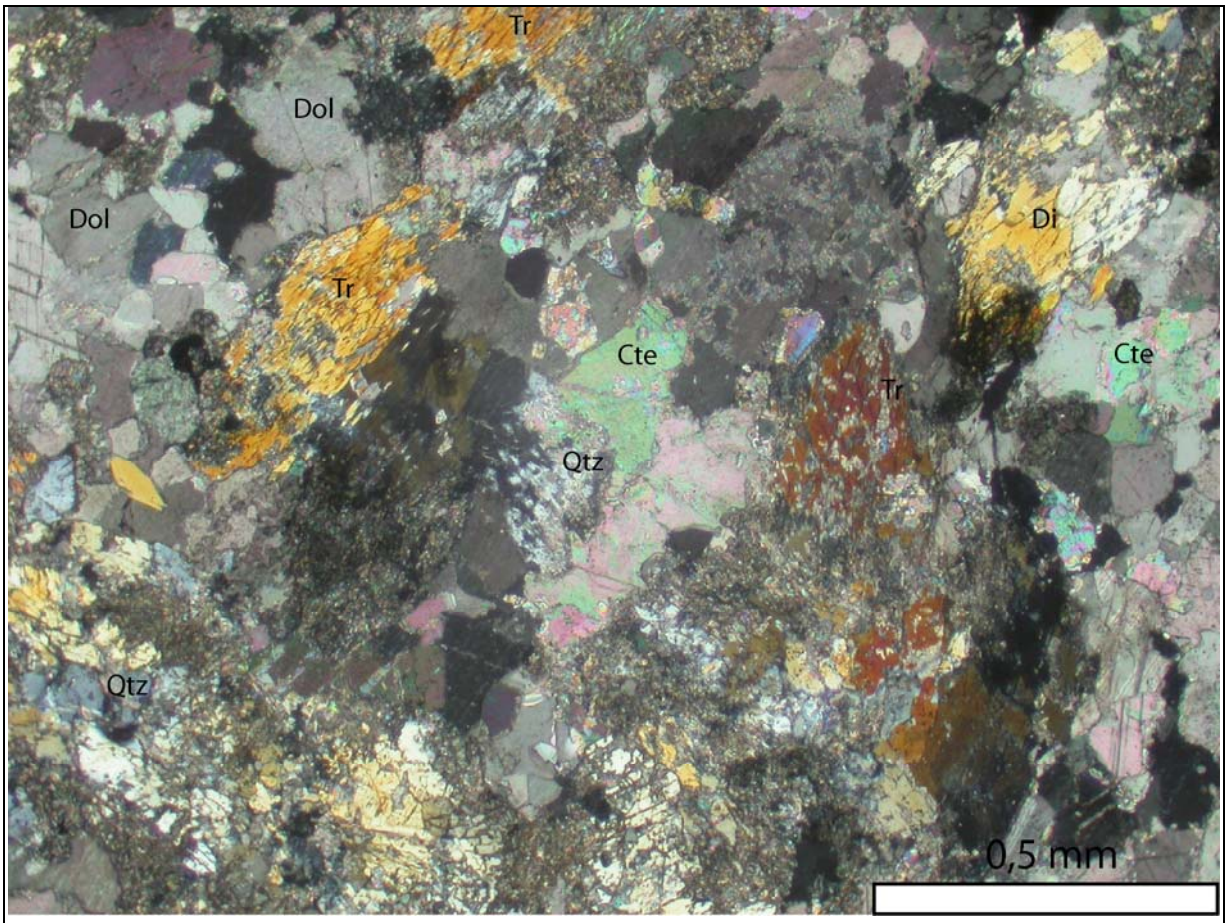

Figure 3.13: Microphotograph under crossed nicols of the mineral assemblage of the impure marble (sample pim04-21) described above. Abbreviations: Cte: calcite, Dol: dolomite, Qtz: quartz, Tr: tremolite.

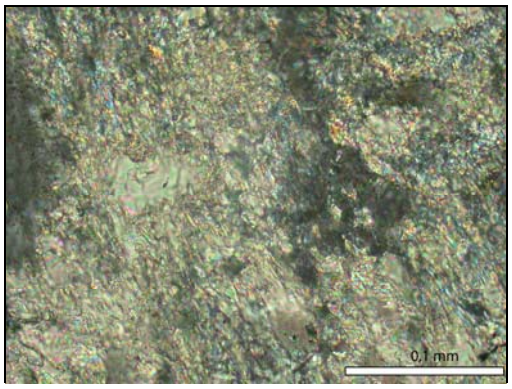

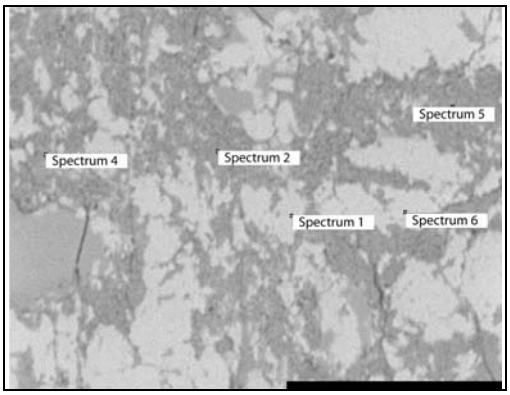

Figure 3.14: Magnified tremolite prophyroblast and calcite. Left: Petrographic microscope photo, crossed nicols. Right: SEM backscatter image, length of scale bar is 0,1 mm. Qualitative (EDX) analyses of the points indicated are given in table 3.1.

Spectrum #	O	Mg	Si	Ca	Phase:
Spectrum 1	39	4	3	38	Cte
Spectrum 2	38	16	28	7	Tr
Spectrum 3	37	17	28	8	Tr
Spectrum 4	37	16	27	7	Tr
Spectrum 5	37	15	28	9	Tr
Spectrum 6	40	3	3	40	Cte

Table 3.1 Semiquantitative abundances of elements based on EDX-spectra from SEM. All values in percent, uncertainties are c. 5 %..

Olistoliths

In the islands in Kongsfjorden and on Løvlandfjellet (figure 3.2, 3.3, 3.4) further north there are some occurences of olistolith deposits. The deposits are coarse-grained carbonate-rich sandstones, carbonates breccias and marble olistostromes. The faults that apparently are controlling the sedimentation in these basins are east-dipping and evident from e.g. fault striae as in figure 3.15:

Figure 3.15: Fault striae on carbonate-coated fault plane within the olistoliths, Lovènøyane, Kongsfjorden. Compass for scale.

3.2: The Krossfjorden area

The Kollerfjorden section

The SW-NE-trending Kollerfjorden lies in the innermost reaches of Krossfjorden. The northern shore comprises a c. 7 km long section perpendicular to the strike consisting, from SW to NE, of mica schist, orthogneiss and migmatite. The inner part, close to the retreating Kollerbreen glacier, has good exposures along the shore.

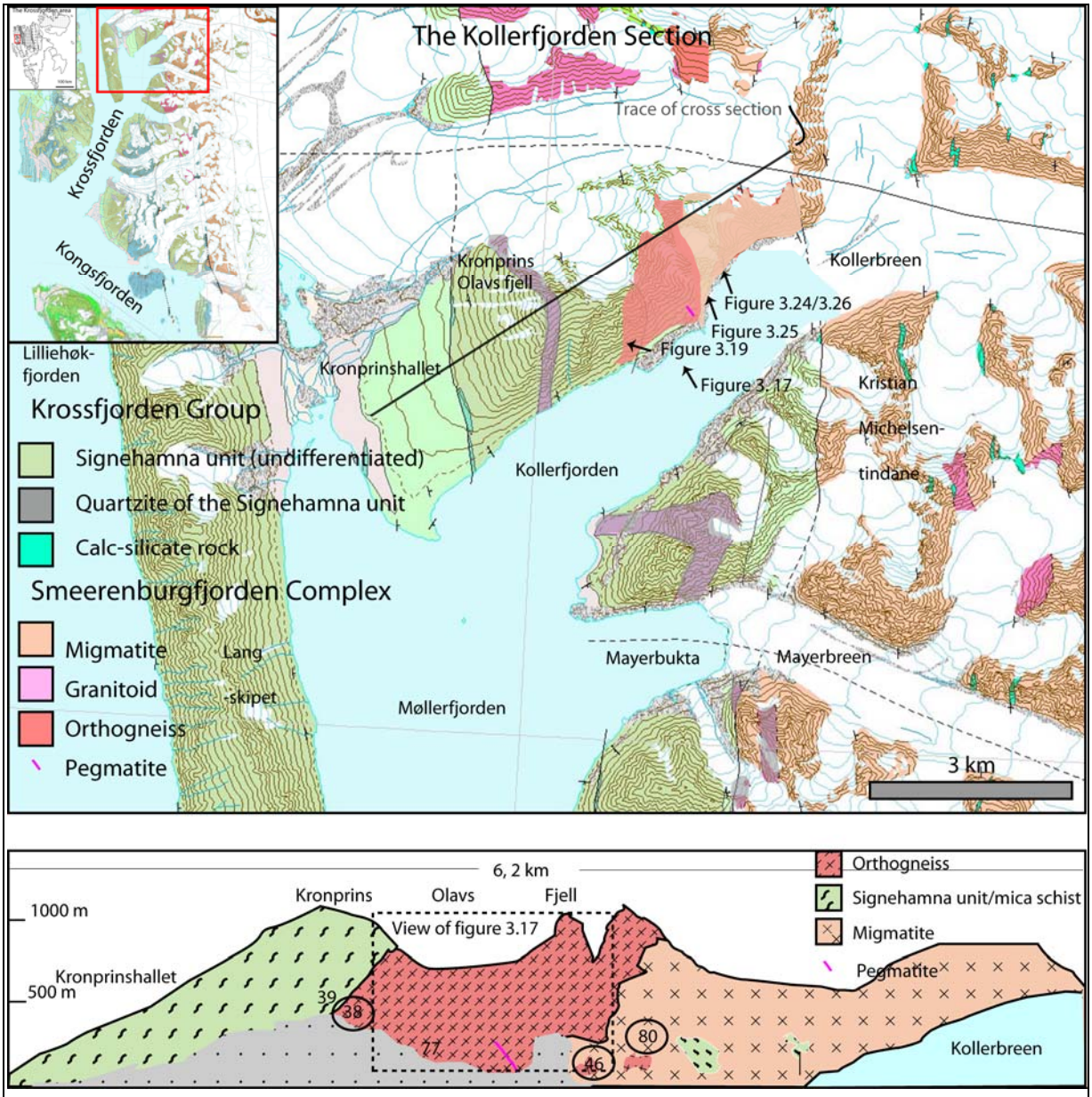

Figure 3.16: The study area in Kollerfjorden. Arrows indicate locality and bearing of photos. Numbers indicate sample locations as referred to in the text. The trace of cross section is given by black line on map. No vertical exaggeration. Map modified from the Norwegian Polar Institue (http://npolar.no).

Figure 3.17: View of Kong Olavs fjell, part of the Kollerfjorden section. The peak to the right is c. 800 meters high.

Mica-schist

Pelitic schist of the Signehamna unit occupies the eastern part of the section. It contains quartzitic lenses ranging in size from a few centimetres to several meters. The lenses are elongated parallel to the schistosity, which is south-west dipping.

The fine grained mica schist consists of c. 30% biotite, 30% muscovite, 30 % quartz, 10% plagioclase and minor amounts of pyrite and radioactive minerals such as zircon. The compositional banding is defined by alternating quartz and mica-dominated bands. Saccharoidal quartz and tapered twins planes in plagioclase occur as results of deformation.

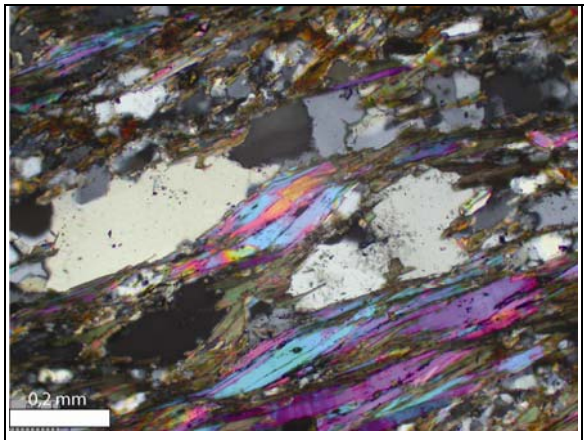

Figure 3.18: Pelitic schist, Kollerfjorden section (pim04-39) with mica fish. Dip direction is to the left, se figure 3.16 (cross section) for location of sample.

Orthogneiss

East of the mica schist c. 967 Ma (chapter 4) leucocratic gneiss crop out. The foliation has the same orientation as the mica schist (west-dipping). The contact to the schist is characterized by a gradual transition from pelitic to felsic gneiss. Xenoliths of mica schist and quartzite occur in the gneiss (Ohta et al. 2002), and suggest an igneous contact to the Signehamna unit. The gneiss is intruded by pegmatite veins that parallel the foliation in some cases and cuts it in other cases. The veins consist mostly of quartz, and contain garnet and tourmalin/amphibole.

Thin sections were prepared from two samples, one close to the mica schist (pim04-38) and the other close to the migmatites (pim04-77). The petrography of these samples is somewhat different, the eastern being slightly more felsic.

Fine grained granodioritic gneiss

pim04-38

Hornblende occurs in elongated bands that make up the foliation together with bands of quartz. On the rims and along cracks hornblende has a coating of limonite (see figure 3.21). Minor amounts of biotite occur associated with the hornblende. Feldspars are strongly sericitized, and have corroded grain boundaries. Also pyrite is affected by retrograde reactions, and is transformed into limonite.

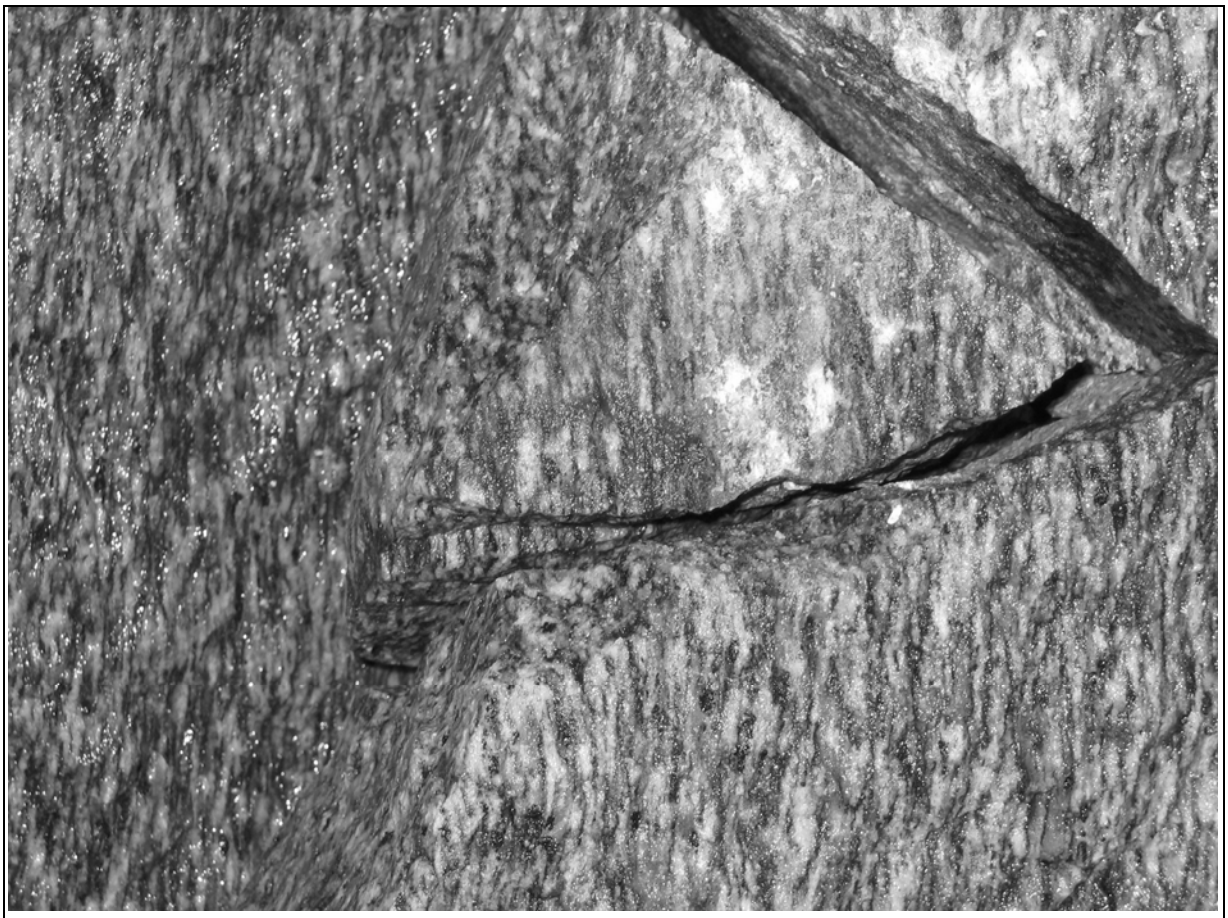

Figure 3.19: Orthogneiss as it crops out in the Kollerfjorden section. Width of photo is 10 cm. View towards north.

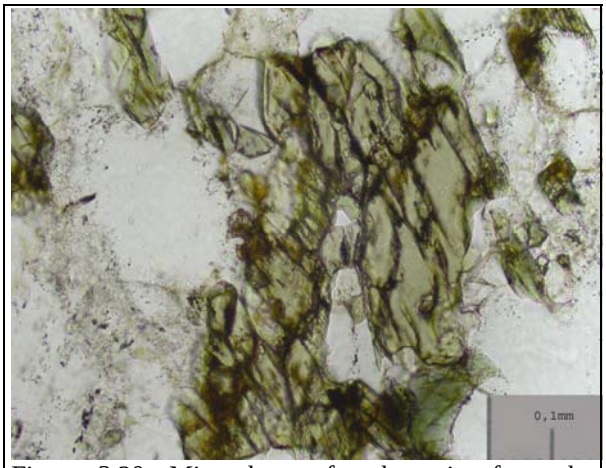

Figure 3.20: Microphoto of orthogneiss from the Kollerfjorden section showing hornblende with corroded rims surrounded by quartz and feldspars. Plane polarized light.

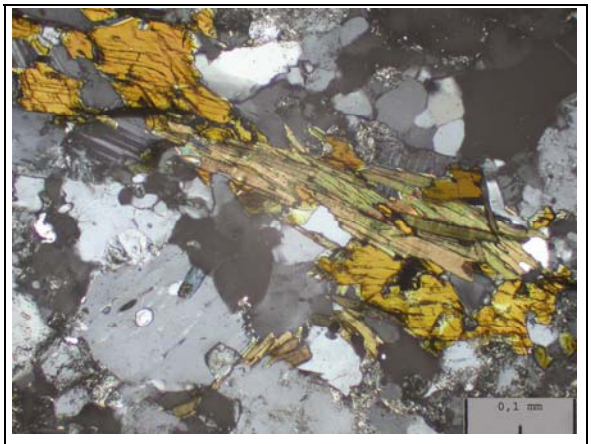

Figure 3.21: Microphoto of hornblende and biotite retrograded to chlorite. (pim04-77). Crossed nicols.

pim04-77

This sample contains the same phases as pim04-38, but significantly more biotite. The field appearance is similar, with a west-dipping foliation. The gneiss is intruded by pegmatite veins that cut the foliation. The absolute grain size is in the range 0,1-1 mm for quartz and slightly higher (0,5-0,2) for hornblende, which occur as porphyroblasts. Quartz grain boundaries are sutured. Biotite is associated with hornblende as a retrogressive phase. Together they occur as bands and porphyroblasts oriented with the long axis parallel to the foliation. Biotite is retrograded as well, and rims of grains are often occupied by green chlorite (see fig 3.21). Calcite and zircon/monazite occur as accessory phases.

	Pim04-38	Pim04-77	Pim04-80
Quartz	43 %	42 %	33 %
Plagioclase	39 %	29 %	39 %
Hornblende	14 %	5 %	-
K-feldspar	2 %	14 %	16
Biotite	<2	10 %	10
Pyrite	<1 %	-	<1
Muscovite			<1
Chlorite	<1 %	< 2%	<1
Zircon	<1	<1	<1
Monazite		<1	<1
Calcite		1	<1
Titanite	<1		-
Chalcopyrite	<1 %	-	-

Table 3.2: Point counter modal analysis of granitoids and gneisses from Kollerfjorden. 1000 counts/sample.

Migmatite

The granitic gneiss described above is intruded by a Caledonian (chapter 4) migmatitic granitoid which constitutes the easternmost unit of the Kollerfjorden section. It contains xenoliths of striped gneiss similar to the in situ gneissic rock described above (figure 3.25) as well as quartzitic and pelitic ones.

Petrology of granodioritic leucosome:

The main phases are quartz, zoned plagioclase, k-feldspar and biotite, and their respective modal abundances are given in table 3.2. Accessory phases are muscovite, chlorite, calcite, pyrite, monazite and zircon. Feldspars are somewhat altered, and occur as medium grained, tabular grains. K-feldspar is commonly acossiated with myrmekite (fig 3.22) and graphic pertites. Biotite occurs as randomly oriented laths, and is sometimes altered to chlorite. Inclusions of zirkon are common in biotite.

Figure 3.22: Microphoto, myrmekite (granodioritic leucosome, pim04-80). Crossed nicols.

Figure 3.23: Microphoto, zoned plagioclase (granodioritic leucosome, pim04-80). Crossed nicols.

Melanosome:

The melanosome consist of dark schistose rock similar to the mica schists of the Signehamna unit, and the primary banding is often folded in tight folds (figure 3.24). The banding consists mainly of alternating quartz or feldspar and biotite. The melanosome is very rich in biotite and some blocks seem to consist almost entirely of biotite. Commonly, the blocks have a leuocratic rim of feldspar and minor quartz in the contact zone with the leucosome. The blocks range in size from a few cm up to large rafts 50 meters across. The leucosome to melanosome-ratio varies on the scale of outcrops, and in some areas the granitic material is homogenous for 50`s of meters of outcrop. This sort of outcrop was chosen for sampling for dating purposes. Other outcrops are dominated by melanosome with only minor veins of leucosome, and these field appearances are indicative of an in situ migmatization (figure 3.26).

Figure 3.24: Melanosome of migmatite, eastern part of the Kollerfjorden section. Notice the folded pelitic schist with common segregations of leucosome.

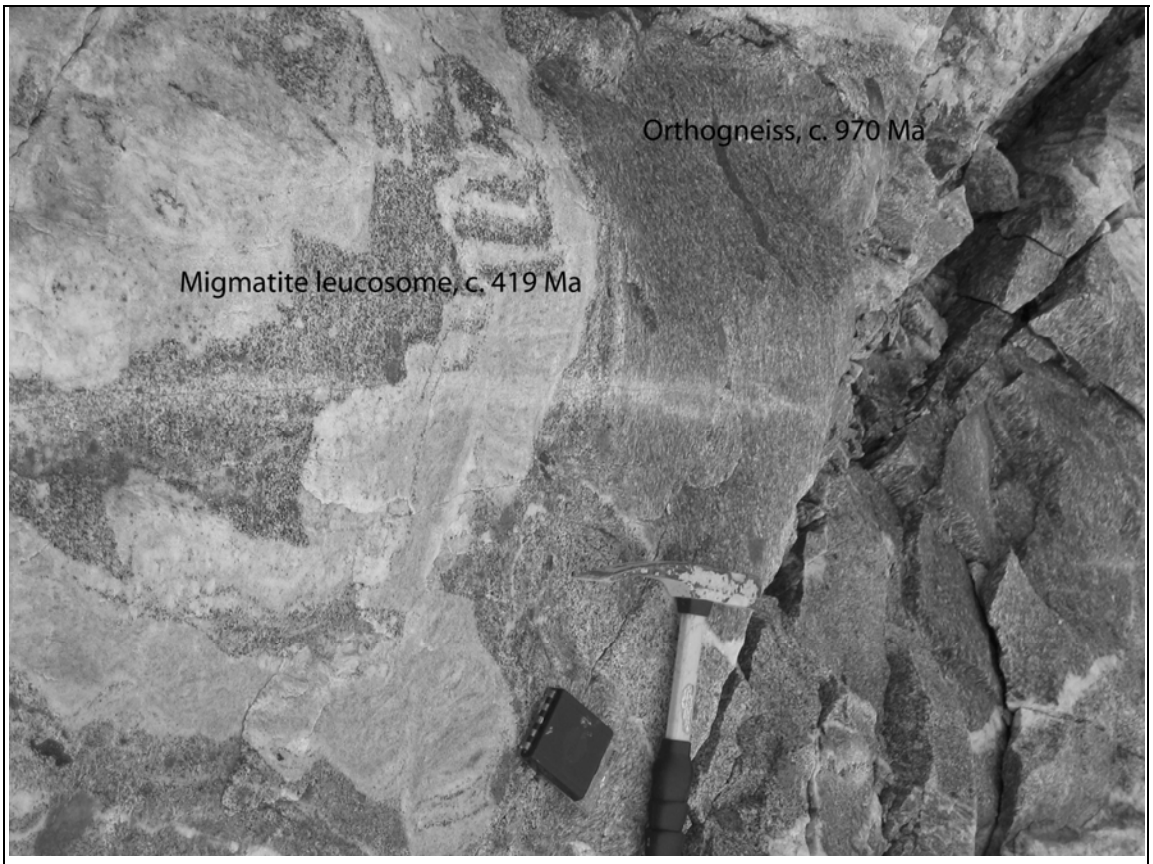

Figure 3.25: Gneissic xenolith (pim04-46-type) in Silurian neosome (pim04-80-type). View towards north. 10 cm long compass for scale

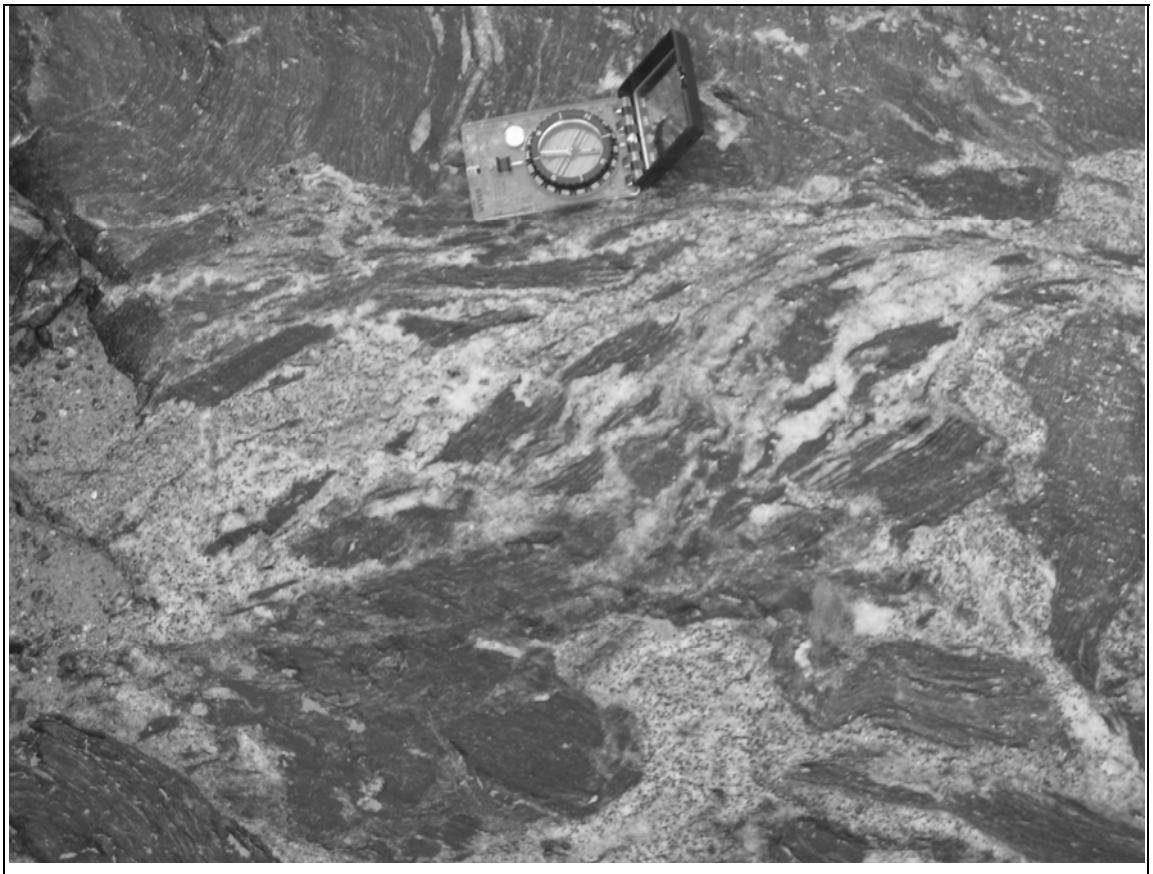

Figure 3.26: Melanosome-rich migmatitic outcrop. View towards north.

3.3: The Smeerenburgfjorden area

Introduction

The study area in the Smeerenburgfjorden area encompasses the two islands of Amsterdamøya and Danskøya and the western part of Vasahalvøya (figure 3.27). The eastern margin of the North-Western Block is represented by the Raudfjorden fault, exposed in the eastern part of Vasahalvøya (figure 3.27). The area was mapped by Hjelle and Ohta, (1974). The main geological units are a basement complex consisting of partially migmatitic para- and orthogneisses and Caledonian granitoids and a Caledonian batholith (the Hornemantoppen granitoid (Hjelle, 1979). Isotopic and geochemical work has been carried out in the area, mainly by Hjelle, (1979); Balasov et al., (1996b); Ohta et al., (2002). (See chapter 2 for a summary of the previous studies.)

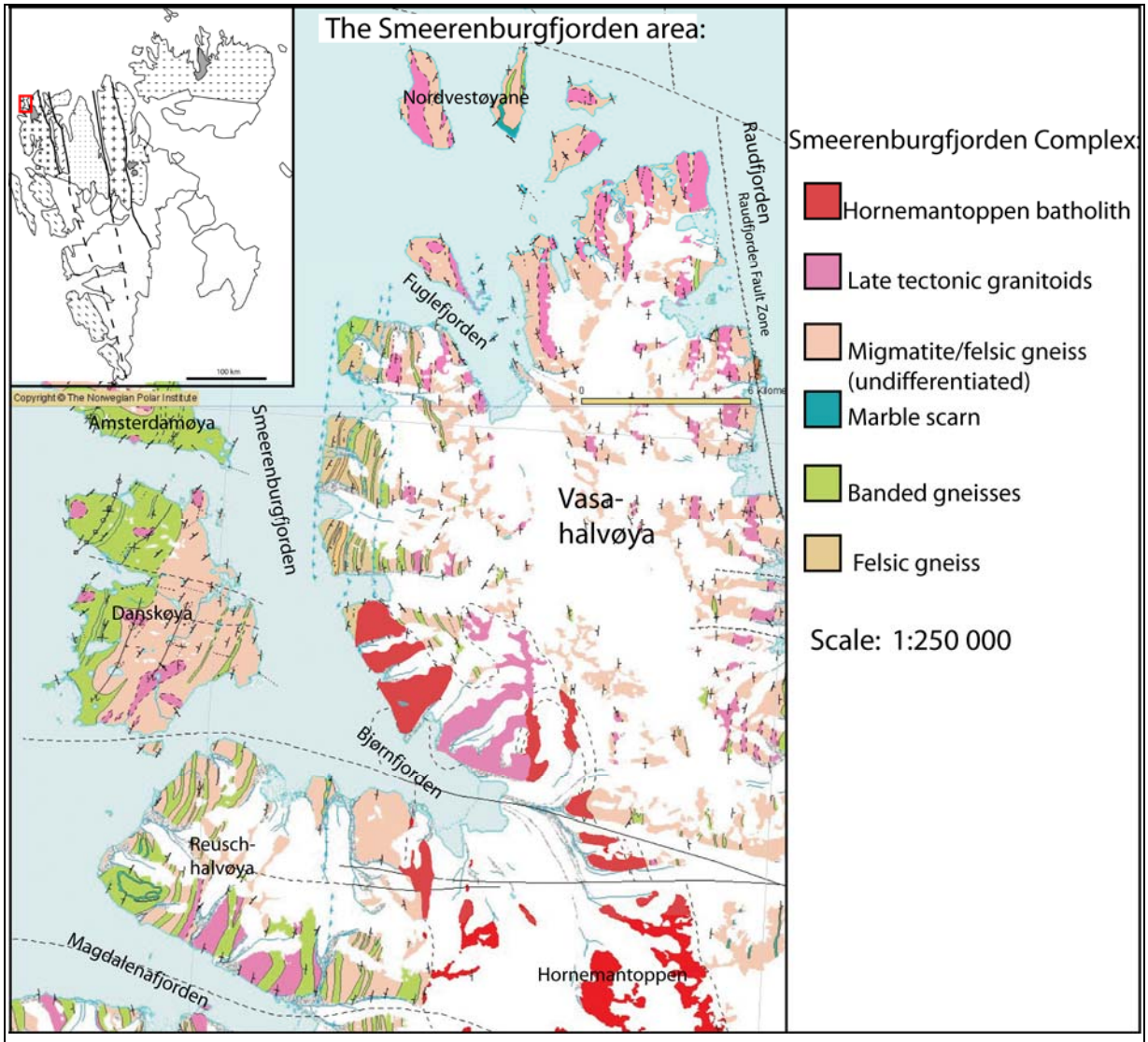

Figure 3.27: Map of the Smeerenburgfjorden area. Modified from the Norwegian Polar Institute (http://npolar.no)

Gneiss complex

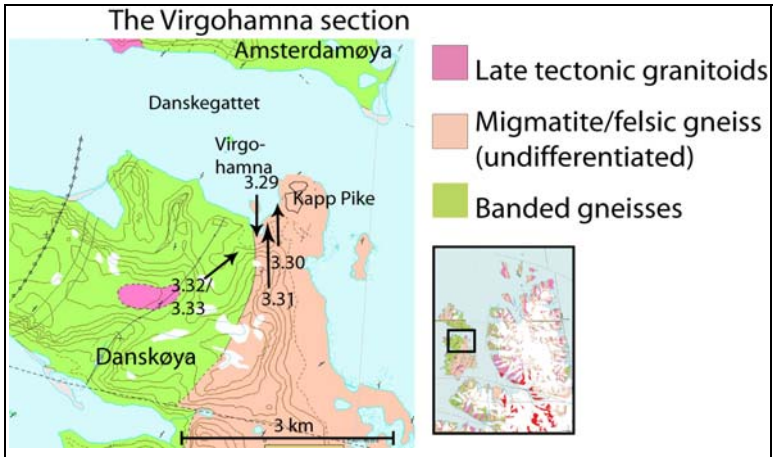

Figure 3.28: The Virgohamna area. Arrows indicate location and bearing of photos. Modified from the Norwegian Polar Institute (http://npolar.no).

Porphyroblastic felsic gneiss dominates the bedrock of a large part of Danskøya and Amsterdamøya as well as the eastern margin of Smeerenburgfjorden. It contains inclusions of various lithologies and is migmatized in some areas.

Pelitic/quartzitic xenoliths

Figure 3.29 shows an outcrop in Virgohamna, Danskøya, where the felsic gneiss contains pelitic xenoliths. Such xenoliths are often boudinaged, and the gneissocity is flexured around the enclave. In some cases the mica schist-xenoliths are garnet-bearing.

Figure 3.29: Pelitic xenolith in steeply west-dipping felsic gneiss. View towards north. 10 cm long strip for scale.

Veins and mafic lenses

The felsic gneiss is cut by at least 3 types of veins; pegmatitic, granittic and gabbroic.

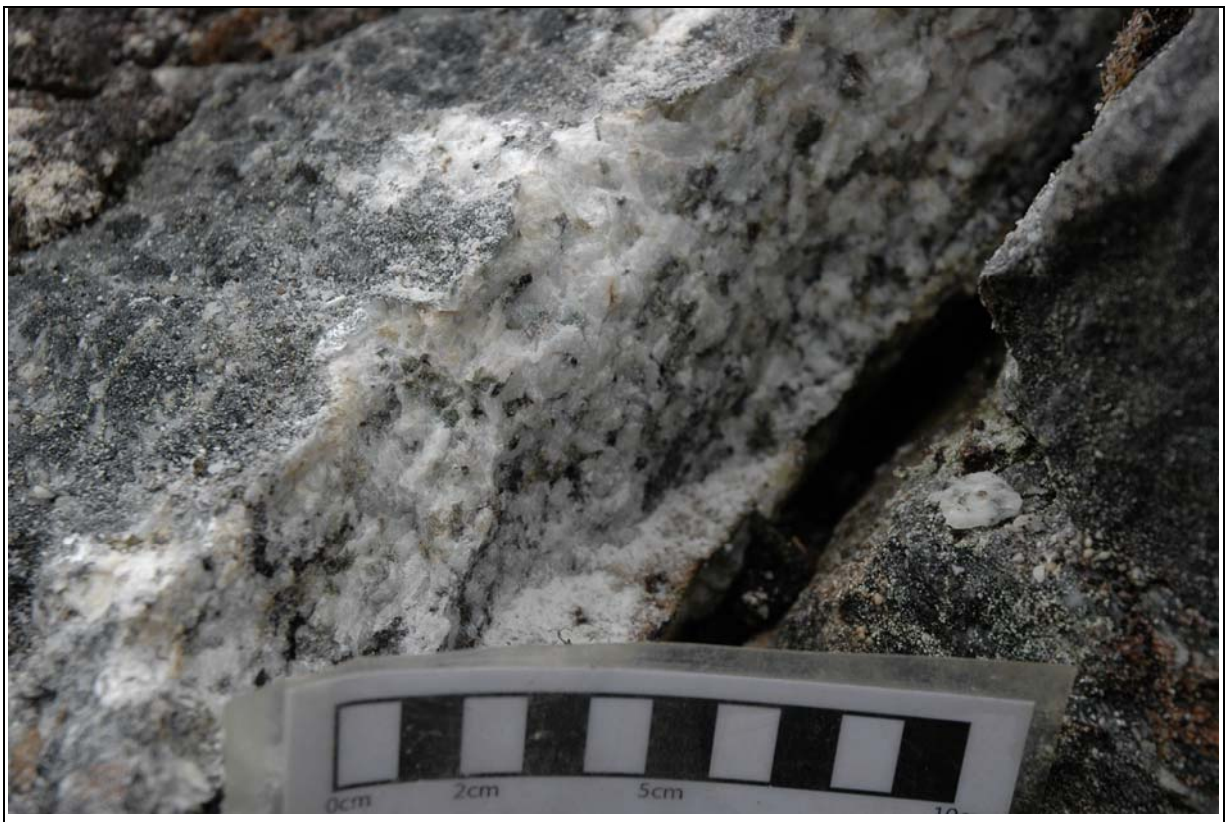

Figure 3.30: Coarse grained granitic vein cutting felsic gneiss, Kapp Pike. View towards north.

Figure 3.31: Granitic vein cutting felsic gneiss, Kapp Pike. View towards north.

Migmatized felsic gneiss

The western part of Danskøya is occupied by partly migmatized gneiss. The felsic gneiss occurs as xenoliths in pods of unfoliated grey medium-grained granitic rock. The melanosome is often rimmed by light, feldspar-rich leucosome. Both leucosome and gneiss are cut by several generations of quartz-rich to granitic veins.

Figure 3.32: Folded felsic gneiss paleosome in granitic neosome. Virgohamna section, Danskøya. View towards north-west. Hammer for scale.

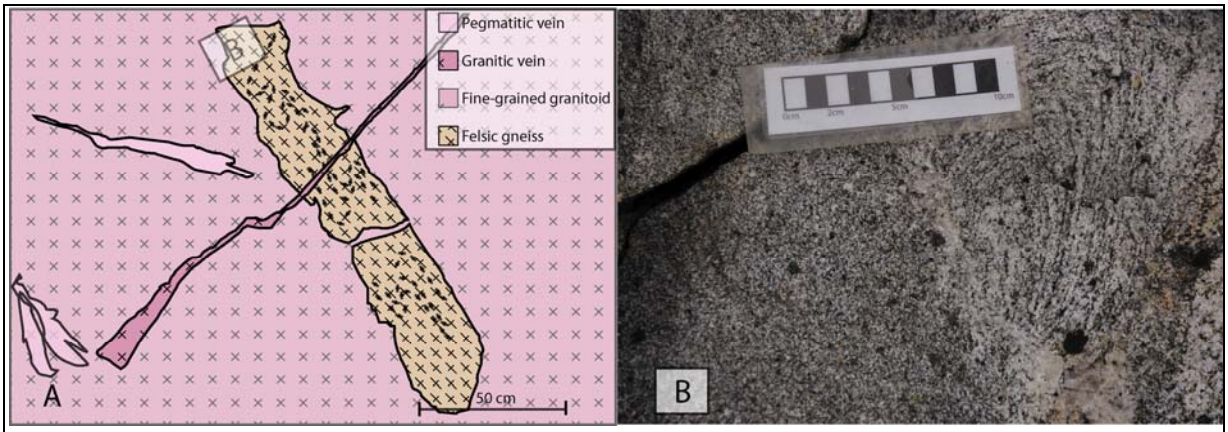

Figure 3.33: **A***: Sketch from figure 3.32 with lithologies indicated. Square in upper left indicates location of close-up photo.* **B***: Close-up on contact zone between folded felsic gneiss (right) and granitic leucosome (left).*

The Bjørnfjorden section

In the inner parts of the Smeerenburgfjorden fjord system, the Bjørnfjorden comprises a c. 10 km long section with orthogneiss, a shear zone and two Caledonian granitoids, named here grey two-mica granitoid and the Hornemantoppen granitoid, respectively.

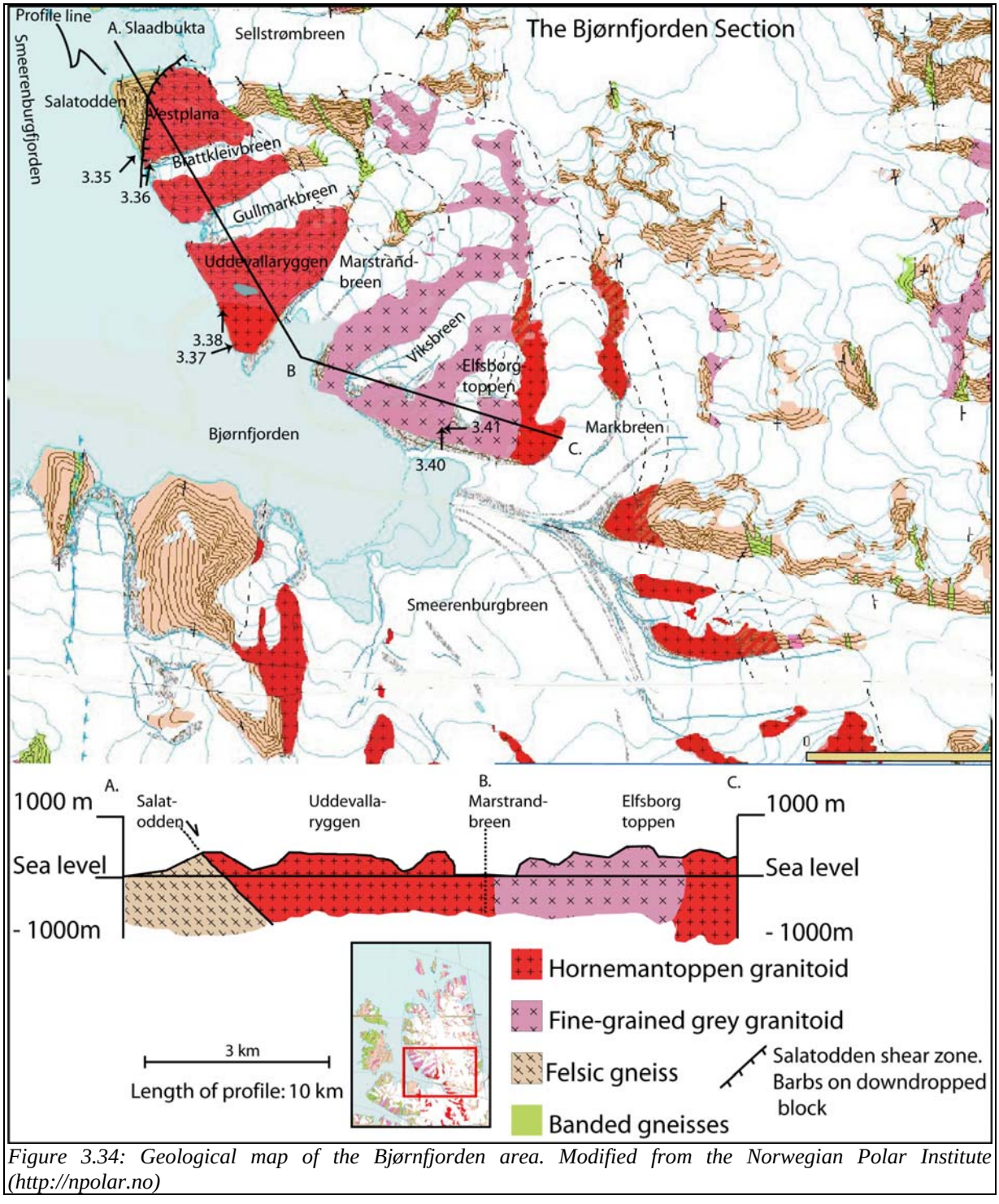

Figure 3.34: Geological map of the Bjørnfjorden area. Modified from the Norwegian Polar Institute (http://npolar.no)

The Salatodden shear zone

In the north-western part of the section, the coarse-grained Hornemantoppen granitoid is in tectonic contact with the basement gneiss complex (Ohta et al., 1996). The rocks have an east-dipping foliation that relates to deformation along the shear zone, and displays shear bands (figure 3.35), brecciation (figure 3.36) and contain ultracataclasite (figure 3.36). The shear zone strikes north-east and dips ~ 60-70^0 to the south-east. The footwall block is occupied by felsic gneiss containing pelitic inclusions (figure 3.34). The shear zone is at least 200 meters wide measured normal to the area of extensively developed mylonitization, but deformation structures like shear bands and cataclasite can also be observed outside of this zone. Presence of cataclasite and shear-bands indicate both ductile/semi-ductile and brittle phases of deformation.

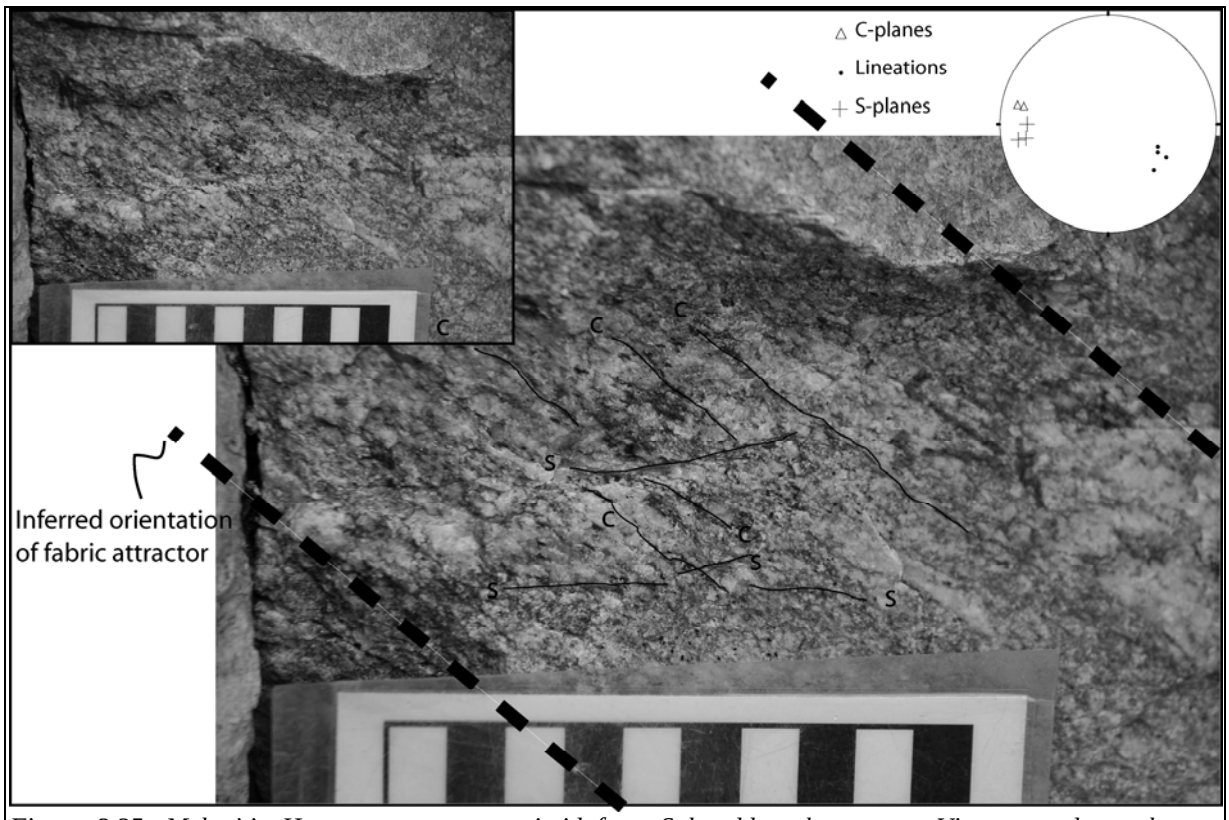

Figure 3.35: Mylonitic Hornemantoppen granitoid from Salatodden shear zone. View towards north-east. Length of scale bar is 10 cm. Inset: Lower hemisphere stereoplot of poles to S-planes (south-east-dipping), C-planes (south-east-dipping) and stretching lineations (south-east-plunging).

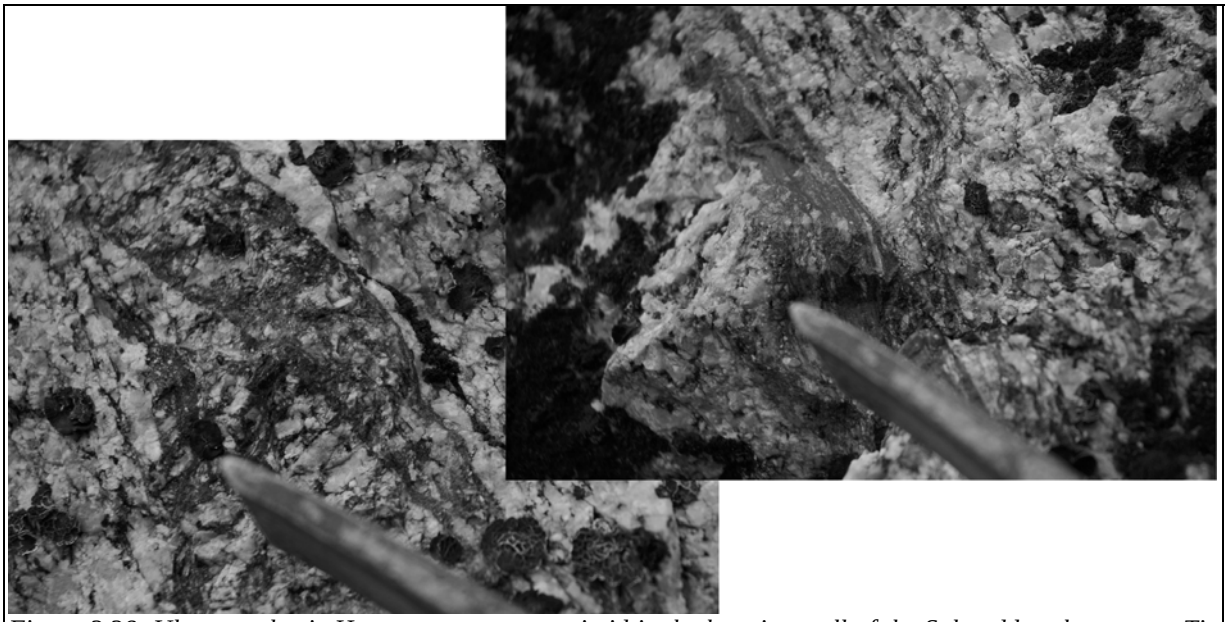

Figure 3.36: Ultracataclastic Hornemantoppen granitoid in the hanging wall of the Salatodden shear zone. Tip of hammer c. 5 cm long for scale. View towards north.

Caledonian granitoid rocks

2 types of granitic rocks can be distinguished based on field observations:

- Coarse grained, often porphyroblastic red granitoid: the Hornemantoppen batholith (Hjelle 1979)
- Fine-grained, grey granitoids

The former crops out in Bjørnfjorden and on nunataks south of Bjørnfjorden, and covers c. 150 km^2, whereas the latter type occurs as leucosome of migmatite (Amsterdamøya and Danskøya) and as a continous xenolith-rich granitoid body in Bjørnfjorden.

Coarse grained red granitoid; the Hornemantoppen granitoid

This rock is rich in K-feldspar which gives it a red colour in outcrop. It contains some felsic and pelitic xenoliths (figure 3.37, 3.38). The contact with the gneiss complex in the north-west is sheared (the Salatodden shear zone, figure 3.35, 3.36). The contact with the grey granitoid is poorly exposed in the localities visited in this study, but it is of primary intrusive nature according to previous mapping (Ohta et al., 1996). Figure 3.39 shows the undeformed nature of the rock. Near the Salatodden shear-zone the rock is more deformed, and fault gouge and an east-dipping mylonitic foliation is developed.

Figure 3.37: Felsic xenolith (centre) in coarse grained granitoid (left and right). Black square: close-up section in figure 3.38. View towards north.

Figure 3.38: Felsic xenolith (right) partly digested by the coarse grained granitoid (left). View towards north. Close-up from part of figure 3.37.

Figure 3.39: The Hornemantoppen granitoid as it crops out on the north shore of Bjørnfjorden. Sample is approximately 15 cm wide.

Fine grained grey granitoid

The grey granitoid covers 5-6 km^2 on the north shore of Bjørnfjorden (figure 3.34). It distinguishes from the Hornemantoppen granitoid in the field by the grey colour, lack of feldspar porphyroblasts and generally fine to medium-grained texture. Another contrast between the two granitoids is the large amount of pelitic, quartzitic and felsic gneiss-xenoliths in the fine-grained granitoid.

Figure 3.40: Grey granitoid as it crops out near Elfsborgtoppen, Bjørnfjorden. Notice the xenolith in the upper left. View towards north. Geologist is Endre Bergfjord.

Figure 3.41: Close-up of folded pelitic inclusion. View towards west. 10 cm long strip for scale.

Chapter 4: U/Pb-chronology; results and interpretation of data

Introduction

8 granitoid samples were dated by the Isotope Dilution–Thermal Ionization Mass Spectrometry (ID-TIMS) dating technique. All sample preparation and analytical work was done in the laboratory facilities of Institute of Geosciences, University of Oslo in September 2004, February-April & Oktober-November 2005. Below are methodology and results of the work.

4.1: Analytical procedure

The samples, weighing around 1 kg, were crushed in a jaw-crusher and milled down to < 0,3-0,5 mm particles in a Retsch crusher. Mineral separation was then carried out using a Wilfley table, Frantz magnetic separators, and finally heavy liquid (DJM, Di-Jod-Methane) flotation.

Mineral grains for analysis were picked in alcohol under a binocular microscope and air-abraded using the method described by Krogh, (1982) to remove material unsuited for analysis. Most mineral samples were photographed using a digital camera attached to the microscope. Phases used for age dating included zircon, titanite and monazite. The mineral samples were washed in HNO_3, H_2O and acetone and ultrasonicated to remove any contamination, weighed on a microscale, spiked and put in Teflon bombs (zircon) or Savillex vials (titanite and monazite). Most samples were spiked with a mixed ^{202}Pb-^{205}Pb-^{235}U tracer, except some grains from samples pim04-80, Newtontoppen, pim04-72 and pim04-75, which were spiked with a mixed ^{205}Pb-^{235}U tracer. The double Pb tracer allows the source fractionation during measurement to be determined, and this value is incorporated into the error calculation for better precision. The zircon was dissolved in HF in the Teflon bombs at 180°C for 5 days. Titanite was dissolved in HF + HNO_3 in the Teflon Savillexes on a hotplate for 5 days. Monazite was dissolved in 6N HCl.

Zircon samples weighing >0,005 mg and all titanite and monazite samples were chemically separated using microcolumns and an ion exchange resin as described in Corfu and Stone, (1998). The solution, once in the column, was treated with HCl (zircon and monazite) and a mixture of HCl and HBr (titanite) to retain U and Pb in the resin, which was subsequently washed out using H_2O and HCl. All samples were loaded on degassed Re filaments with H_3PO_4 and a silicagel.

The samples were measured on a Finnigan MAT 262 mass spectrometer. Most samples were measured on Faraday (FAR) cups in static mode whereas low-intensity samples and all $^{207}Pb/^{204}Pb$-ratios were measured on a Secondary Electron Multiplier (SEM) in peak-jumping mode. The SEM data was corrected for non-linearity based on measurements of the standard NBS 982 U500 + Pb. This standard is also used to monitor the reproducibility of the mass spectrometer. Standard measurements are conducted for every 5-6 measured samples (once a day).

The measurements were corrected for a 2 pg Pb and 0,1 pg U blank with blank compositions: $^{206}Pb/^{204}Pb = 18,4 \pm 2$ %, $^{207}Pb/^{206}Pb = 0,85 \pm 1$ % and $^{207}Pb/^{204}Pb = 15,555 \pm 2$ %. Common Pb was corrected for using the Pb-evolution model by Stacey and Kramers, (1975), with assumed crystallization age for the sample as initial age. U source fractionation was estimated to be 0,12 %/a.m.u with an error of ± 0,06 for Faraday data and ± 0,1 for secondary electron

multiplier data. Pb source fractionation was corrected for using the measured value for the $^{205}Pb/^{202}Pb$ tracer-ratio normalized to the certified value of 0,44050. Additionally, a standard fractionation uncertainty of 0,06 %/a.m.u. was incorporated into the calculation. This factor becomes significant for analysis where the $^{205}Pb/^{202}Pb$-ratio is determined very precisely and the fractionation correction becomes unrealistically precise. This procedure yields Pb fractionation values in the order of c. 0,05-0,15 %/a.m.u. For the samples that was only spiked with the mixed ^{205}Pb-^{235}U-tracer, Pb source fractionation was estimated to 0,1 %/a.m.u. Errors of the fractionation estimate for such samples was set to ± 0,05 %/a.m.u for Faraday data and ± 0,1 %/a.m.u for secondary electron multiplier data.

Finally, analytical errors and the corrections described above were incorporated and propagated using the ROMAGE 5.1 program originally developed by T. E. Krogh. Concordia plots were made using the ISOPLOT program (Ludwig, 1991).

4:2: Results

4.2.1: Granodioritic hornblende gneiss (pim04-38)

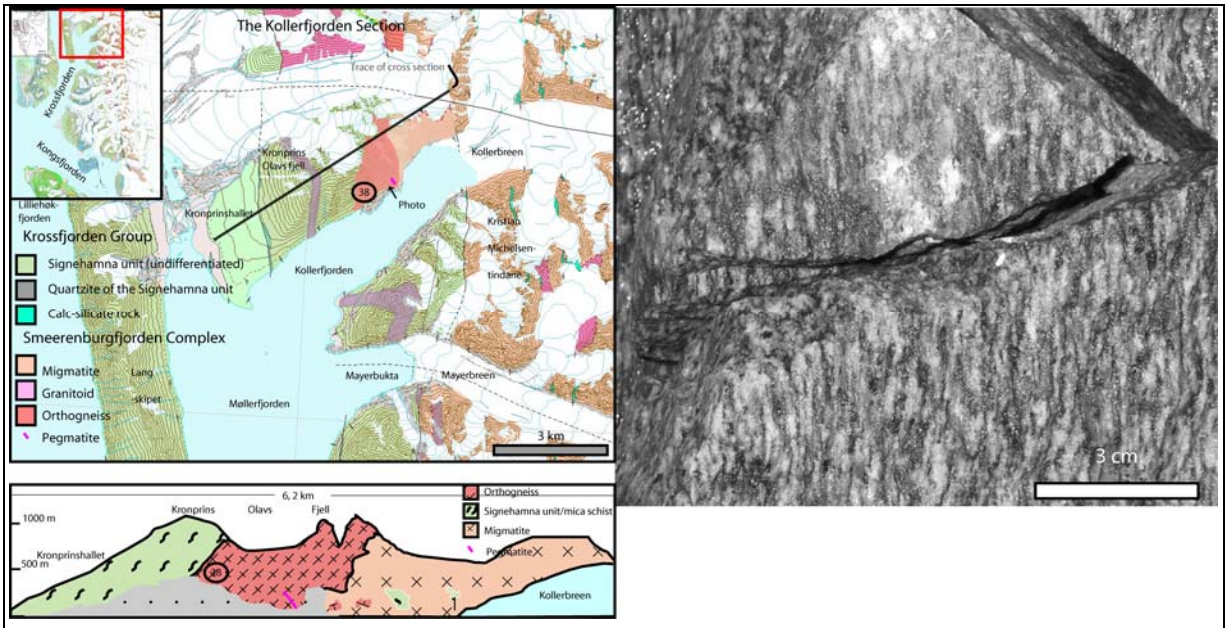

Figure 4.1: Map location of sample pim04-38 and field appearance of Grenvillian orthogneiss in Kollerfjorden. Sample location and number is indicated by an ellipse. Bearing and location of photo is indicated on map by arrow. Map modified from the Norwegian Polar Institute (http//:npolar.no).

Field relations and sample description

This west-dipping orthogneiss occupies a c. 2 km stretch of the Kollerfjorden section. In the east it is intruded by anatectic granodiorite (pim04-80-type). In the western reaches of the section the orthogneiss is in contact with the Signehamna unit pelitic schist. This contact is modified by Caledonian deformation, and may be either intrusive or sedimentary. The modal composition of the sample is granodioritic to tonalitic with c. 14 % hornblende and minor amounts of biotite, calcite, zircon, titanite, pyrite, chalcopyrite, chlorite and limonite.

Analytical results

A total of 5 zircon fractions of 1-8 grains and 2 titanite fractions of 9 and 7 grains were analysed, and the results are given in figure 4.2 and table 4.1.

Zircon

All the analysed grains had high length to width ratios from 3-6, and were dominated by the prismatic ([100] & [101]) forms. Some of the zircon crystals contained black inclusions, and 2 fractions of these were analysed (101/58 & 101 /54, table 4.1). Commonly zircon crystals contain elongated melt inclusions, and two of the analyses was done using such grains (101/55 & 101/59). Some grains are very clear without inclusions and one analysis of such grains was carried out as well. All the fractions have low common Pb, and U content varies from 70 ppm to 1040 ppm. Zircon are 0,6- 6,9 % discordant, and all but one single-grain analysis plot on a discordia line manually anchored at 418,8 Ma. The upper intercept of this line is at 961,9 ± 6,2 Ma. One single grain analysis (101/55) plots below this line, and is 6,9 % discordant.

Titanite

The heavy, non-magnetic fraction of the sample contains titanite and allanite. These minerals was distinguished in the binocular microscope by the colour (allanite is darker) and by the cleavage commonly displayed by allanite. To verify that the phases were correctly identified, some grains were mounted in epoxy and analysed qualitatively in a scanning electron microscope (SEM) equipped with an energy dispersive x-ray (EDX) system. Dark titanite grains were preferred because of the often higher U content and igneous nature of such grains (Corfu and Stone, 1998). The picked grains were 0,1-0,5 mm large. The U content is 170 and 260 ppm, respectively, and the grains contain 1,6 ppm common Pb. The total Pb content is c. 30 & 45 ppm., with errors of 0,7 % and 0,9 % (table 4.1).

Interpretation

Most of the zircon analyses and both titanite analyses plots on a discordia line manually anchored at c. 418 Ma, the time of crystallisation of the neighbouring late-intruding anatectic granodiorite (pim04-80). One zircon analysis plots below this line, and is more complex. This may indicate that also recent Pb-loss affected the zircon crystals, in which case the upper intercept age should be considered a maximum age. Alternatively, inherited zircon may complicate the grain.

Assuming all Pb-loss occurred during the Caledonian orogeny and ignoring one analysis, the upper intercept of 961, 9 ± 6,2 Ma is interpreted as the crystallisation age of the granodioritic orthogneiss. Subsequent Caledonian tectonic activity caused Pb-loss in titanite and zircon and developed a foliation.

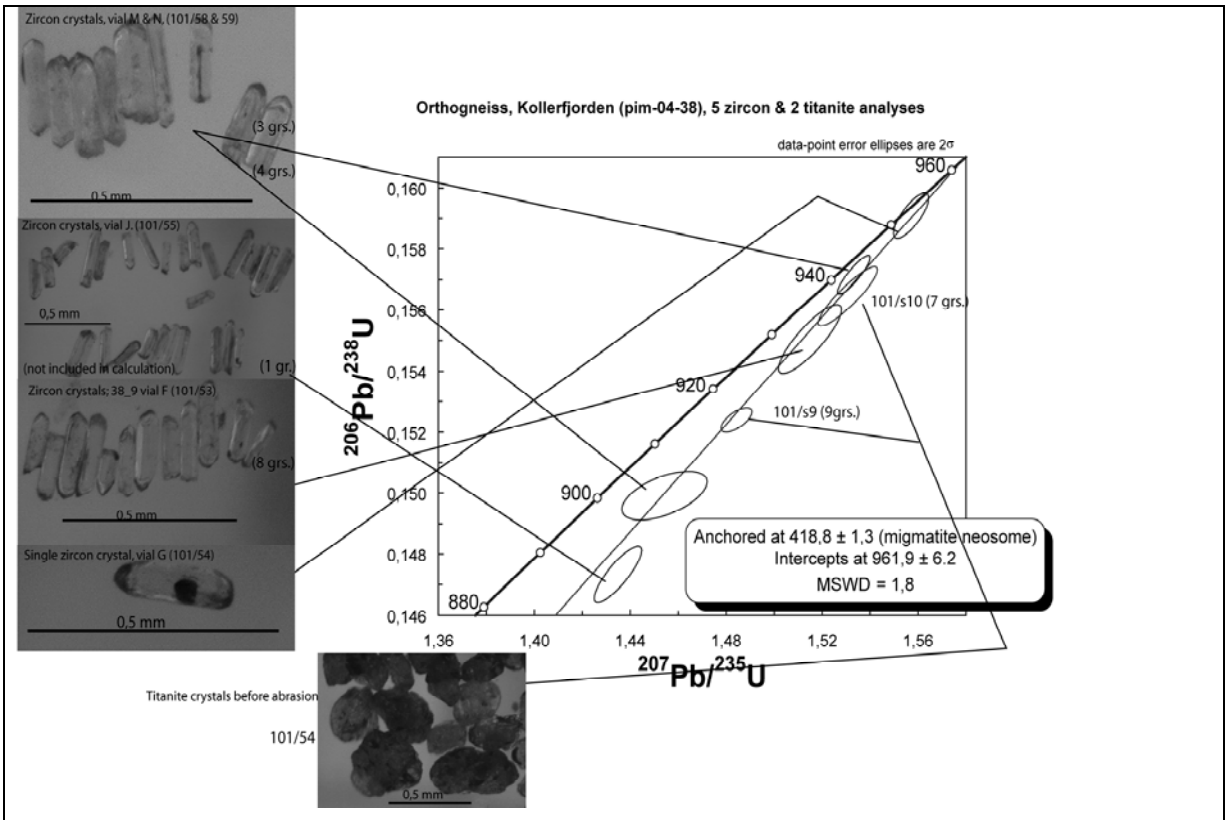

Figure 4.2: Concordia plot of sample pim04-38. 4 zircon and 2 titanite analyses constitutes a discordia line manually anchored at c. 418 Ma with an upper intercept of 961,9 ± 6,2 Ma, which is interpreted as the crystallization age of the now foliated orthogneiss.

4.2.2: Gneissic granitic xenolith (pim04-46) in Silurian granitoid (pim04-80)

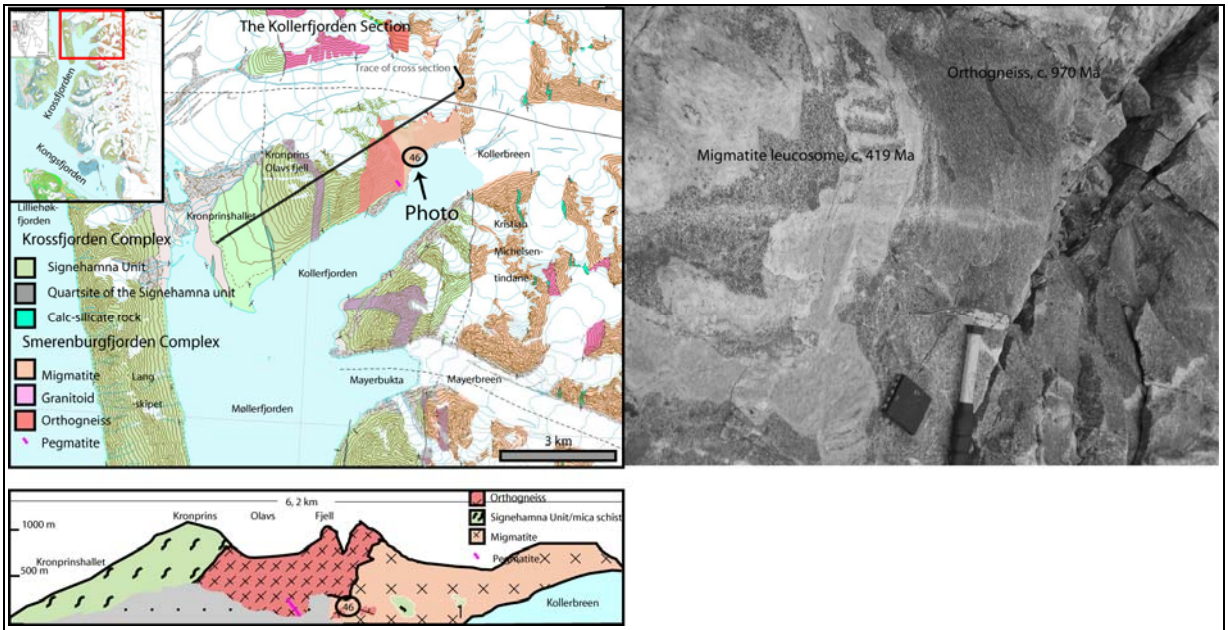

Figure 4.3: Map location of sample pim04-46 and field appearance of Grenvillian gneissose xenoliths in Silurian granitic migmatite in Kollerfjorden. Sample location and number is indicated by an ellipse. Bearing and location of photo is indicated on map by an arrow. Map modified from the Norwegian Polar Institute (http://npolar.no).

Field relations and sample description

This rock occurs as xenoliths in the Silurian granitic migmatite (section 4.2.8). This particular sample was taken from a xenolith c. 1,5 meters across. It contains quartz, plagioclase, k-feldspar, biotite and hornblende, and minor amounts of chlorite, zircon and monazite. A similar rock was dated by Ohta et al. (2002). They used the Kober method on zircon and Ar/Ar mica thermochonometry, and obtained ages ranging from 940 to 963 Ma for zircon and 419 ± 1 Ma for the micas (see table in chapter 3).

Analytical results

A total of 4 zircon fractions (3 single-grains and one consisting of 2 grains) and three monazite fractions consisting of 3-4 grains were analysed, and the results are given in table 4.1 and plotted in figure 4.4.

Zircon

The zircon crystals chosen for analysis were prismatic, needle-shaped with length/with-ratios from 3-5. They commonly contained elongate melt inclusions, and the magmatic (Corfu et al., 2003) grains were not likely to contain xenocrystic cores. All analyses but one is 1-10 % discordant, and fall on a discordia line anchored at c. 419 Ma (the time of crystallization of metamorphic monazite) with an upper intercept at 970 ± 7 Ma.

Monazite

Monazite crystals in the separated sample are small (0,05-0,2 mm) and often cracked and have turbid interior. Inclusions of dark minerals are common. Three analyses of 3-4 grains (5-12 µg) give a concordia age of 419,7 ± 0,5 Ma. The 2 most precise analyses are slightly discordant, which causes a high MSWD for the concordia age of 8,9. This seems to be a reproducible feature of monazite in the sample.

Interpretation

The upper intercept of the anchored 5-point (4 zircon analyses and anchor-point) discordia-line represents the crystallization age of granitoid magma at 970 ± 7 Ma. Zircon lost Pb in the late Silurian when monazite formed metamorphically at 419,7 ± 0,5 Ma and the gneissic rock was incorporated into the 418,8 ± 0,7 Ma granite body (pim04-80-type).

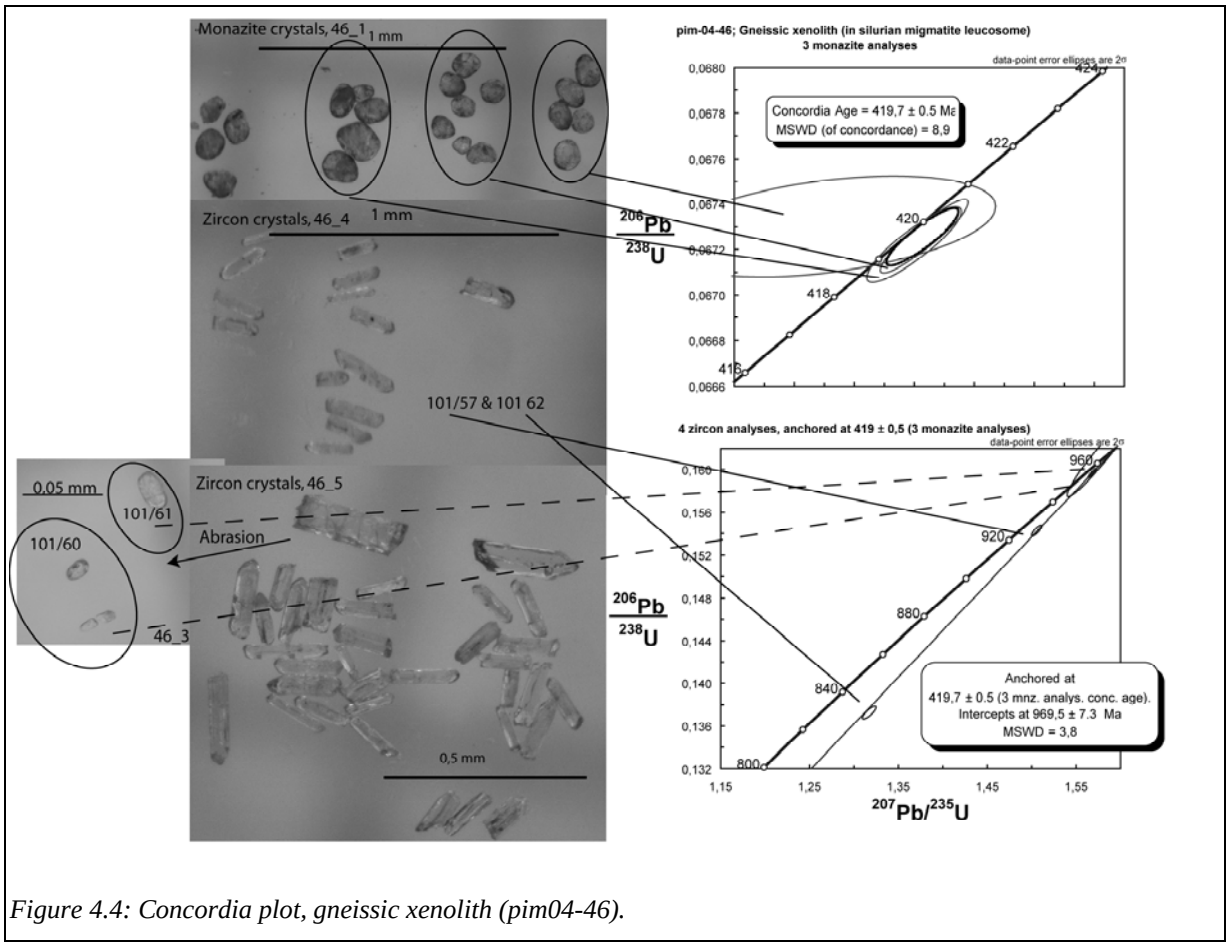

Figure 4.4: Concordia plot, gneissic xenolith (pim04-46).

4.2.3: Newtontoppen granitoid.

Field relations and sample description

The sample was taken near the summit of Newtontoppen, Svalbards highest mountain (1713 m.a.s.l.). The Newtontoppen granitoid suite intrudes Precambrian basement in southern Ny Friesland, (Tebenkov et al., 1996) and constitutes one of the batholiths in Svalbard. The basement is assigned to the Nordaustlandet terrane (chapter 2), bordered to the west of Newtontoppen by the Lomfjorden Fault. Unconformably overlaying are unmetamorphosed Carboniferous strata.

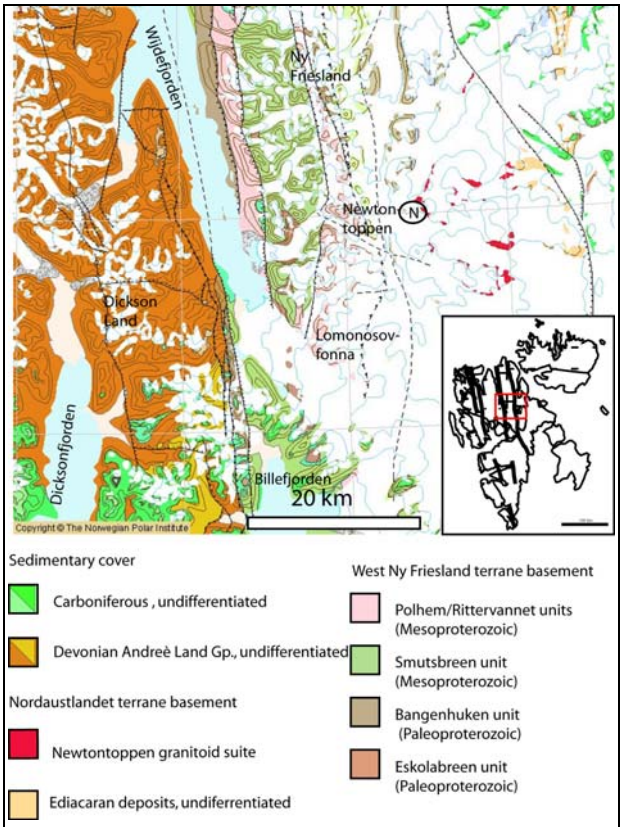

Figure 4.5: Map of southern Ny Friesland and the Newtontoppen granitoid suite. The tectonic border (Lomfjorden Fault zone) between the West Ny Friesland Terrane and the Nordaustlandet Terrane runs in the Lomonosovfonna glacier west of Newtontoppen. In the eastern part of the outcrop area, the Newtontoppen granitoid suite intrudes Ediacaran strata of the Nordaustlandet terrane. Sample locality is indicated by an ellipse. Map modified from the Norwegian Polar Institute (http://npolar.no).

Analytical results

A total of 4 fractions of zircon, 2 fractions of titanite and 2 fractions of allanite were analysed. All results are given in figure 4.6 and table 4.1.

Zircon

Zircon crystals in the sample are euhedral and relatively stubby with length to width-ratios up to c. 2,5 to 3,5. Cracked and metamict grains were not considered for analysis. The abundance of grains with obvious cores is low. One fraction of broken-off tips of prismatic zircon crystals gives a slightly discordant age ($^{207}Pb/^{206}Pb$-age of 435 Ma, 0,9 % discordance). Another fraction of similar grains was not spiked by mistake, and the U/Pb-ratios could not be determined. The $^{207}Pb/^{206}Pb$-ratio was measured, however, and the fraction has a $^{207}Pb/^{206}Pb$-age of c. 445 Ma, with an uncertainty of 6,4 Ma. The single-grain fraction analysed in 99/54 (figure 4.6) was a poor mass spectrometer run and yields an imprecise age because of that. The 3-grain fraction (99/56) gives a concordant age of c. 430 Ma.

Accessory minerals

Titanite ($CaTiO(SiO_4)$) and allanite ($(Ca,Ce)_3(Fe)(Al_2O(SiO_4)(Si_2O_7)(OH)$) is abundant in the sample, and 2 multigrains fractions of each mineral were analysed. Allanite belongs to the epidote group and was distinguished from titanite based on the black to dark brown colour and cleavage. The two allanite fractions give a concordant upper Devonian age of 359 ± 2 Ma, but highly uncertain $^{207}Pb/^{206}Pb$-age (± >100 Ma). The present isotopic composition of the allanite may be a result of post-crystallization alteration, and the age is not considered to be related to the emplacement of the Newtontoppen granitoid. Because it is reproducible, the upper Devonian age probably represents a geological event of some sort.

Titanite occurs as pale brown to dark brown anhedral grains. The darkest of these were chosen for analysis because of assumed higher U content (Corfu and Stone 1998), which turned out to be c. 250 ppm. Titanite grains are generally clear, and do not have signs of extensive metamictization. Two fractions consisting of 3 grains (170µg & 90 µg) give ages overlapping with the zircon ages (c. 430-435 Ma), but not as precise because of the uncertainty represented by the Stacey-Kramers common Pb-correction.

Interpretation

The 4 analyses described above (2 zircon and 2 titanite fractions) plot at the concordia except for the one zircon fraction (99/54), which is slightly discordant (0,9 %). Because it is backed up by the 3 other analyses it is unlikely that the discordance seen in analysis 99/54 is due to inheritance or Pb-loss. Therefore, the discordance seen in the one fraction may be due to other causes, like excess ^{207}Pb as a result of ^{231}Pa disequilibrium (Anczkiewicz et al., 2001; Mortensen et al., 1997; Parrish and Noble, 2003) or inaccuracy in the value for the decay constants for one or both of the U-isotopes (Schoene et al., in press).

The ^{206}Pb/^{238}U-age of analysis 99/54 is interpreted as the closest to the real age. The weighted mean of ^{206}Pb/^{238}U-ages for 4 analyses is 430 ± 0,7 Ma, identical to the 3-point concordia age, and this is interpreted as the crystallization age for the Newtontoppen granitoid.

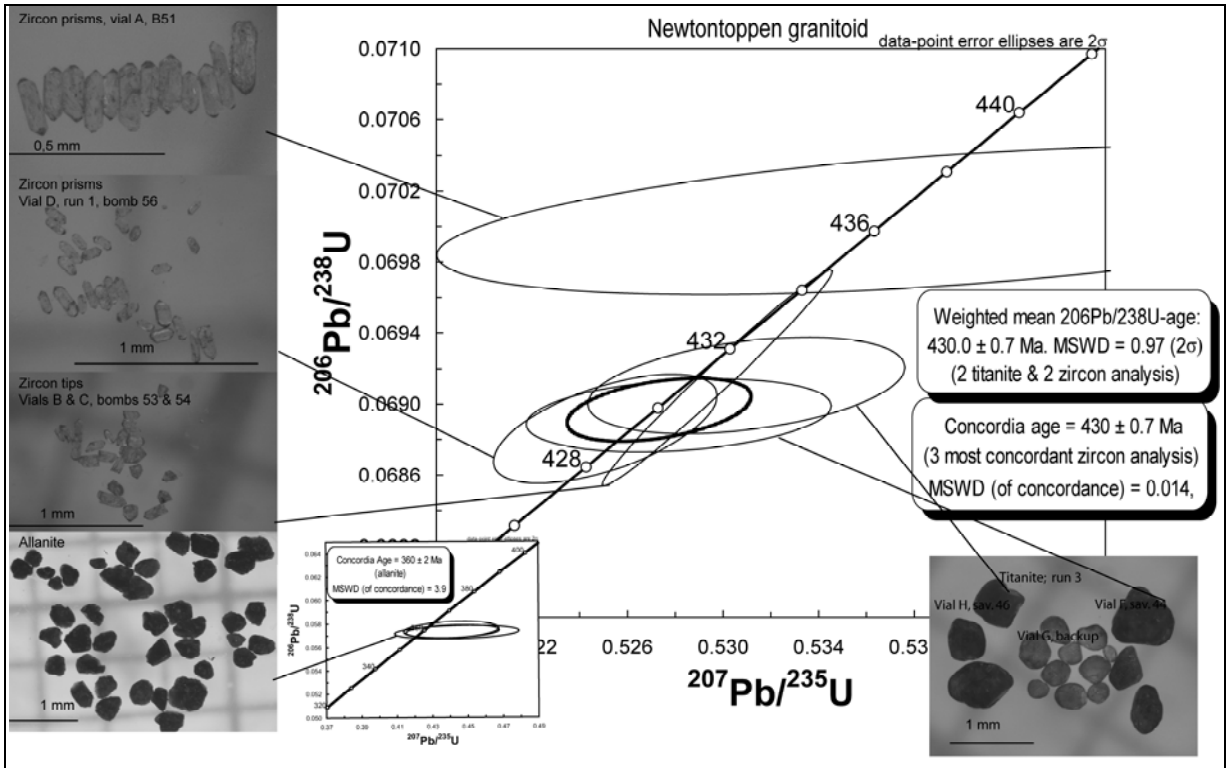

Figure 4.6: Concordia plot for the Newtontoppen sample. The weighted mean $^{206}Pb^{238}U$- age for 2 zircon and 2 titanite analyses and the concordia age for the 3 most concordant analyses (both 430 ± 0,7 Ma) is preferred as the crystallisation age for the Newtontoppen sample. The allanite concordia age dicussed above is shown in the inset. The geological meaning of this is unclear.

4.2.4: Grey two-mica granitoid, Bjørnfjorden (pimsm-22-05)

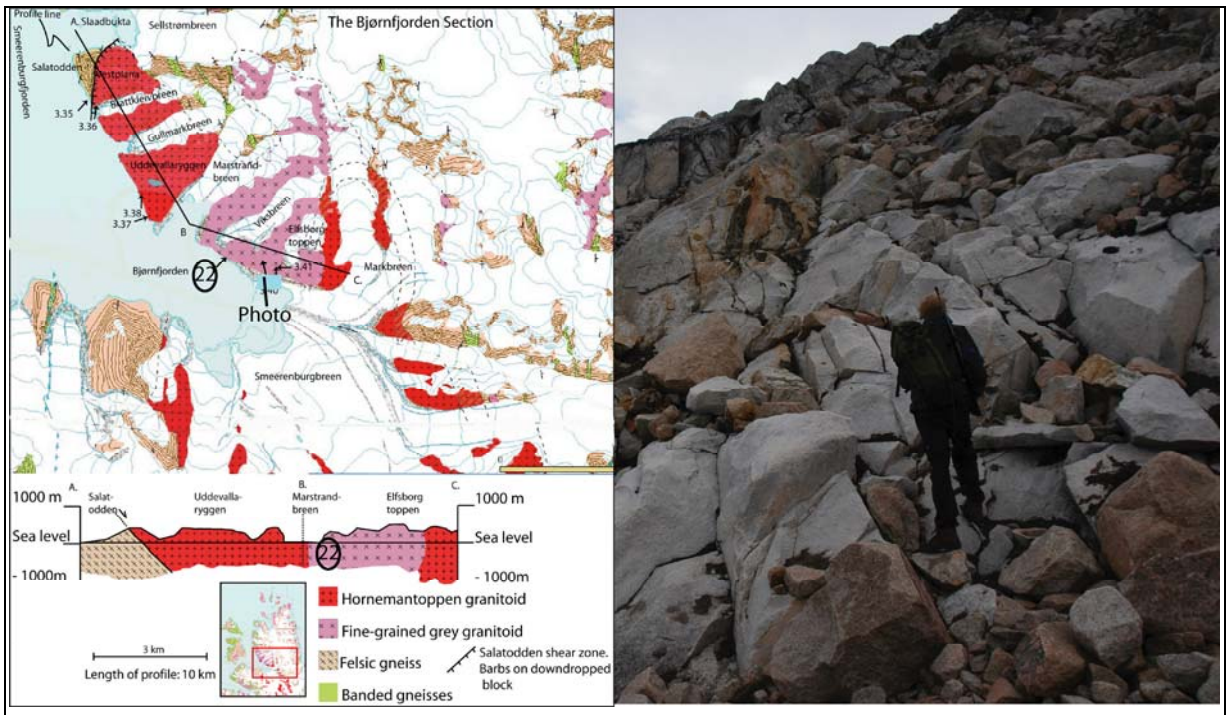

Figure 4.7 Location and field appearance of sample pimsm22-05(grey granitoid). Location of sample is indicated by ellipses with sample number, location and bearing of photo is given by arrow. Trace of cross-section is indicated by black line on the map. Note that the section turns c. 120 deg, indicated by stippled line on the cross-section. Geologist: Endre Bergfjord. Map modified from the Norwegian Polar Institute (http://npolar.no).

Field relations and sample description

This granitoid crops out near the Hornemantoppen granitoid in Bjørnfjorden, Smeerenburgfjorden area (see map above), and covers 5-6 km^2. The contact relationships between the grey granite and migmatites and Hornemantoppen granitoid are poorly exposed in this mountainous fjord area, but are probably of intrusive nature (Ohta et al. 1996). The rock contains numerous xenoliths of pelitic rock, quartzite and orthogneiss. A thin section contains quartz, plagioclase, K-feldspar, biotite and muscovite, and minor amounts of chlorite, zircon, monazite and opaque phases (sulphides).

Analytical results

A total of 3 zircon fractions were analysed (2 single-grain and one 5-grain), as well as two multigrain (15 & 16 grains) monazite fractions.

Zircon

Most zircon crystals in the sample are short, euhedral grains with length to width-ratios of <2. Many of these seem to consist of a relict core with overgrowths of new zircon. Another group of grains consist of high quality elongate prisms, sometimes fragmented. These often have elongate melt inclusions, some inclusions of other phases and length to width-ratios of 3 to 6. Zircon from this group was used for all analytical work. A single-grain analysis (115/61) yielded a 40 % discordant age of c. 1350 Ma (^{207}Pb/^{206}Pb-age), whereas fraction 115/62 has a

$^{207}Pb/^{206}Pb$-age of c. 800 Ma (no U-ages were obtained). These 2 analyses represent inheritance. One of the single-grain fractions yielded a concordia-age of 423,6 ± 1,5 Ma.

Monazite

Monazite occur as 0,2-0,4 mm subhedral to anhedral grains. Two analyses were carried out using non-turbid grains with few inclusions of other phases. The results reveal a high U-content of 1000-4000 ppm and Pb-content of 200-850 ppm. The common Pb-content is <0,5 ppm. The resulting ages are around 420 Ma, but negatively discordant by c. 1 % and poorly overlapping. (See below for a discussion of monazite disturbances.)

Interpretation

The concordant zircon-age of 423 ± 1,5 Ma is interpreted as the crystallization age of the grey granitoid. Thus, it predates the neighbouring Hornemantoppen granitoid. An alternative interpretation is that the overlapping $^{207}Pb/^{235}U$-ages of the monazite grains represent the real age, and that the zircon crystal is affected by slight inheritance. In that case, 421,7 ± 0,2 Ma would be the crystallisation age.

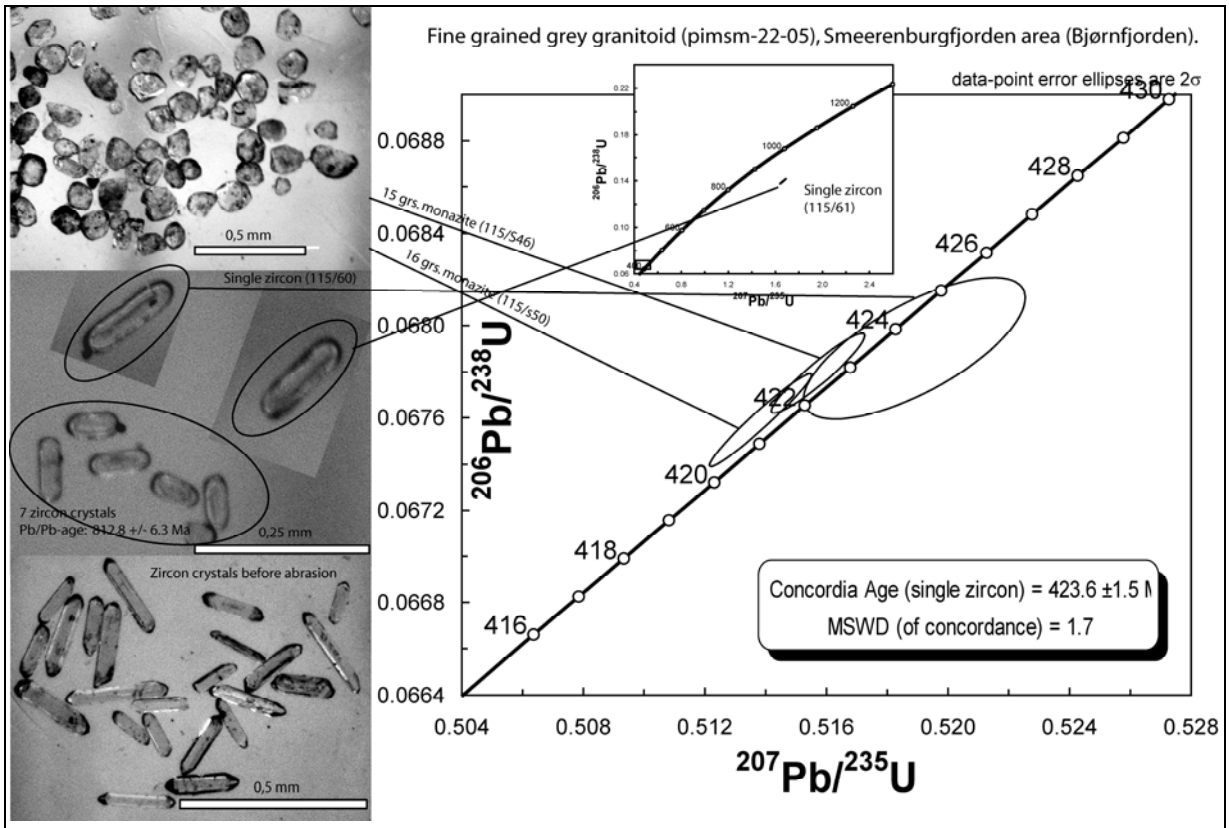

Figure 4.8: Concordia plot from grey granitoid, Bjørnfjorden (sample pimsm22-05). Binocular microscope photos on the left.

4.2.5: Grey migmatitic granitoid, inner Kongsfjorden (pim04-72)

Field relations and sample description

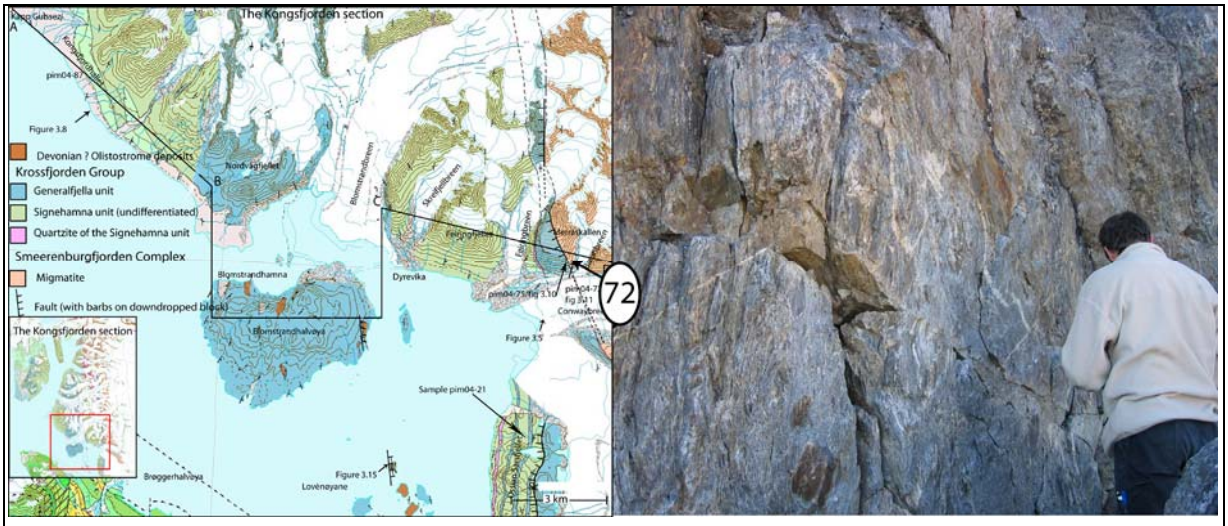

Figure 4.9: Location and field appearance of migmatitic 2-mica granitoid, inner Kongsfjorden. Sample locality and bearing of photo is indicated by arrow and ellipse. Geologist is Carl F. Petterson. Map modified from the Norwegian Polar Institute (http://npolar.no).

This rock crops out in the south-eastern part of the study area, where the migmatitic Smeerenburgfjorden Complex is in tectonic contact with marbles of the Krossfjorden Gp. metasediments. The migmatitic complex constitutes a narrow horst (see inset map above) bounded to the west by the southern extension of the Raudfjorden fault (Dallmann et al., 2002) and in the east by the Merraskallen fault which is interpreted here to be west-dipping with top-to-the west (extensional) displacement. (See chapter 3 for further discussion of field relationships.)

The exposures in inner Kongsfjorden are dominated by migmatitic, quartzofeldspatic rocks, in some cases foliated. Sample pim04-72 is from the locality in the figure above, where the leucosome is somewhat enriched and pods of unfoliated granitoids occur. The sample locality is c. 200 meters east of the Merraskallen fault. The modal composition is c. 40 % quartz, 34 % plagioclase, 10 % K-feldspar, 15 % biotite and minor amounts of chlorite, muscovite, calcite, epidote and opaques.

Analytical results

Zircon

Zircon crystals from this sample can be grouped into 4 morphologies;

- crystals dominated by the prismatic forms with length to width ratios of 1, 5-2 and 2, 5 to 3;
- crystals with a distinctively developed pyramidal form;
- resorbed, stubby prisms with length to width ratios of ~2 or less;
- tips of prisms.

One multigrain (5-7) fraction from each morphology was analysed (analyses 99/53/60/59 & 101/51). The results are 13-16 % discordant ages between c. 1100 and 1300 Ma (see table 4.1

and concordia plot in figure 4.10). To be able to reveal xenocrystic cores 30 clear crystals with the developed pyramidal form were mounted in epoxy and imaged by cathodoluminescence (CL) imaging on SEM. Some crystals with clearly magmatic zoning (figure 4.10, 5 grains) were removed from the epoxy and analysed as single grains with the ID-TIMS-method. The results are highly discordant late Proterozoic (4 crystals, 22-30 % discordant) or Archean (one crystal, $^{206}Pb/^{207}Pb$ age of 2,7 Ga, 20 % discordant) ages. Because the grains were not abraded, these analyses give more discordant ages than the former.

Monazite

Monazite in the sample occur as 100-250 µm large grains. They are commonly clear and non-turbid and some have inclusions of other phases. 4 fractions give middle Silurian ages, but the reproducibility is poor (see below for a discussion of monazite chronology). To take this into account, the age in fig 4.10 is given by the two analyses with the greatest deviation (99/s56 & 104/s47). They give an age between 422,1 ± 0,8 and 427,3 ± 1,7 Ma, or 424,6 ± 4,4 Ma.

Interpretation

The Middle Silurian monazite age of 424,6 ± 4,4 Ma represents the Caledonian event for the inner Kongsfjorden rocks. This may also be the time of migmatization and formation of the granitoid leucosome. In that case, the zircon data represents inherited zircon that did not dissolve during melting because of low temperatures (Miller et al., 2003; Watson and Harrison, 1983). Alternatively, the zircon crystals represent the magmatic event, and the monazite ages are merely metamorphic. In that case, the protolith granitoid crystallized some time in the Mesoproterozoic.

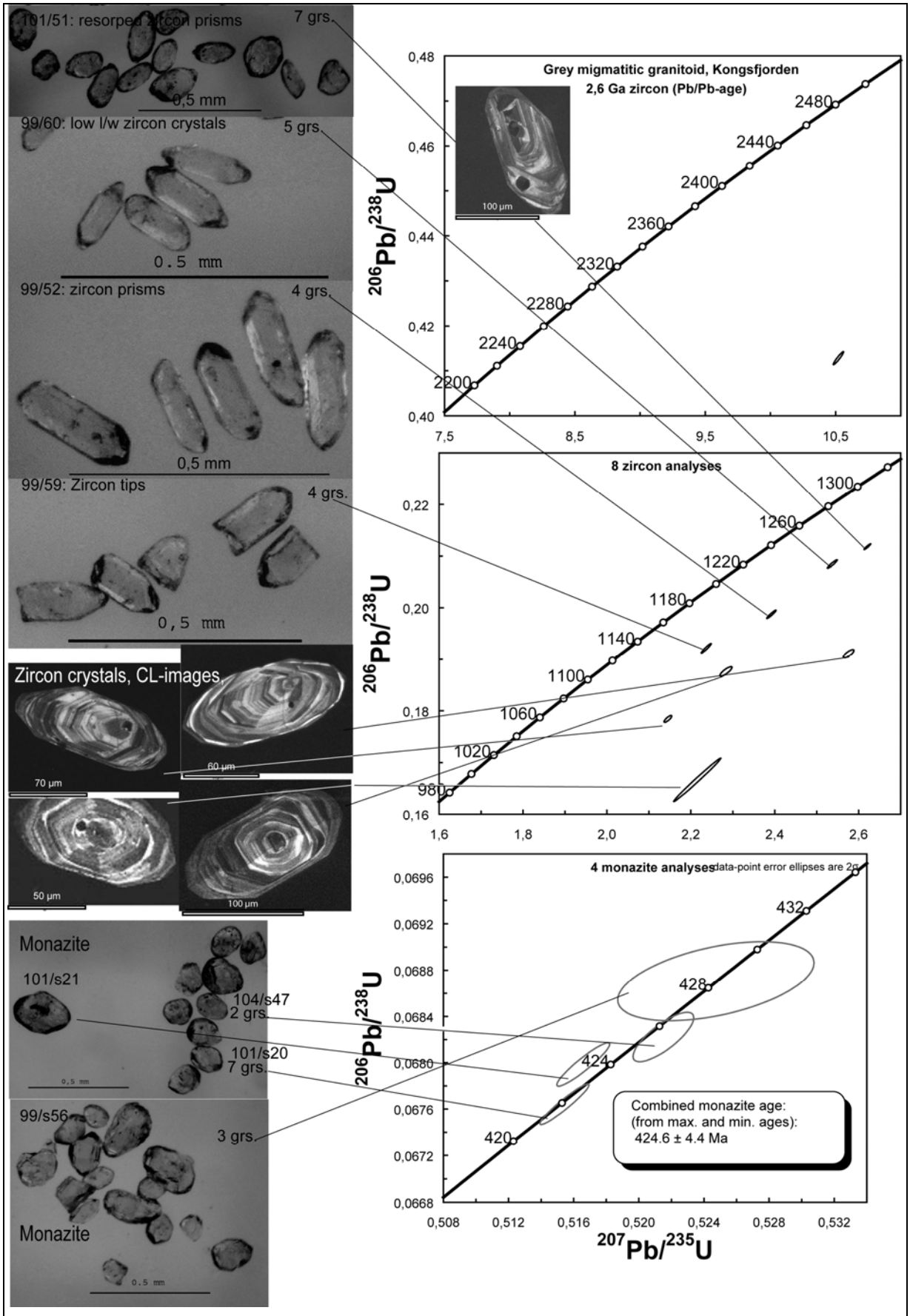

Figure 4.10: Concordia plot of pim04-72, migmatitic granitoid. Analysis numbering refers to table 4.1. The concluded age is combined from the oldest and the youngest monazite analyses.

4.2.6: Foliated granitoid leucosome, inner Kongsfjorden (pim04-75)

Field relations and sample description

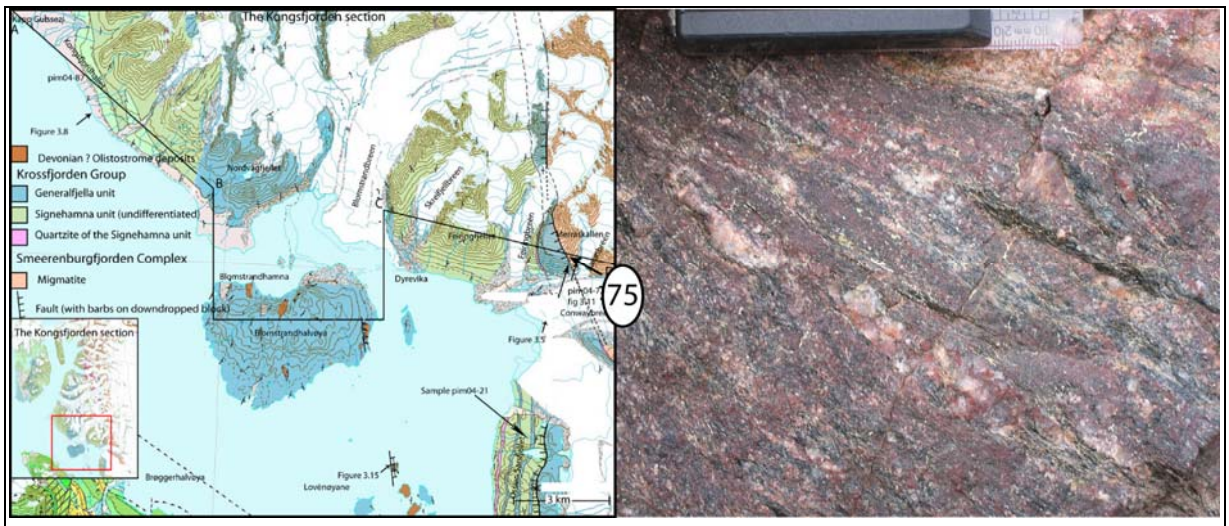

Figure 4.11: Location and field appearance of foliated and limonitized migmatite leucosome in Kongsfjorden. 10 cm long compass for scale. Map modified from the Norwegian Polar Institute (http://npolar.no).

The sample was collected in the footwall block of the Merraskallen fault, where it constitutes the western margin of a north-south trending basement horst. East of the Merraskallen fault the complex is dominated by migmatitic gneiss and pods of granitoid leucosome (sample pim04-72-type). Near the fault the rock is foliated and has a distinct red colour due to limonite. The modal composition is c. 50 % quartz, 25% plagioclase, 10 % biotite, 4 % K-feldspar, 4 % muscovite, 4 % chlorite with minor amounts of zircon, monazite and ilmenite.

Analytical results

Zircon

A total of 3 morphologies of zircon were analysed (see fig 4.12 for photos):

- Long prisms (length to width ~ 3-3,5) dominated by well developed prismatic forms. These crystals gave discordant Mesoproterozoic ages (2 analyses).
- Stubby prisms (length to width ~ 2-3) with significantly developed pyramidal forms. A single grain analysis gave discordant Neoproterozoic ages.
- Tips of prismatic grains. A 6-grain analysis gave discordant Mesoproterozoic ages.

Monazite

Small (<0.1mm), colourless monazite grains occur in minor amounts, and a 13-grain analysis weighing 5 µg gave a concordant age of 422,6 ± 0,9 Ma.

Interpretation

The 3 zircon analyses do not fall on one obvious discordia line. There are two possible interpretations: Either the zircon ages represents a Mesoproterozoic protolith and the monazite ages represents metamorphic resetting, or, alternatively, the 422,6 ± 0.9 Ma monazite age is the time of crystallization of the granitoid and the zircon crystals are remnants of the source rock.

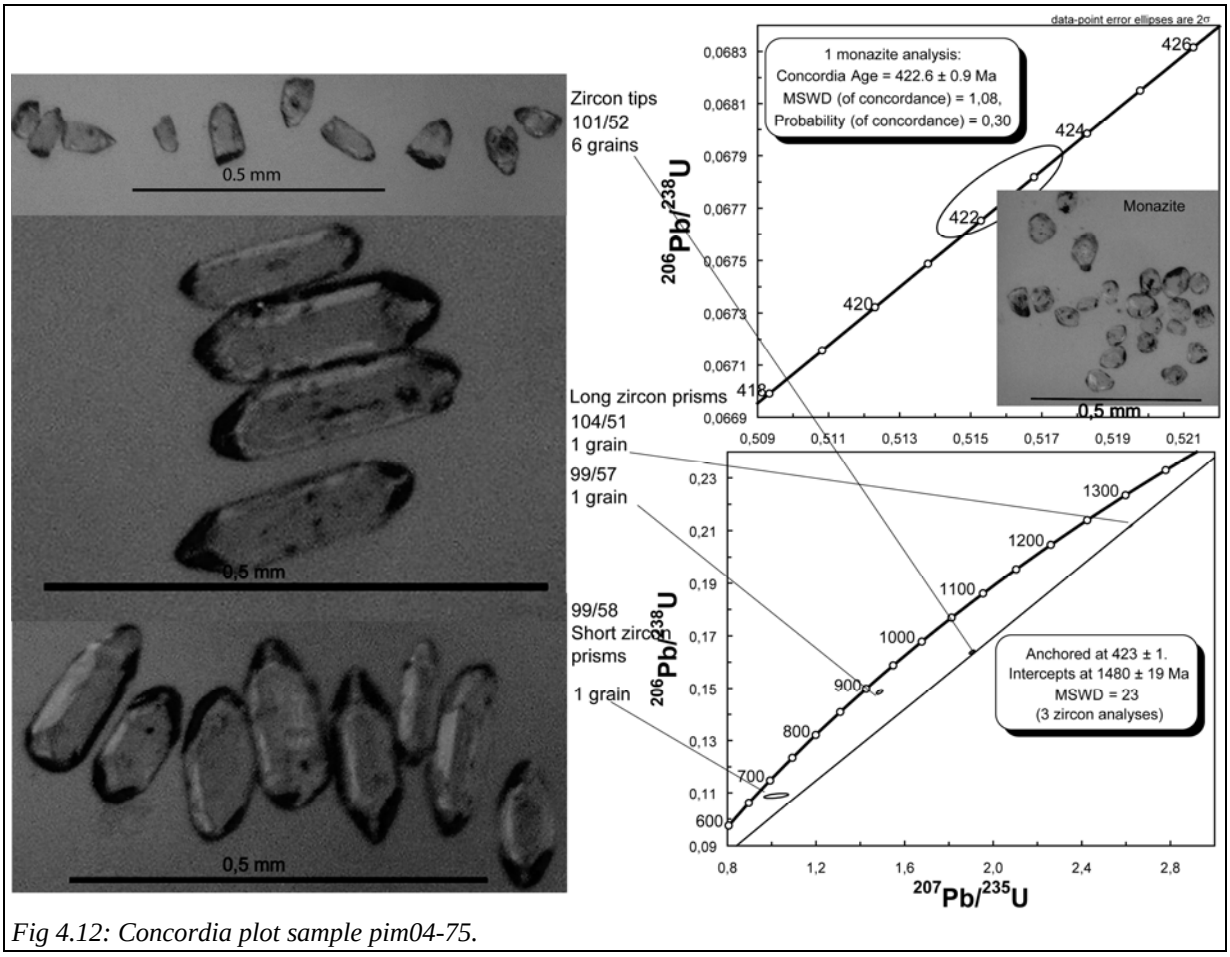

Fig 4.12: Concordia plot sample pim04-75.

4.2.7: Hornemantoppen granitoid (pimsm19-05)

Field relations and sample description

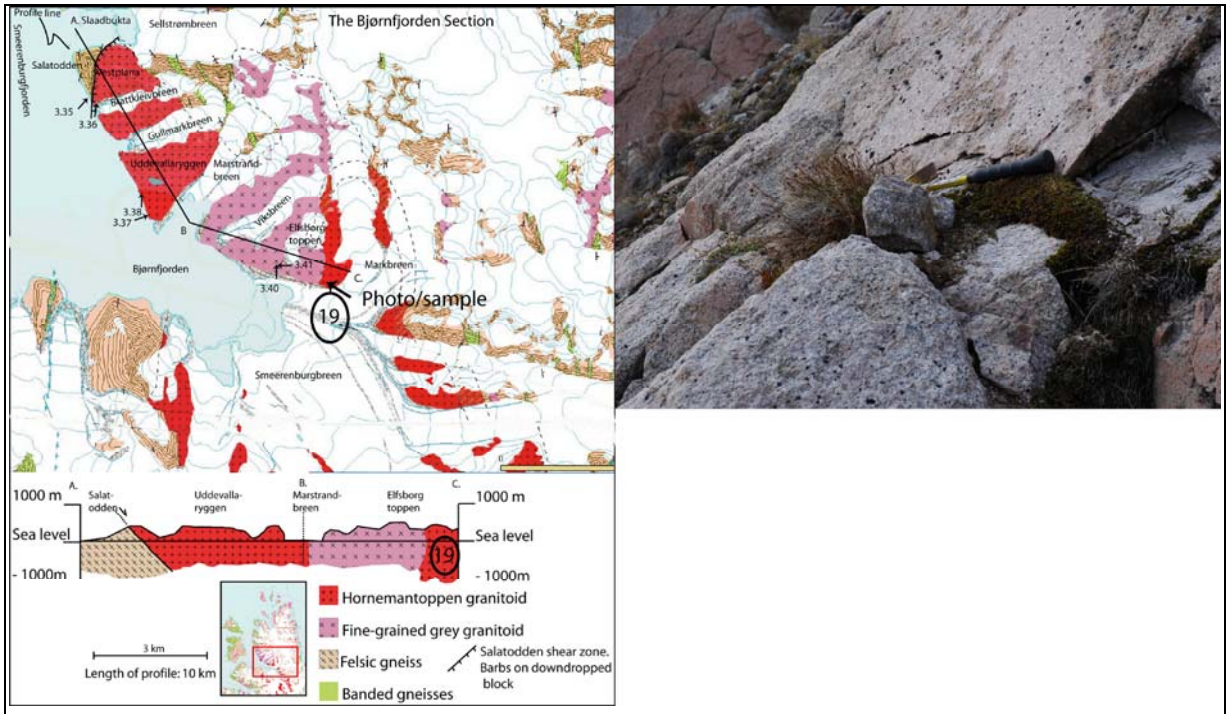

Figure 4.13: Location and field appearance of sample pimsm19-05 (Hornemantoppen granitoid). Location of sample and photo and bearing of photo is indicated by arrow. Trace of cross-section is indicated by black line on the map. Note that the section turns c. 120 deg. Hammer for scale on photo. Map modified from the Norwegian Polar Institute (http://npolar.no).

The Hornemantoppen granitoid is a large batholith that occupies c. 150 km^2 in the Smeerenburgfjorden area and the mountainous areas south of Smeerenburgfjorden. It intrudes the older basement rocks (e.g. Balasov et al., 1996a) in the south and west, but in the north it is in tectonic contact to a basement gneiss complex along the Salatodden shear zone (see map). This shear zone is interpreted to be a top to the south-east extensional shear zone based on S-C-fabric (chapter 3). This particular sample is from the north shore of Bjørnfjorden, where the granitoid crops out as a homogenous coarse grained reddish rock. It consists of quartz, plagioclase, K-feldspar, biotite and minor amounts of chlorite, titanite, zircon and magnetite.

Analytical results

A total of 3 analyses were carried out from this sample; 2 zirkon fractions and one titanite fraction.

Zircon

Zircon commonly occurs as euhedral, prismatic crystals with high length to width-ratios. The grains contain inclusions of other phases like biotite in some cases (see figure 4.14), and melt inclusion are also common. Grains with obvious cores seem to be rare. The two analysed fractions yield overlapping but slightly discordant ages of c. 418 Ma.

Titanite

Titanite occurs as relatively pale, clear grains as well as turbid, inclusion-rich varieties. One analysis of c. 15 clear grains yields a concordant age of 418,4 ± 1,0 Ma. The common Pb-content of 1,1 ppm was corrected for using a 425 Ma initial Stacey-Kramers age. The uncertainty associated with this correction constitutes most of the error on the age.

Interpretation

The discordant zircon analyses are supported by titanite with similar, but concordant, ages. This and the fact that one would not expect inherited cores or Pb-loss to affect both analysed zircon fractions equally, supports the interpretation that the $^{206}Pb/^{238}U$-ages are the closest to the real zircon age. The discordance may be a result of other causes, such as ^{231}Pa disequilibrium (e.g. Anczkiewicz et al., 2001), inaccuracy in the U decay constants (Schoene et al., in press) or other factors. Consequently, the most correct ages for crystallisation of the zircon are given by the $^{206}Pb/^{238}U$-ages, which are 418,4 ± 0,9 and 418 ± 1,8, respectively.

The Hornemantoppen granitoid crystallized at 418,4 ± 0,8 Ma, based on the $^{206}Pb/^{238}U$-ages of two zircon and one titanite analyses.

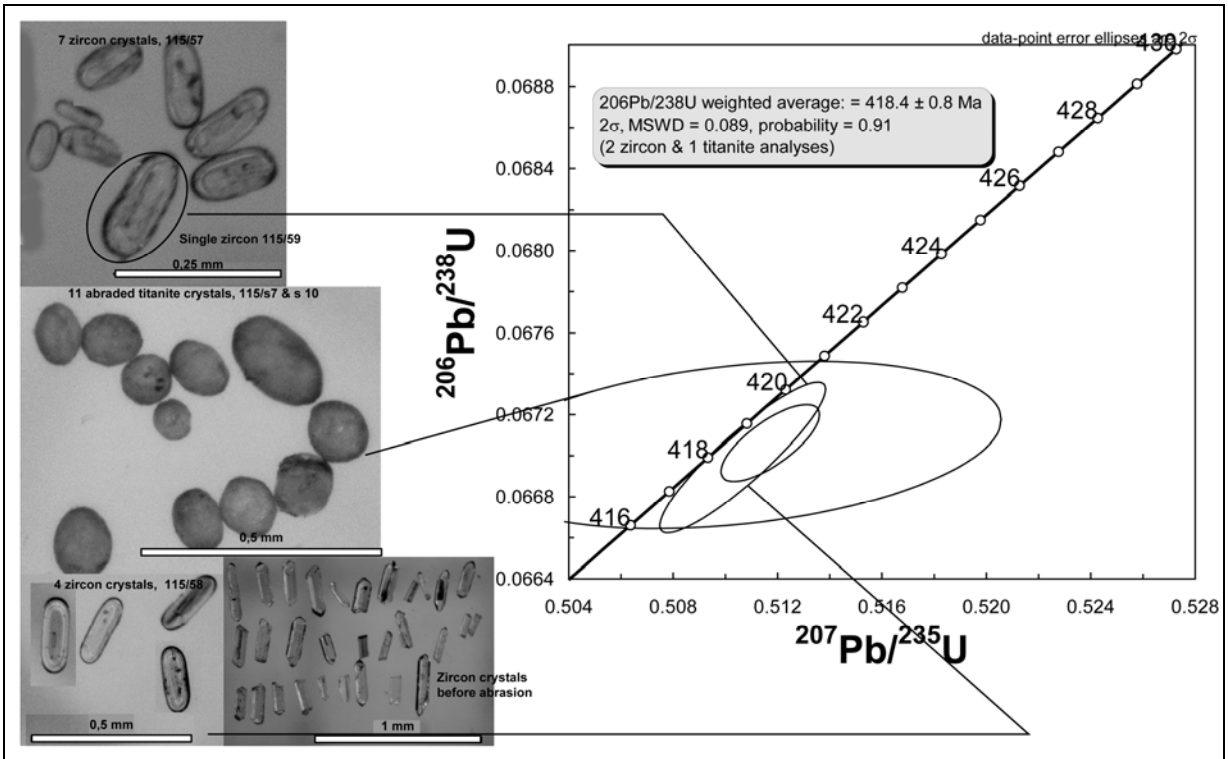

Figure 4.14: Concordia plot for the Hornemantoppen granitoid, sample pimsm19-05.

4.2.8: Two-mica leucosome of migmatite, Kollerfjorden (pim04-80)

Field relations and sample description:

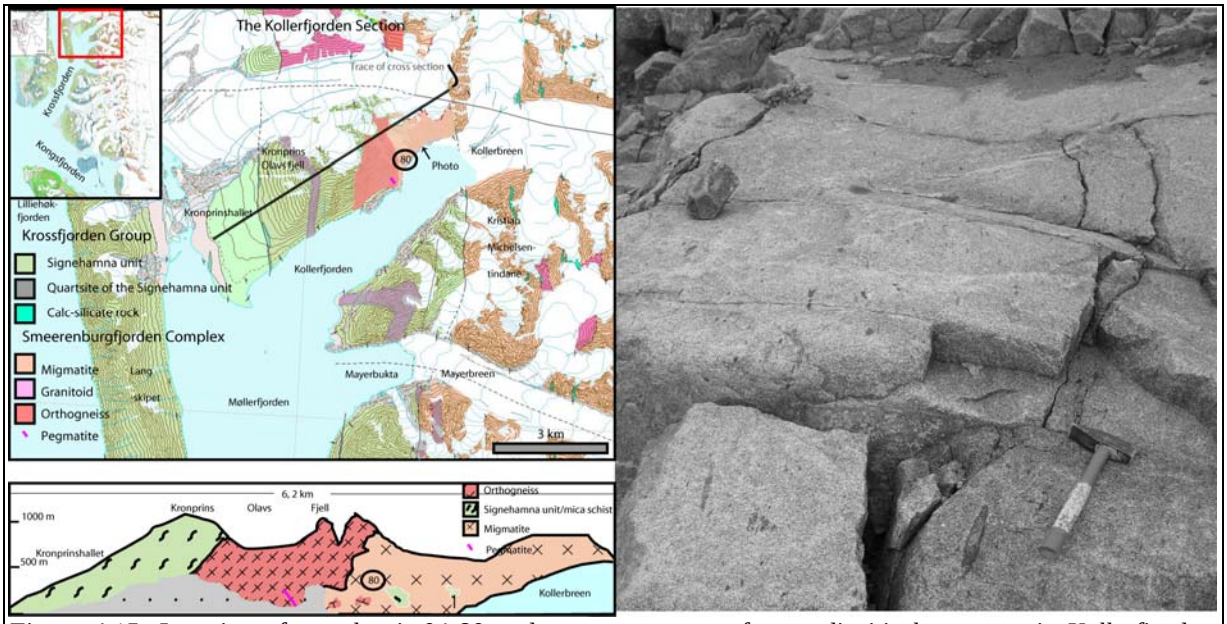

Figure 4.15: Location of sample pim04-80 and outcrop pattern of granodioritic leucosome in Kollerfjorden. Sample location is indicated by an ellipse and locality and bearing of photo is indicated by an arrow. Map modified from the Norwegian Polar Institute (http://npolar.no).

The migmatite complex in inner Kollerfjorden (see map in Figure 4.15) intrudes an orthogneiss and is the youngest unit exposed here. It contains xenoliths of orthogneiss and metapelitic rocks and partly digested schlieren and ghosts of dark, biotite-rich melanosome. This sample was taken from a locality where the leucosome is quite homogenous for some tens of meters (figure 4.15). The modal composition of the sample is granodioritic, with two micas. Accessory phases are zircon, monazite, (retrograde) chlorite, calcite and pyrite.

Analytical results:

Both zircon (5 fractions) and monazite (3 fractions) were analysed from this sample (figure 4.16 and table 4.1).

Zircon

Analyses 92/27, 104/57 & 104/58 were done using high length to width (4-5) prismatic grains, some of which had melt inclusions. The single-grain in analysis 104/58 had a black inclusion. These fractions give a concordia age of 418,8 ± 0,7 Ma. One zircon-fraction of short, prismatic grains (92/26) (not shown in fig 4.14) give a discordant age of c. 450 Ma, probably caused by xenocrystic zircon. Zircon fraction 92/25 consisted of euhedral, high length to width-grains, some fragmented. These grains contained minor inclusions of dark minerals, and the analysis reveals a common Pb-content of 24 ppm (26 pg, table 4.1) which can be explained by Pb-bearing inclusions. Correcting for the common Pb using a 450 Ma initial common Pb-age (Stacey and Kramers, 1975) results in an imprecise age of ~ 417 Ma.

Monazite

Monazite in this sample occurs as 0,05-1 mm grains. The analysed grains were clear with no cracks. These were abraded to remove parts affected by Pb-loss and impurities of other minerals like biotite. Three fractions of 1-15 µg (1, 4 & 5 grains) were analysed and yield ages in the range 420-430 Ma. Two of the analyses overlap with the concordia within error whereas one fraction plots above concordia. One fraction (92/s10) has a $^{207}Pb/^{235}U$-age overlapping with the concordant zircon-age described above, whereas the other fractions have older ages.

Interpretation

The concordia age of 418,8 ± 0,7 Ma, based on the 3 zircon fractions (104/57, 104/58 & 92/27), is interpreted as the crystallization age of leucosome of the migmatite. Monazite yields negatively discordant ages older than this, and may be affected by inheritance, unsupported ^{206}Pb etc. (see section on monazite chronology below).

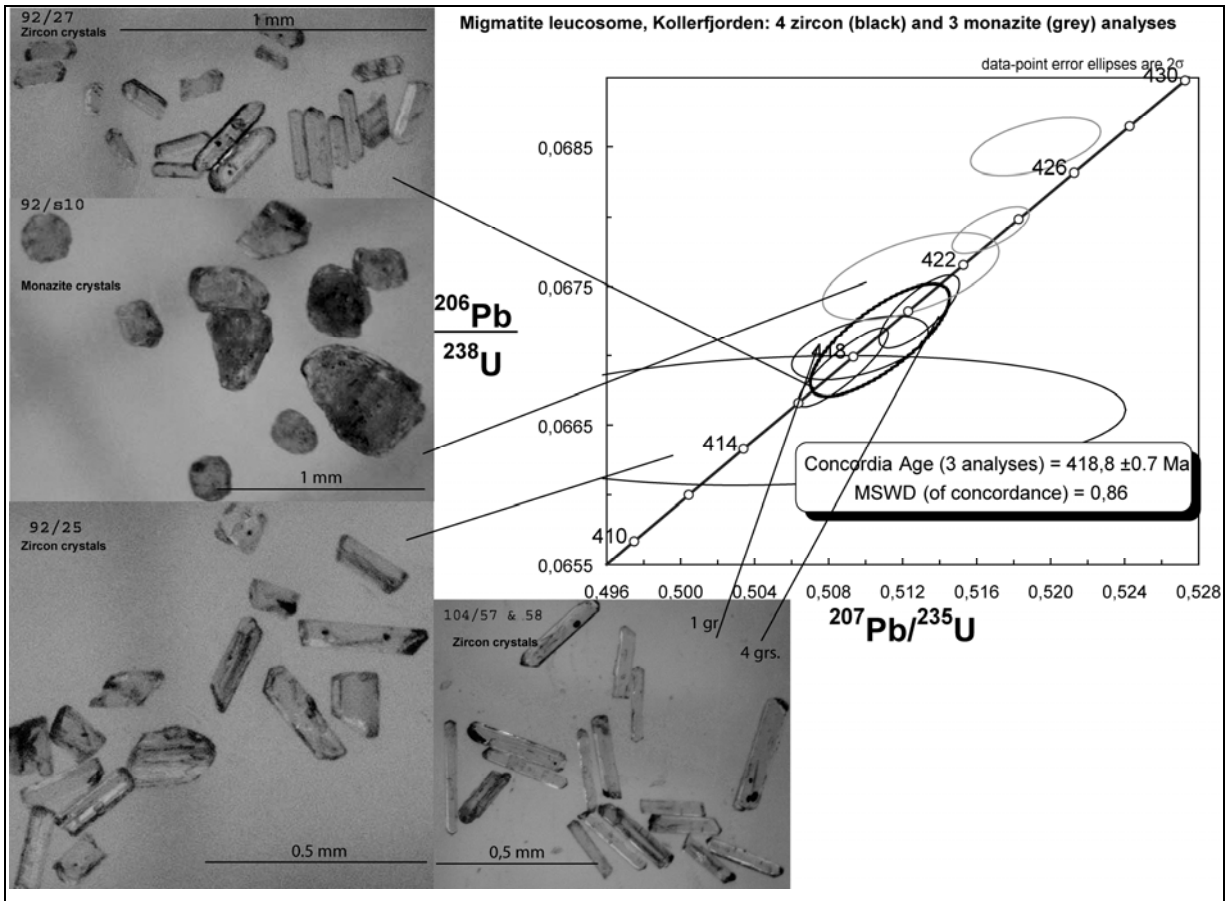

Figure 4.16: Concordia plot sample pim04-80. Grey ellipses: monazite, black: zircon. Concordia age is based on zircon data.

pim04-38: Granodioritic hornblende gneiss																					
101/s9 light tit.	9	54	30	169	0.61	1.68	95.2	935	1.4843	0.0053	0.15239	0.00032	0.67	0.07064	0.00019	914.4	1.8	924.0	2.2	947.0	5.4	3.7
101/s10 dark tit.	7	70	45	259	0.56	1.60	117.3	1534	1.5307	0.0101	0.15645	0.00080	0.90	0.07096	0.00021	937.0	4.5	942.8	4.0	956.3	6.0	2.2
101/59 zrc . prisms w/melt incl. l/w 3-4	4	1	11	70	0.43	0.00	1.1	620	1.4543	0.0145	0.14991	0.00065	0.56	0.07036	0.00059	900.5	3.6	911.6	6.0	938.7	17.0	4.4
101/58 zrc, prism w/black incl. l/w 5	3	1	37	223	0.58	0.00	1.5	1468	1.5149	0.0107	0.15505	0.00091	0.85	0.07087	0.00026	929.2	5.1	936.4	4.3	953.5	7.5	2.7
101/55 zrc. w/melt incl., l/w 5-6	1	5	11	73	0.47	0.00	1.2	2816	1.4349	0.0081	0.14734	0.00075	0.85	0.07063	0.00021	886.0	4.2	903.6	3.4	946.8	6.1	6.9
101/54 zrc. prism w/bio. incl. l/w 3	1	1	90	528	0.57	0.00	1.5	3541	1.5571	0.0060	0.15909	0.00061	0.78	0.07099	0.00018	951.7	3.4	953.3	2.4	957.0	5.2	0.6
101/53 zrc. clear prisms l/w 4	8	1	178	1040	0.62	0.00	1.8	5671	1.5332	0.0055	0.15715	0.00052	0.89	0.07076	0.00012	940.9	2.9	943.8	2.2	950.4	3.4	1.1
pim04-46: Gneissic granitic xenolith in Silurian granitoid																						
101/s.5 mnz., clear, few incl.	3	12	22	44	23.94	0.33	6.0	389	0.5091	0.0046	0.06730	0.00018	0.39	0.05486	0.00046	419.9	1.1	417.9	3.1	406.7	18.5	-3.4
101/s.4 mnz., turbid, w/incl.	4	12	248	576	19.68	0.30	5.7	5133	0.5123	0.0012	0.06726	0.00013	0.92	0.05525	0.00005	419.6	0.8	420.0	0.8	422.2	2.1	0.6
101/s.3 mnz., turbid, w/incl.	4	5	835	1704	22.77	1.86	11.6	3111	0.5120	0.0013	0.06722	0.00013	0.88	0.05524	0.00007	419.4	0.8	419.8	0.9	421.9	2.7	0.6
101/57 1 zrc. prismatic w/ melt incl. & black incl. l/w 4	1	1	60	354	0.67	0.00	0.8	4107	1.5057	0.0047	0.15428	0.00041	0.84	0.07078	0.00012	924.9	2.3	932.7	1.9	951.1	3.5	3.0
101/61 1 zrc. needle-like w/elongated melt incl. l/w 4-5	1	1	13	74	0.51	0.00	0.7	1152	1.5776	0.0309	0.16129	0.00311	0.96	0.07094	0.00038	964.0	17.2	961.4	12.1	955.7	10.8	-0.9
101/60 1 zrc.needle-like w/elongated melt incl. l/w 4-5	1	1	394	1957	1.26	0.00	0.6	32275	1.5682	0.0039	0.15968	0.00035	0.95	0.07123	0.00006	955.0	2.0	957.7	1.5	963.9	1.6	1.0
101/62 2 zrc. needle-like, l/w 4	2	1	57	378	0.63	0.00	1.1	2860	1.3172	0.0063	0.13727	0.00050	0.83	0.06959	0.00019	829.2	2.8	853.3	2.8	916.3	5.5	10.1
Newtontoppen granitoid																						
99/51 zrc. l/w 3 prism	1	1	2	28	0.36	0.00	0.6	219	0.5395	0.0175	0.07004	0.00034	0.48	0.05587	0.00170	436.4	2.1	438.1	11.5	447.1	66.4	2.5
99/56 zrc. l/w <2,5 small prisms	3	1	27	386	0.36	0.00	1.5	1131	0.5251	0.0038	0.06886	0.00025	0.60	0.05530	0.00032	429.3	1.5	428.5	2.5	424.4	13.0	-1.2
99/54 zrc. 4 tips w/incl.	4	1	345	5045	0.30	0.00	1.7	12524	0.5298	0.0039	0.06915	0.00050	0.99	0.05556	0.00007	431.0	3.0	431.6	2.6	435.0	2.8	0.9
104/S44 tit. VIAL F	3	170	26	257	1.22	3.45	588.7	339	0.5310	0.0054	0.06910	0.00022	0.38	0.05573	0.00053	430.8	1.3	432.5	3.6	441.5	20.9	2.5
104/S46 tit. VIAL H	3	90	24	240	1.19	3.35	303.1	326	0.5281	0.0052	0.06894	0.00017	0.26	0.05556	0.00053	429.8	1.0	430.6	3.5	435.0	21.1	1.2
99/53 aln.	>5	107	9	8	65.09	0.51	56.9	69	0.4438	0.0287	0.05727	0.00047	0.21	0.05621	0.00357	359.0	2.8	373.0	20.0	460.6	"<100"	22.7
99/54 aln.	>5	202	52	38	77.43	2.02	409.6	85	0.4407	0.0219	0.05747	0.00057	0.22	0.05562	0.00270	360.2	3.5	370.7	15.4	437.1	"<100"	18.1
99/53 zrc. tips no spike	3	1													0.00016					445.4		

Fraction Analysed	No. of	Weight	Pbt	U	Th/U	Pbc	Pbc	$^{206}Pb/^{204}Pb$	$^{207}Pb/^{235}U$	2 sigma	$^{206}Pb/^{238}U$	2 sigma	rho	$^{207}Pb/^{206}Pb$	2 sigma	$^{206}Pb/^{238}U$	2 sigma	$^{207}Pb/^{235}U$	2 sigma	$^{207}Pb/^{206}Pb$	2 sigma	Disc.
	grs.	[ug]	[ppm]	[ppm]		[ppm]	[pg]			[abs]		[abs]			[abs]	[abs]			[abs]		[abs]	[%]
pimsm-22-05: Grey two-mica granitoid, Bjørnfjorden																						
115/60 zrc. prism l/w 3-4 w/ melt incl some w/ black incl.	1	1	22	323	0.31	0.00	0.8	1710	0.5189	0.0030	0.06790	0.00025	0.71	0.05542	0.00022	423.5	1.5	424.4	2.0	429.4	9.0	1.4
115/61 zrc. prism l/w 3-4 w/ melt incl no black incl.	1	1	56	408	0.20	0.00	0.5	7073	1.6640	0.0199	0.13939	0.00167	0.99	0.08658	0.00016	841.2	9.4	994.9	7.6	1351.2	3.5	40.2
115/62 zrc. prism l/w 3-4 w/ melt incl some frags. small	5	1	54																	812.8	6.3	
115/S46 mnz. non-turbid, few incl.	16	23	209	1002	7.73	0.50	13.5	7271	0.5157	0.0013	0.06779	0.00014	0.94	0.05517	0.00005	422.8	0.9	422.3	0.8	419.3	1.9	-0.9
115/S50 mnz. non-turbid, few incl.	15	23	851	4480	6.81	0.36	10.3	42254	0.5138	0.0014	0.06759	0.00016	0.97	0.05513	0.00004	421.6	1.0	421.0	0.9	417.7	1.5	-1.0
pim04-72: Grey migmatitic granitoid, inner Kongsfjorden																						
99/52 L. zrc. Prisms, l/w 2.5	4	10	50	246	0.29	0.03	2.29189	13381	2.3919	0.0089	0.19873	0.00065	0.96	0.08729	0.00010	1168.5	3.5	1240.2	2.7	1366.9	2.1	15.9
99/60 P. zrc. short prisms, l/w 1.5-2	5	8	26	114	0.56	0.00	1.8	6508	2.5371	0.0094	0.20846	0.00066	0.95	0.08827	0.00011	1220.6	3.5	1282.7	2.7	1388.3	2.4	13.3
99/59 P. zrc. 4 tips	4	1	142	711	0.41	0.00	0.6	13471	2.2366	0.0094	0.19215	0.00074	0.96	0.08442	0.00010	1133.0	4.0	1192.6	2.9	1302.3	2.4	14.2
101/51 7 zrc. resorped	7	18	41	177	0.58	0.01	2.1	20053	2.6209	0.0062	0.21183	0.00044	0.96	0.08973	0.00006	1238.6	2.3	1306.5	1.7	1419.9	1.4	14.0
104/53/30 zrc. grain mount prism, l/w 2.5-3	1	1	46	249	0.33	0.00	1.0	2725	2.1453	0.0073	0.17845	0.00052	0.82	0.08719	0.00017	1058.5	2.9	1163.5	2.4	1364.7	3.8	24.3
104/55/37 zrc. grain moumt prism, l/w 2.5-3	1	1	27	135	0.50	0.00	1.0	1581	2.2838	0.0115	0.18764	0.00075	0.84	0.08827	0.00024	1108.6	4.1	1207.3	3.6	1388.4	5.3	21.9
104/56/25 zrc. grain mount prism, l/w 2.5-3	1	1	34	177	0.65	0.00	1.1	1766	2.2150	0.0457	0.16665	0.00342	0.99	0.09640	0.00022	993.6	18.8	1185.8	14.3	1555.5	4.3	38.9
104/52/36 zrc. grain mount prism, l/w 2.5-3	1	1	54	261	0.46	0.00	1.8	1752	2.5761	0.0101	0.19109	0.00064	0.78	0.09777	0.00024	1127.3	3.5	1293.9	2.9	1582.1	4.6	31.3
104/54/34 zrc. grain mount prism, l/w 2.5-3	1	1	67	153	0.18	0.00	0.8	5187	10.5219	0.0317	0.41280	0.00116	0.95	0.18487	0.00017	2227.7	5.3	2481.8	2.8	2697.0	1.5	20.5
99/s.56M mnz.	3	1	319	2252	3.58	23.82	26.6	382	0.5247	0.0049	0.06870	0.00028	0.47	0.05539	0.00046	428.3	1.7	428.3	3.3	428.1	18.4	-0.1
101/s.20 mnz.	8	25	78	504	4.89	0.01	2.346	22763	0.5154	0.0012	0.06764	0.00014	0.95	0.05527	0.00004	421.9	0.9	422.1	0.8	423.0	1.6	0.3
101/s.21 mnz.	1	15	142	993	4.36	0.35	7.2	8834	0.5166	0.0013	0.06799	0.00015	0.93	0.05511	0.00005	424.0	0.9	422.9	0.9	416.7	2.1	-1.8
104/S47 mnz.	2	1	230	1532	4.64	0.00	1.4	4795	0.5215	0.0015	0.06822	0.00017	0.78	0.05544	0.00010	425.4	1.1	426.2	1.0	430.1	4.1	1.1
99/62 zrc. "211" no spike	1	1	135					1493						0.09577	0.00021					1543.2	4.1	

Fraction Analysed	No. of	Weight	Pbt	U	Th/U	Pbc	Pbc	$^{206}Pb/^{204}Pb$	$^{207}Pb/^{235}U$	2 sigma	$^{206}Pb/^{238}U$	2 sigma	rho	$^{207}Pb/^{206}Pb$	2 sigma	$^{206}Pb/^{238}U$	2 sigma	$^{207}Pb/^{235}U$	2 sigma	$^{207}Pb/^{206}Pb$	2 sigma	Disc.
	grs.	[ug]	[ppm]	[ppm]		[ppm]	[pg]			[abs]		[abs]			[abs]	[abs]			[abs]		[abs]	[%]
pim04-75: Foliated granitoid leucosome, inner Kongsfjorden																						
99/57 zrc. prism, l/w 3-3.5	1	1	26	162	0.60	0.00	1.8	848	1.4868	0.0113	0.14861	0.00063	0.64	0.07256	0.00043	893.2		925.0		1001.7	11.9	11.6
99/58 zrc. stubby short prism, l/w 2-3	1	1	2	19	0.43	0.00	1.0	146	1.0202	0.0447	0.10886	0.00076	0.52	0.06796	0.00276	666.1		714.0		867.5	82.1	24.4
101/52 zrc. tips	6	1	109	625	0.33	4.01	6.1	1061	1.9043	0.0093	0.16388	0.00056	0.74	0.08428	0.00028	978.3		1082.6		1299.0	6.4	26.6
104/51 zrc. prism, l/w 3-3.5	1	1	42	169	0.54	0.00	0.6	4248	2.9625	0.0087	0.23267	0.00064	0.86	0.09235	0.00014	1348.5	3.3	1398.0	2.2	1474.5	2.8	9.5
101/s12 mnz. small, light	13	5	84	511	5.41	0.53	4.7	2305	0.5158	0.0014	0.06776	0.00014	0.79	0.05521	0.00009	422.7		422.4		420.6	3.8	-0.5
pimsm-19-05:Hornemantopppen granitoid																						
115/58 zrc., l/w 3-4, prisms	4	8	19	237	0.96	0.00	2.0	3976	0.5117	0.0015	0.06706	0.00015	0.74	0.05534	0.00011	418.4	0.9	419.6	1.0	426.1	4.5	1.9
115/59 zrc. l/w 3-4, prisms	1	1	55	676	1.14	0.00	0.7	4175	0.5107	0.0026	0.06699	0.00030	0.91	0.05529	0.00012	418.0	1.8	418.9	1.7	423.8	4.8	1.4
115/s7 tit.	>5	21	11	53	7.21	1.10	25.1	203	0.5104	0.0083	0.06705	0.00033	0.30	0.05521	0.00086	418.4	2.0	418.7	5.6	420.7	34.2	0.6
pim04-80: Two-mica leucosome of migmatite, Kollerfjorden																						
92/25 zrc. l/w 2-3 black incl. frag.	2	1	69	631	0.52	24.29	26.3	118	0.5062	0.0146	0.06653	0.00038	0.17	0.05518	0.00157	415.2	2.3	415.9	9.8	419.6	62.2	1.1
92/27 zrc. l/w 4-5, some w/ melt incl.	11	11	3	38	0.50	0.00	0.2	7817	0.5088	0.0020	0.06692	0.00023	0.87	0.05514	0.00011	417.5	1.4	417.6	1.3	418.1	4.4	0.1
104/58 zrc. l/w 4-5, black incl.	1	1	19	262	0.66	0.00	0.9	1288	0.5097	0.0030	0.06706	0.00019	0.53	0.05513	0.00028	418.4	1.1	418.2	2.0	417.4	11.2	-0.2
104/57 zrc. l/w 4-5, some w/ melt incl.	4	1	72	995	0.58	0.00	1.0	4076	0.5129	0.0018	0.06732	0.00021	0.76	0.05526	0.00013	420.0	1.3	420.4	1.2	422.7	5.1	0.7
104/S52 mnz.	5	15	56	354	5.03	1.08	18.2	1261	0.5168	0.0017	0.06791	0.00014	0.69	0.05519	0.00013	423.5	0.8	423.0	1.1	420.0	5.3	-0.9
104S63 mnz.	4	13	28	151	6.79	0.15	3.9	2180	0.5192	0.0029	0.06850	0.00017	0.51	0.05497	0.00026	427.1	1.0	424.6	1.9	410.9	10.6	-4.1
92/s.10 mnz.	>5	1	217	513	19.52	0.41	2.4	916	0.5124	0.0039	0.06757	0.00026	0.57	0.05500	0.00035	421.5	1.6	420.1	2.6	412.3	14.0	-2.3
92/26 zrc. l/w 2-3	1	2	16	200	0.75	0.00	0.7	2766	0.5686	0.0029	0.07304	0.00031	0.80	0.05646	0.00017	454.5	1.9	457.1	1.9	470.5	6.6	3.5

Table 4.1: Analytical results. Sample names in bold.
Explanation:
Numbers on the form "115/(s)57" indicates sample numbers of individual grains or fractions of grains
Weight is given in µg and with an uncertainty of <10 % for the fractions weighing more than the detection limit of the scale of 1 µg. The U and Pb concentrations are given in ppm with uncertainties according to weight uncertainties.
Th/U-ratio is modelled based on the $^{208}Pb/^{206}Pb$-ratio.
$^{206}Pb/^{204}Pb$-ratio is corrected for fractionation and blank. All other ratios and uncertainties are corrected for and calculated as explained in section 4.1.
All errors are given as absolute errors on the 2 sigma level
Abbreviations: Pbt: total Pb, Pbc: common Pb, Disc.: discordancy (in percent), Tit.: titanite, zrc.: zircon, incl.: inclusion, l/w: length to with-ratio, mnz.: monazite, aln.: allanite.

4.3: Comment on monazite results

Monazite suffers from negative discordance (it plots above concordia) in some of the samples (pimsm22-05, pim04-72, pim04-80). This is a common feature, and is mainly caused by two factors: Unsupported ^{206}Pb and U-loss.

Unsupported ^{206}Pb is derived from excess ^{230}Th (Harrison et al., 2002; Oberli et al., 2004), an intermediate daughter-product in the ^{238}U-^{206}Pb series with a half life of c. 75 Ka. Monazite has a strong affinity for Th, and may contain 2 to <40 % ThO_2 (Deer et al. 1992), and thus can incorporate a significant amount of ^{230}Th if it is available. The effect of this on the concordia plot is to bring the analysis up parallel to the $^{206}Pb/^{238}U$-axis.

Loss of U will have a similar effect except that the point will move up and to the right in the concordia diagram because both the $^{206}Pb/^{238}U$ and $^{207}Pb/^{235}U$ ages will be too old.

Also, some analysis may be affected by inheritance (e.g. pim04-72), which is a well documented feature for monazite (e.g Be Mezeme et al., In press; Cocherie et al., 1998).

Complicated cases occur when several factors disturb the isotopic composition of monazite, and in such cases it is difficult to come to conclusive ages.

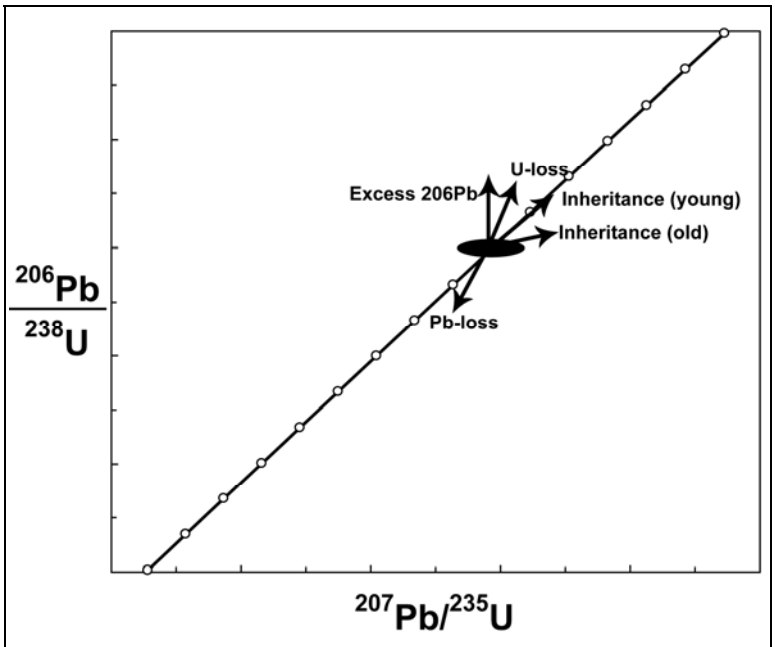

Figure 4.17: Discordance effects commonly observed in monazite.

Chapter 5: Discussion

5.1: Introduction:

The main points made here are 3-fold; a model for the genesis of the magmatic rocks of the North-Western Block in terms of isotopic ages; the similarities of this evolution with the Caledonian Laurentian margin, and finally a model for the transport of the Svalbard basement terranes.

A model for the tectonic evolution of the North-Western Block has to comprise development of Proterozoic sedimentary basins, involvement the old crust in the Grenvillian orogeny and polyphased Caledonian structural and metamorphic evolution. Furthermore, such a model needs to take into account subsequent structural features that are observed in the Devonian rocks as well as the stages that led to the establishment of extensional basins in the Carboniferous and subsequent stable platform sedimentation throughout the late Palaeozoic and Mesozoic.

Pre-Caledonian evolution of the North-Western Block

Pre-Grenvillian zircon xenocrysts of Mesoproterozoic age are present in the migmatites in Kongsfjorden, and may point to an igneous event in the early Paleoproterozoic to late Mesoproterozoic (chapter 4). Deposition of the Krossfjorden Group metasediments is poorly constrained. The absence of post-Grenvillian zircons in quartzites reported by Ohta et al., (2002) indicates that the Krossfjorden Group sediments can be pre-Grenvillian (but also post-Grenvillian), in age.

The presence of 962 ± 6 Ma and 970 ± 7 Ma orthogneiss in Krossfjorden provides evidence of the influence of the Grenvillian orogeny also in this terrane. Grenvillian magmatic rocks has previously been well documented from eastern Svalbard, as summarized by Johansson et al., (2005).

Caledonian magmatic evolution

Reported ages for the Caledonian rocks in the North-Western Block range between c. 470 and c. 410 Ma, spanning over a c. 60 Ma long time interval (chapter 2). Following an early phase of HP metamorphism and subduction part of the block crust was subject to extensive high-T metamorphism and intrusion of granites. Two generations of granitoids within the migmatite area of north-west Spitsbergen was recognized by Schetelig, (1912), who suggested that the Hornemantoppen granitoid was the youngest of the intrusives.

Figure 5.1 illustrates the chronology of the Caledonian intrusive rocks. Two phases of intrusions, the grey granitoids and the Hornemantoppen granitoid, are separated in time by minimum 2 Ma based on ID-TIMS data from this study. The first episode of granitoid emplacement, represented in this study by the two-mica grey granitoid from Bjørnfjorden (pimsm22-05), is characterized by fine-grained two-mica petrography and abundant inherited zircon crystals (chapter 4). The amount and nature of the inherited zircon crystals points towards a low-temperature origin of the magma (Miller et al., 2003) for this sample. Contrastingly, the Hornemantoppen granitoid is characterized by little inherited zircon. Also, the size of the Hornemantoppen intrusion indicates that it must have been associated with a greater magnitude of heat influx. Temperature estimates for the marble skarns within the

migmatized area and non-migmatitic garnetiferous pelites are in the range of 650 -700^0 C within the upper 10-15 km of the crust (Bucher-Nurminen, 1981; Klaper, 1986; Lange, 1999), and give some clue of the temperature conditions in the crust during (peak) metamorphism.

The melting of continental crustal rocks to form granitoids is controlled by 3 main factors: The requirement of a suitable protolith, an adequate source of heat and a melting mechanism (e.g. decompression melting, dehydration reactions or high H_2O-activity) for the protolith to reach sub-solidus. A suitable protolith (e.g.Patino, 1999) in north-west Spitsbergen is found in the metasedimentary Krossfjorden Group. Evidence for the nature of heat sources and mechanisms for melting is more difficult to point at. Underplating of mantle-derive basaltic magmas (e.g. Clemens, 2003; Harris et al., 2000; Petford et al., 2000 and references therein) and radiogenic heating in the crust (e.g. England et al., 1992; Ledru et al., 2001 and references therein) are two possible sources for heat. The latter requires a significant period of thermal maturation, and may have contributed to the latest stage of granitic intrusion in north-west Spitsbergen. Evidence for basaltic underplating is difficult to point to because such melts would be less likely to reach higher crustal levels. However, mafic dykes, seemingly undeformed, are present in the Smeerenburgfjorden area (chapter 3, this study and Hjelle and Ohta, (1974).

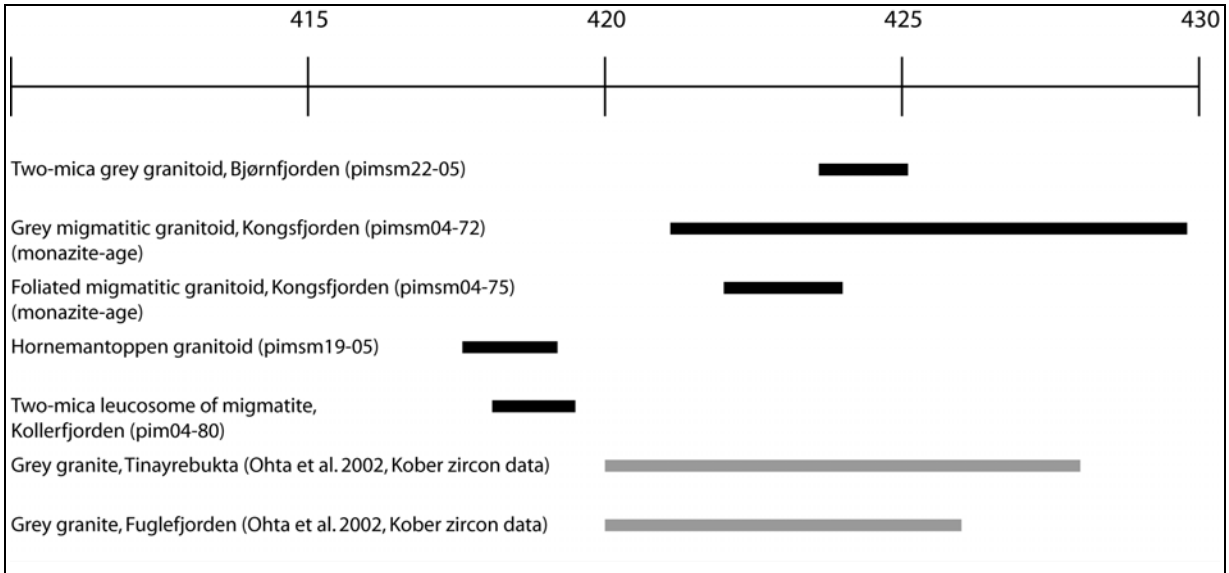

Figure 5.1: The Caledonian magmatic evolution of the North-Western Block. Uncertainties are included in age bars. The ages for pimsm-04-72 & pim04-75 may not date crystallization of granitoids (chapter 4) but rather represent metamorphic ages. The two lower samples are located in eastern Krossfjorden (grey granite, Tinayrebukta, chapter 3) and northern Vasahalvøya (grey granite, Fuglefjorden). The ages reported in Ohta et al., (2002) for these two samples are $^{207}Pb/^{206}Pb$-ages obtained by the Pb-evaporation (Kober) method.

The abundance and differing characteristics of granitoids in north-west Spitsbergen makes it an exciting area for studies of granitoid genesis and high-temperature metamorphism. A base for such studies is precise age data.

5.2: Laurentian affinities of the Western Terranes

Eastern Svalbard and the North-East Greenland Caledonides has been correlated based on similarities in pre-Grenvillian supracustal record, Grenvillian tectonic and magmatic evolution, Neoproterozoic to middle Ordovician sedimentary record and Caledonian tectonic and magmatic evolution. This is summarized in Johansson et al., (2005). Additionally, present data from the Newtontoppen granitoid show that this batholith crystallized at 430 ± 1 Ma, simultaneously with the Grejsdalen pluton in North-East Greenland (Andresen et al., in press).

As mentioned in chapter 2, great similarities also exist between Svalbards western terranes and North-East Greenland:

The sedimentary record of the North-Western Terrane is poorly understood, partly because of the high metamorphic grade of these rocks. The present knowledge indicates that the Krossfjorden Group could have been deposited in the late Mesoproterozoic, Neoproterozoic or even, although less likely, in the Cambrian-Ordovician. Because of the fragmented knowledge, correlation based on sedimentary similarities is uncertain, and correlation with other basement provinces must be aided by other tectonic fingerprinting:

Radiometric data pointing towards a Grenvillian tectonometamorphic event has been presented by Ohta et al., (2003); Ohta et al., (2002); Peucat et al., (1989). Data obtained in this study show that a magmatic event dates to 970-960 Ma. This age is slightly older than most data from the East Greenland Grenvillian rocks, which record ages of c. 915-955 Ma (e.g. Kalsbeek et al., 2000; Leslie and Nutman, 2003; Strachan et al., 1995; Watt et al., 2000) (Table 5.1, age data).

The Caledonian thermal record of western Svalbard consists of 2 main stages: middle/late Ordovician HP metamorphism and late Silurian HT metamorphism and related granitoid intrusion. The c. 450 Ma HP metamorphic event in Biscayarhuken in the north and a slightly older, but more poorly constrained in time, event in Motalafjella further south (see chapter 2) represents the first stage. These rocks may have formed in a subduction complex where Iapetan oceanic crust was subducted under the Laurentian continent. Bjørnerud et al., (1991) pointed out that Ordovician thrusting in south-western Spitsbergen may relate to the Motalafjella event. Simultaneously, I-type calc-alkaline granitoids crystallized in North-East Greenland (Scoresby Sund region, Rehnstrøm, pers. comm., Nutman & Kalsbeek, unpubl. data in Higgins et al., (2004). These intrusions may represent a magmatic arc developed as a response to the subduction going on further east. In the outboard reaches of this margin, metamorphic zircon growth is recorded in Smallefjord Group metasediments at 445 ± 10 Ma (Strachan et al., 1995).

The late Silurian HT event in north-western Spitsbergen is recorded by ID-TIMS U/Pb data as 2 discrete magmatic events at c. 419 Ma and 422 Ma, respectively (see chapter 4). This event has its counterpart in Laurentia in the S-type, two mica granites and migmatites described by Andresen et al., (in press); Gilotti and McClelland, (2005); Hartz et al., (2001); Kalsbeek et al., (2001); Leslie and Nutman, (2003) and others. The ages reported here from Svalbard fall within the youngest group of granitoid ages from North-East Greenland, where 425-430 Ma seems to dominate, but recent studies show younger (c. 410-415) ages (Gilotti and McClelland, 2005). A summary of North-East Greenland and West Spitsbergen age data is given in table 5.1.

South-western Spitsbergen bear evidence of pre-(or early?) Grenvillian magmatism, unfortunately poorly constrained (1100-1300 Ma, table 2.1) (Balasov et al., 1995, 1996b) followed by a Grenvillian tectonic event (Bjørnerud et al., 1990). Unconformably above this are Neoproterozoic supracrustals that was deformed during the Caledonian orogeny. The Neoproterozoic and underlying rocks can be correlated with Nordaustlandet (Gee and Tebenkov, 2004) and also bear similarities with North-East Greenland, although the tectonic evolution of the area is not as well understood as e.g. Nordaustlandet.

Some differences in geologic evolution exist between North-East Greenland and the Western Terranes of Svalbard: Paleoproterozoic (c. 1740 Ma) basement are not documented in the Western Terranes of Svalbard, but are present in North-East Greenland (Pedersen et al., 2002) (and Eastern Svalbard, (Witt-Nilsson, 1998)). Thermal post-410 Ma events in Svalbard are not distinguished except for Ar/Ar cooling ages, whereas in North-East Greenland 390-410 Ma eclogites occur in an extensive area (“the North-East Greenland eclogite province”), as documented by (Gilotti and Krogh, 2002; Gilotti et al., 2004).

Time (in Ma)	**North-East Greenland**	**Western Spitsbergen Terranes**
2000-1740	Paleoproterozoic basement	Inherited zircons (also pre-2000 Ma)
1600(?)- 1050	Late Archean, Paleoproterozoic and Mesoproterozoic inherited and detrital zircons, Zig-Zag Dal basalts (Eastern North Greenland): 1382 ± 2 Ma	Deposition of Proterozoic sedimentary sequence (Eimfjellet & Isbjørhamna Gp`s) & c. 1200-1300 Ma magmatism in SW. Deposition of Krossfjorden Gp? (NW)
1050-960	Deposition of Krummedal and Smallefjord sequences	Deposition of Deilegga Group siliclastics? (SW) & Krossfjorden Group? (NW)
970-920	Grenvillian metamorphism, magmatism and deformation	Grenvillian metamorphism, magmatism and deformation
800-470	Deposition of Eleonore Bay Supergroup, Vendian Tillite Group & and locally Ordovician sediments.	Deposition of siliclastic, carbonates and Vendian tillites. Upper Proterozoic event followed by Cambrian-Early Ordovician sedimentation (SW) Deposition of Krossfjorden Group? (NW)
470?-440	Caledonian back-arc magmatism (Scoresby Sund) and metamorpishm (75^0N)	Caledonian HP/LT metamorphism (Biscayarhuken & Motalafjella Complexes).
430-410	Caledonian anatectic granites	Caledonian anatectic granites & batholiths
410-390	Late Caledonian HP metamorphism	Caledonian Ar/Ar-(K/Ar) cooling ages
>Carboniferous	Devonian Old Red Sandstone deposition & deformation	Devonian Old Red Sandstone deposition & transcurrent deformation
Lower Carboniferous-Tertiary	Deposition of Carboniferous to Cretaceous sediments, Tertiary basalts	Deposition of Carboniferous to Cretaceous sediments
Tertiary	Opening of the Atlantic	West Spitsbergen Fold and thrust belt

Table 5.1: Summary of the geological evolution of the Western Spitsbergen Terranes and North-East Greenland. References for the Western Spitsbergen Terrane are given in the text. North-East Greenland summary largely from Johansson et al., (2005) and Upton et al., (2005) (Zig Zag Dal Basalts), Rehnstrøm, pers. comm; Strachan et al., (1995) (Scoresby Sund I-type magmatism).

A transcurrent transport and amalgamation regime

The issues discussed above for the evolution of the Western Terranes indicates a common crustal evolution history with the North-East Greenland Caledonides, in accordance with (Harland and Wright, 1979) and most subsequent studies, the latest being (Gee and Tebenkov, 2004). The general idea that the Svalbard Terranes originated in Laurentia is accepted by most authors, and several, but similar, models for the evolution of Svalbard in the aftermath of the Caledonian orogeny are based on Harland`s original idea illustrated in figure 5.2

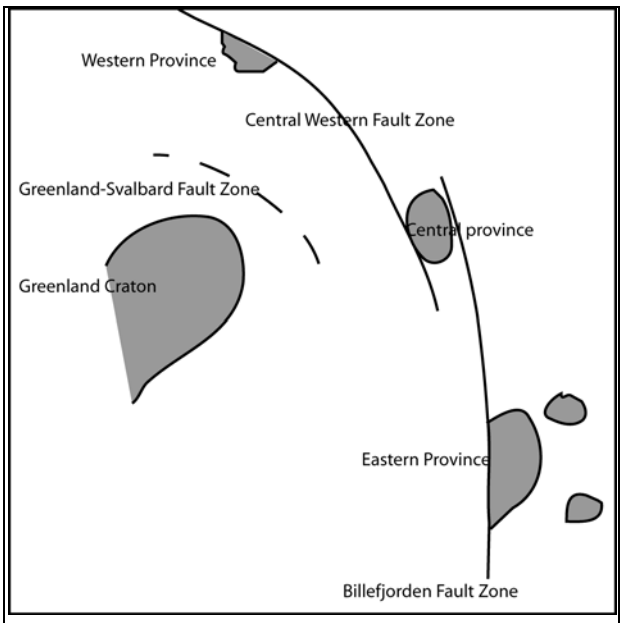

Figure 5.2: Harland 1979`s view on the transccurent movements responsible for Svalbards terrane, (or province), configuration

The evidence found in Svalbard of transcurrent movement is twofold: direct evidence is found in the Devonian rocks (McCann, 2000) as well as in some of the basement domains (Western Ny Friesland, Gee and Page, (1994)). Indirect evidence comes from the contrasting geology across north-south-trending lineaments described in chapter 2. An upper time constraint for the transcurrent movement on the Breibogen-Bockfjorden fault is given by the Pragian-Emsian Wood Bay Formation (McCann 2000), whereas the overlap assemblage on the Billefjorden fault zone and the Lomfjorden fault is Lower Carboniferous in age (Piepjohn et al, (2000b). Lower time-constraints are not as easy definable, but Gee and Page, (1994) suggest a Silurian age for the major movements. Some of the faults were reactivated later, i.e. the Billefjorden Fault Zone, which was a basin-controlling fault in the Carboniferous and also active in the Tertiary. However, it seems that post-middle Carboniferous activity was mostly of dip-slip nature (Witt-Nilsson, 1998).

Gee and Page, (1994); Gee and Tebenkov, (2004) prefer a model for the terrane assembly where the Eastern and Western Svalbard Terranes were located on the eastern margin of East Greenland. In this model it is assumed that the Motalafjella-bearing central West Spitsbergen originated north of Greenland, and constitutes a fragment of the Paleozoic Ellesmerian orogeny, based on correlation with a HP complex there (e.g. Trettin et al., 1987).

Andresen (2002, 2004) presented a model for the transport and amalgamation of the Svalbard terranes where all the terranes originated on the North-East Greenland margin. This model thus implies that the HP/UHP-rocks of Spitsbergen all formed in a mid-late Ordovician subduction zone between Baltica and Laurentia (see figure 5.3).

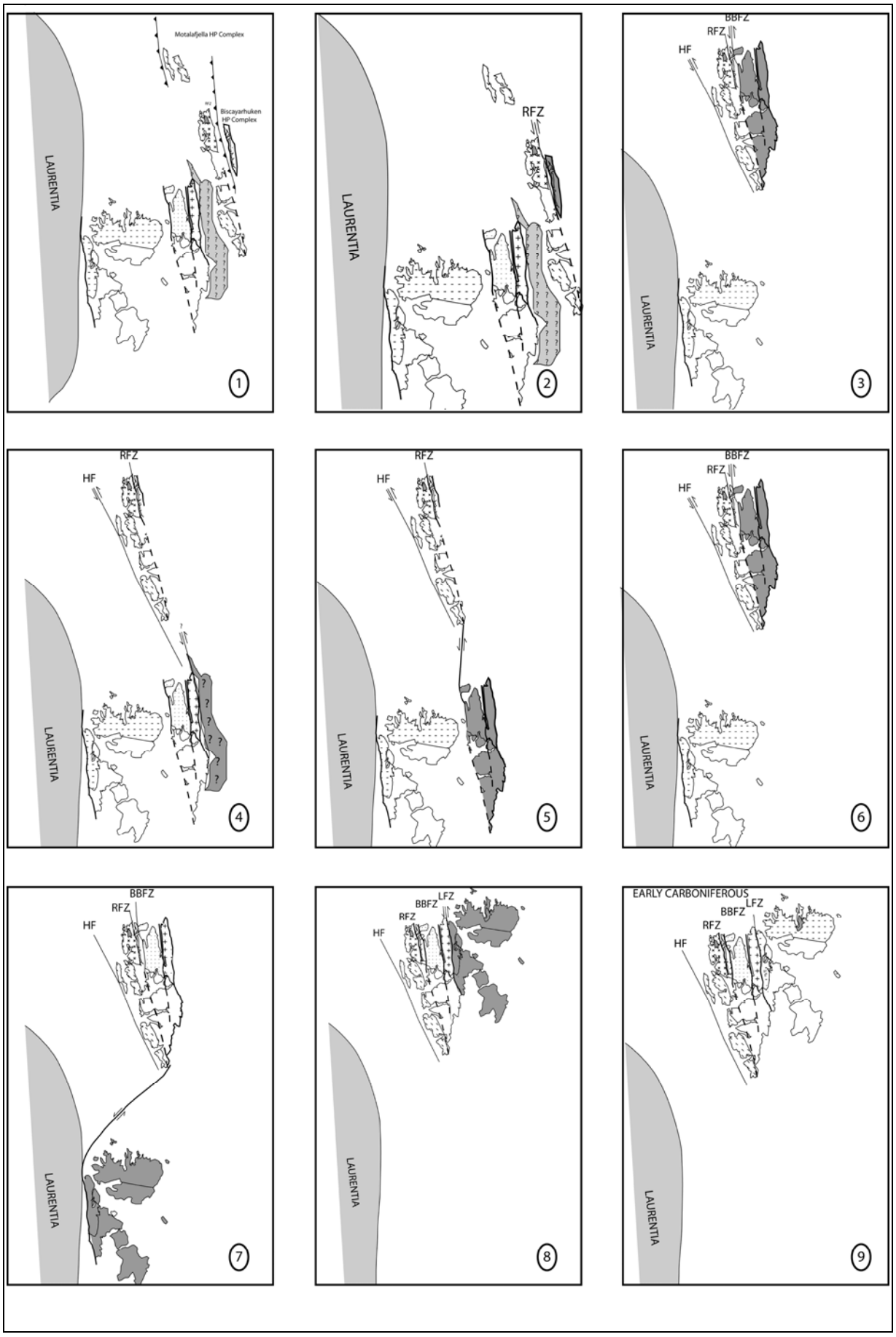
Motalafjella HP Complex
Biscayarhuken HP Complex
RFZ
LAURENTIA
1
2
BBFZ
RFZ
HF
3
4
5
6
LFZ
7
8
EARLY CARBONIFEROUS
9

Figure 5.3: Proposed sequence of events during the transport and amalgamation of Svalbards Caledonian Terranes. ***1****.: Subduction between Laurentia and Baltica. Formation of the HP Complexes of Western Spitsbergen.* ***2****.: Accretion of Biscayar-Holtedalfonna Block with the Western Block along Raudfjorden Fault Zone (RFZ).* ***3****: Activation of the Hornsund (?) Fault Zone.* ***4****.:Detachment of an unkown terrane (Andreè Land Basement?)* ***5****. Activation of the Breibogen-Bockfjorden Fault (BBFZ).* ***6****: Amalgamation of the West Ny Friesland Terrane + unknown Andreè Land Basement with the Western Terranes.* ***7*** *&* ***8****: Activation of the Lomfjorden Fault Zone (LFZ) and transport and amalgamation of the Nordaustlandet terrane.* ***9*** *Final transport to a position north-east of Greenland (Roberts et al., 2003).*
Abbreviations:
HF: Hornsund fault zone (Breivik et al., 2005), RFZ: Raudfjorden fault zone ,BBFZ, Breibogen-Bockfjorden Fault Zone, LFZ, Lomfjorden fault zone

Left-lateral transcurrent detachment and northwards transport of the terranes from the eastern margin of Laurentia must imply that the most outboard terranes where detached first followed by terranes originally situated further away from the Caledonian margin of the Laurentian continent. The terranes may have been detached in the following sequence; the Biscayar-Holtedalfonna block, the North-Western Block, the Ny Friesland Terrane and finally the Nordaustlandet Terrrane. The cover sequences of the Billefjorden fault zone/Lomfjorden fault (lower Carboniferous, (Piepjohn et al. 2000b) and the Breibogen-Bockfjorden fault zone (lower-middle Devonian, (McCann 2000) suggests that movement on the latter ceased first.

Some advantages of the model presented by (Andresen 2002, 2004) are:
-It does not require a major rotation of the dominant N-S structural grain of the Caledonian rocks in Svalbard
-The Terranes are “born” in the right order in the Caledonian margin: Terranes with oceanic rocks (Western Terranes, Biscayar-Holtedalfonna Block) are closest to the subduction zone and continental terranes (Ny Friesland, Nordaustlandet) originated closer to the hinterland.
-The previous remark allows for a more logical detachment sequence:
Most outboard terranes are detached first, exposing inboard terranes to subsequent transcurrent faulting.

A more recent analogue to the transccurent regime discussed above is found in one of the worlds most intensively studied continental margins: The western North America, where a similar tectonic regime is constantly transporting exotic terranes from north to south along strike slip faults, e.g. the San Andreas Fault.

5.3: Conclusions:

Following the discussion above, the following conclusions can be made:

- The North-Western Spitsbergen Block took part in the Grenvillian orogeny also affecting Eastern Svalbard and North-East Greenland
- Caledonian batholith intrusion in Eastern Svalbard is constrained to 430 ± 1 Ma.
- Caledonian migmatization and HT metamorphism in the North-Western Spitsbergen Block is constrained to c. 422-418 Ma.
- Intrusion of Caledonian granitoids occurred in two stages;
    - 422,5 ± 1,5 Ma: Fine-grained grey granitoids
    - 418,4 ± 0,8 Ma: The Hornemantoppen batholith
- An attempt can be made to integrate knowledge from Svalbard and North-East Greenland into a transcurrent model for the amalgamation of Svalbards various Terranes (based on (Andresen, 2004),(2002)

Agard, P., L. Labrousse, et al. (2005). Discovery of Paleozoic Fe-Mg carpholite in Motalafjella, Svalbard Caledonides; a milestone for subduction-zone gradients. *Geology (Boulder)* **33**(10): 761-764

Anczkiewicz R., Oberli F., Burg J. P., Villa I. M., Gunther D., and Meier M. (2001) Timing of normal faulting along the Indus Suture in Pakistan Himalaya and a case of major 231Pa/235U initial disequilibrium in zircon. *Earth and Planetary Science Letters* **191**(1-2), 101-114.

Andersen, T.B. & Jamtveit, B. 1990. Uplift of deep crust during orogenic extensional collapse: a model based on field studies in the Sogn-Sunnfjord region, W. Norway. *Tectonics*, **9**, 1097-1111.

Andersen, T.B., Jamtveit, B., Dewey, J.F. & Swensson, E. 1991. Subduction and eduction of continental crust: major mechanism during continent-continent collision and extensional collapse, a model based on the south Norwegian Caledonides, *Terra Nova*, **3**, 303-310

Andresen A. (2004) Origin of the Caledonian terranes of Svalbard. *Geologiska foreningens forhandlingar*, 77.

Andresen A., Rehnstrøm E. F., and Holte M. (in press) Timing of syn-contractional and syn-extensional intrusions in the NE Greenland Caledonides.

Agard, Philippe, Labrousse, L., Elvevold, S., Lepvrier, C (2005) Discovery of Paleozoic Fe-Mg carpholite in Motalafjella, Svalbard Caledonides; a milestone for subduction-zone gradients Geology (Boulder), 33; 10, 761-764

Armstrong H. A., Nakrem H. A., and Ohta Y. (1986) Ordovician conodonts from the Bulltinden Formation, Motalafjella, central-western Spitsbergen. *Polar Research* **4**(1), 17-23.

Balasov J. A., Peucat J. J., Teben k. A. M., Ohta Y., Larionov A. N., and Sirotkin A. N. (1996a) Additional Rb-Sr and single-grain zircon datings of Caledonian granitoid rocks from Albert I Land, Northwest Spitsbergen. *Polar Research* **15**(2), 153-165.

Balasov J. A., Teben k. A. M., Ohta Y., Larionov A. N., Sirotkin A. N., Gannibal N. F., and Ryungenen G. I. (1995) Grenvillian U-Pb zircon ages of quartz porphyry and rhyolite clasts in a metaconglomerate at Vimsodden, southwestern Spitsbergen. *Polar Research* **14**(3), 291-302.

Balasov Y. A., Peucat J. J., Teben k. A. M., Ohta A. M., Larionov A. N., Sirotkin A. N., and Bjornerud M. (1996b) Rb-Sr whole rock and U-Pb zircon datings of the granitic-gabbroic rocks from the Skalfjellet Subgroup, Southwest Spitsbergen. *Polar Research* **15**(2), 167-181.

Be Mezeme E., Cocherie A., Faure M., Legendre O., and Rossi P. (In press) Electron microprobe monazite geochronology of magmatic events: Examples from Variscan migmatites and granitoids, Massif Central, France. *Lithos* **In Press, Corrected Proof**.

Bergh S. G. and Andresen A. (1990) Structural development of the Tertiary fold-and-thrust belt in East Oscar II Land, Spitsbergen. *Polar Research* **8**(2), 217-236.

Bergh S. G., Ohta Y., Andresen A., Maher H. D., Braathen A., and Dallmann W. K. (2003) Geological map of Svalbard 1:100,000, sheet B8G St.Jonsfjorden. *Norsk Polarinstitutt Temakart.*

Bernard G. J., Peucat J. J., and Ohta Y. (1993) Age and nature of protoliths in the Caledonian blueschist-eclogite complex of western Spitsbergen; a combined approach using U-Pb, Sm-Nd and REE whole-rock systems. *Lithos* **30**(1), 81-90.

Bjørnerud M. (1990) An upper Proterozoic unconformity in northern Wedel Jarlsberg Land, Southwest Spitsbergen; lithostratigraphy and tectonic implications. *Polar Research* **8**(2), 127-139.

Bjørnerud M., Craddock C., and Wills C. J. (1990) A major late Proterozoic tectonic event in southwestern Spitsbergen. *Precambrian Research* **48**(1-2), 157-165.

Bjørnerud, M., P. L. Decker, et al. (1991). Reconsidering Caledonian deformation in Southwest Spitsbergen. *Tectonics* **10**(1): 171-190.

Breivik, A. J., R. Mjelde, et al. (2005). Caledonide development offshore-onshore Svalbard based on ocean bottom seismometer, conventional seismic, and potential field data. *Tectonophysics* **401**(1-2): 79-117.

Bucher-Nurminen K. (1981) Petrology of chlorite-spinel marbles from NW Spitsbergen (Svalbard). *Lithos* **14**(3), 203-213.

Clemens J. D. (2003) S-type granitic magmas; petrogenetic issues, models and evidence. *Earth-Science Reviews* **61**(1-2), 1-18.

Cocherie A., Legendre O., Peucat J. J., and Kouamelan A. N. (1998) Geochronology of polygenetic monazites constrained by in situ electron microprobe Th-U-total lead determination; implications for lead behaviour in monazite. *Geochimica et Cosmochimica Acta* **62**(14), 2475-2497.

Corfu F., Hanchar J. M., Hoskin P. W. O., and Kinny P. D. (2003) Atlas of zircon textures. In *Zircon*, Vol. **53**;, pp. 469-500. Mineralogical Society of America and Geochemical Society.

Corfu F. and Stone D. (1998) The significance of titanite and apatite U-Pb ages; constraints for the post-magmatic thermal-hydrothermal evolution of a batholithic complex, Berens River area, northwestern Superior Province, Canada. *Geochimica et Cosmochimica Acta* **62**(17), 2979-2995.

Dallmann W. K., Ohta Y., Elvevold S., and Blomeier D. E. (2002) Bedrock map of Svalbard and Jan Mayen, 1:750,000, selected areas 1:250,000. . *Norsk Polarinstitutt Temakart*.

Dallmann W. K., Piepjohn K., and Ohta Y. (2005) Geological map of Svalbard, sheet B4G, Reinsdyrflya. *Norsk Polarinstitutt temakart nr. 38*.

Dallmeyer R. D., Peucat J. J., Hirajima T., and Ohta Y. (1989) Tectonothermal chronology within a blueschist-eclogite complex, west-central Spitsbergen, Svalbard; evidence from (super 40) Ar/ (super 39) Ar and Rb-Sr mineral ages. *Lithos* **24**(4), 291-304.

Deer, Howie and Zussmann, (1992): *An Introduction to the Rock-Forming Minerals*, 2nd ed.

England P., Le F. P., Molnar P., and Pecher A. (1992) Heat sources for Tertiary metamorphism and anatexis in the Annapurna-Manaslu region, central Nepal. *Journal of Geophysical Research, B, Solid Earth and Planets* **97**(2), 2107-2128.

Fairchild I. J. and Hambrey M. J. (1995) Vendian basin evolution in East Greenland and NE Svalbard. In *Neoproterozoic stratigraphy and Earth history*, Vol. **73**; 1-4, pp. 217-233. Elsevier.

Friend P. F., Harland W. B., Rogers D. A., Snape L., and Thornley R. S. W. (1997) Late Silurian and Early Devonian stratigraphy and probable strike-slip tectonics in northwestern Spitsbergen. *Geological Magazine* **134**(4), 459-479.

Friend P. F. and Moody-Stuart M. (1972) Sedimentation of the Wood Bay Formation (Devonian) of Spitsbergen: Regional analysis of a late orogenic basin. *Norsk polarinstitutt skrifter* **157**, 77 pp.

Gavrilenko B. V., Balashov Y. A., Teben k. A. M., and Larionov A. N. (1993) Ranneproterozoyskiy U-Pb-vozrast "reliktovogo" tsirkona iz vysokokaliyevykh kvartsevykh porfirov Zemli Vedel'-Yarlsberga (U/Pb Early Proterozoic age of "relict" zircon from high potassium quartz porphyries of Wedel Jarlsberg Land, southwest Spitsbergen.). *Geokhimiya* **1993**(1), 154-158.

Gee D. G. (1972) Late Caledonian (Haakonian) movements in northern Spitsbergen. *Norsk Polarinstitutt årbok*, **1970**, 92-101.

Gee D. G. and Hjelle A. (1966) On the crystalline rock of northwest Spitsbergen. *Norsk Polarinstitutt årbok*, **1964**, 31-45

Gee D. G. and Moody-Stuart M. (1966) The base of the Old Red Sandstone in central north Haakon VII Land, Vestspitsbergen. *Norsk Polarinstitutt årbok* **1964**, 57-68.

Gee D. G. and Page L. M. (1994) Caledonian terrane assembly on Svalbard; new evidence from (super 40) Ar/ (super 39) Ar dating in Ny Friesland. *American Journal of Science* **294**(9), 1166-1186.

Gee D. G. and Tebenkov A. M. (2004) Svalbard: A fragment of the Laurentian margin. *The Neoproterozoic Timanide orogen of Eastern Baltica, Geol. soc. of London Mem.* **30**, 191-206.

Gee D. G., Witt-Nilsson P., Johansson Å., and Hellman F. J. (2001) Continental collision and lateral escape deformation in the lower and upper crust; an example from Caledonide Svalbard; discussion and reply. *Tectonics* **20**(5), 788-796.

Gilotti J. A. and Krogh R. E. J. (2002) First evidence for ultrahigh-pressure metamorphism in the north-east Greenland Caledonides. *Geology (Boulder)* **30**(6), 551-554.

Gilotti J. A. and McClelland W. C. (2005) Leucogranites and the time of extension in the East Greenland Caledonides. *Journal of Geology* **113**(4), 399-417.

Gilotti J. A., Nutman A. P., and Brueckner H. K. (2004) Devonian to Carboniferous collision in the Greenland Caledonides; U-Pb zircon and Sm-Nd ages of high-pressure and ultrahigh-pressure metamorphism. *Contributions to Mineralogy and Petrology* **148**(2), 216-235.

Gjelsvik T. (1979) The Hecla Hoek Ridge of the Devonian graben between Liefdefjorden and Holtedahlfonna, Spitsbergen. *The geological development of Svalbard during the Precambrian, lower Palaeozoic, and Devonian. Oslo, Norway, Norsk Polarinstitutt Skrifter* **167**, 63-71.

Gromet L. P. and Gee D. G. (1998) An evaluation of the age of high-grade metamorphism in the Caledonides of Biskayerhaloya, NW Svalbard. In *Tectonics and geological history of some Phanerozoic orogens; honorary volume to David G. Gee on the occasion of his 60th birthday.*, Vol. **120**; 2 (ed. B. Sundquist and B. Stephens Michael), pp. 199-208. Geological Society of Sweden.

Harland W. B. (1985) Caledonide Svalbard. In *The Caledonide Orogen; Scandinavia and related areas; Vol 2*. John Wiley & Sons.

Harland W. B. (1997) *The geology of Svalbard*. Blackwell [for the] Geological Society of London.

Harland W. B., Cutbill J. L., Friend P. F., Gobbette D. J., Holliday D. W., Maton P. I., PArker J. R., and Wallis R. H. (1974) The Billefjorden Fault Zone, Spitsbergen the long history of a major tectonic lineament,. *Norsk polarinstitutt skrifter* **161**, 72.

Harland W. B., Hambrey M. J., and Waddams P. (1993) The Vendian geology of Svalbard. *Norsk Polarinstitutt skrifter* **193**, 1-130.

Harland W. B. and Horsfield W. T. (1974) West Spitsbergen orogen. In *Mesozoic-Cenozoic orogenic belts; Data for Orogenic Studies; other orogens*, Vol. **4**;, pp. 747-755. Geological Society of London.

Harland W. B., Horsfield W. T., Manby G. M., and Morris A. P. (1979) An outline pre-Carboniferous stratigraphy of central western Spitsbergen. In *The geological development of Svalbard during the Precambrian, lower Palaeozoic, and Devonian*, Vol. **167**, pp. 119-144. Norsk Polarinstitutt.

Harland W. B. and Wright N. J. R. (1979) Alternative hypothesis for the pre-Carboniferous evolution of Svalbard. In *The geological development of Svalbard during the Precambrian, lower Palaeozoic, and Devonian*, Vol. **167**, pp. 89-117. Norsk Polarinstitutt.

Harris N. B. W., Vance D., and Ayres M. (2000) From sediment to granite; timescales of anatexis in the upper crust. In *Rates and timescales of magmatic processes*, Vol. **162**; 2, pp. 155-167. Elsevier.

Harrison T. M., Catlos E. J., and Montel J. M. (2002) U-Th-Pb Dating of Phosphate Minerals. In *Phosphates*, Vol. **48** (ed. J. M. Kohn, J. Rakovan, and J. M. Hughes). Mineralogical Society of America and Geochemical Society.

Hartz E. H., Andresen A., Hodges K. V., and Martin M. W. (2001) Syncontractional extension and exhumation of deep crustal rocks in the East Greenland Caledonides. *Tectonics* **20**(1), 58-77.

Hartz, E., Andresen, A., Martin, M.W. & Hodges, K.V. 2000. U-Pb and $^{40}Ar/^{39}Ar$ constraints on the Fjord Region Detachment Zone; a long-lived extensional fault in the central East Greenland Caledonides. *Journal of the Geological Society, London,* **157** 795-809.

Helman F. J., Gee D. G., Gjelsvik T., and Tebenkov A. M. (1998) Provenance and tectonic implications of Palaeoproterozoic (c. 1740 Ma) quartz porphyry clastics in the basal Old Red Sandstone (Lilljeborgfjellet Conglomerate Formation) of northwestern Svalbard's Caledonides. *Geological Magazine* **135**(6), 755-768.

Higgins A. K., Elvevold S., Escher J. C., Frederiksen K. S., Gilotti J. A., Henriksen N., Jepsen H. F., Jones K. A., Kalsbeek F., Kinny P. D., Leslie A. G., Smith M. P., Thrane K., and Watt G. R. (2004) The foreland-propagating thrust architecture of the East Greenland Caledonides 72 degrees -75 degrees N. *Journal of the Geological Society of London*. **161,** 1009-1026

Hirajima T., Banno S., Hiroi Y., and Ohta Y. (1988) Phase petrology of eclogites and related rocks from the Motalafjella high-pressure metamorphic complex in Spitsbergen (Arctic Ocean) and its significance. *Lithos* **22**(2), 75-97.

Hjelle A. (1974) The geology of Danskøya and Amsterdamøya, North-west Spitsbergen. *Skrifter - Norsk Polarinstitutt* **158,** Contribution to the geology of north western Spitsbergen, 7-37.

Hjelle A. (1979) Aspects of the geology of Northwest Spitsbergen. In *The geological development of Svalbard during the Precambrian, lower Palaeozoic, and Devonian.*, Vol. **167** (ed. S. Winsnes Thore), pp. 37-62. Norsk Polarinstitutt.

Hjelle A. and Ohta Y. (1974) Contribution to the geology of north western Spitsbergen. *Norsk Polarinstitutt skrifter nr.* **158**, 107 pp.

Hjelle A., Piepjohn K., Saalmann K., Ohta Y., Salvigsen O., Thiedig F., and Dallmann W. (1999) Geological map of Svalbard, 1:100 000, sheet A7C Kongsfjorden. In *Norsk Polarinstitutt Temakart nr.* **30**.

Johansson A. (2001) The Eskolabreen granitoids revisited; an ion microprobe study of complex zircons from late Palaeoproterozoic granitoids within the Ny Friesland Caledonides, Svalbard. *Geologiska foreningen Stockholms forhandlingar* **123**(1), 1-5.

Johansson A., Gee D. G., Larionov A. N., Ohta Y., and Tebenkov A. M. (2005) Grenvillian and Caledonian evolution of eastern Svalbard - a tale of two orogenies. *Terra Nova* **17**(4), 317-325.

Johansson Å., Larionov A. N., Gee D. G., Ohta Y., Tebenkov A. M., and Sandelin S. (2004) Grenvillian and Caledonian tectono-magmatic activity in northeasternmost Svalbard. In *The Neoproterozoic Timanide Orogen of Eastern Baltica*, Vol. **30** (ed. D. G. Gee and V. Peace), pp. 207-232. The Geological Society of London.

Johansson A., Larionov A. N., Tebenkov A. M., Gee D. G., Whitehouse M. J., and Vestin J. (2000) Grenvillian magmatism of western and central Nordaustlandet, northeastern Svalbard. *Transactions of the Royal Society of Edinburgh: Earth Sciences*, **90**, 221-254

Johansson A., Larionov A. N., Tebenkov A. M., Ohta Y., and Gee D. G. (2002) Caledonian granites of western and central Nordaustlandet, northeast Svalbard. *Geologiska foreningen Stockholms forhandlingar* **124**(3), 135-148.

Kalsbeek F., Jepsen H. F., and Nutman A. P. (2001) From source migmatites to plutons; tracking the origin of ca. 435 Ma S-type granites in the East Greenland Caledonian Orogen. *Lithos* **57**(1), 1-21.

Kalsbeek F., Thrane K., Nutman A. P., and Jepsen H. F. (2000) Late Mesoproterozoic to early Neoproterozoic history of the East Greenland Caledonides; evidence for Grenvillian orogenesis *Journal of the Geological Society of London,* **157,** 1215-1225.

Klaper E. M. (1986) The metamorphic evolution of garnet-cordierite-sillimanite gneisses of NW Spitsbergen (Svalbard). *Schweizerische Mineralogische und Petrographische Mitteilungen = Bulletin Suisse de Mineralogie et Petrographie* **66**(3), 295-313.

Krogh T. E. (1982) Improved accuracy of U-Pb zircon ages by the creation of more concordant systems using an air abrasion technique. *Geochimica et Cosmochimica Acta* **46**(4), 637-649.

Lange M. H., B. (1999) Metamorphic conditions of the metasedimentary rocks of the crystalline basement in the southwestern Haakon VII Land, Northwest-Spitsbergen, Svalbard, using microprobe analysis on garnets. *Munst. Forsch. Geol. Palaontol.* **86**, 1-10.

Ledru P., Courrioux G., Dallain C., Lardeaux J. M., Montel J. M., Vanderhaeghe O., and Vitel G. (2001) The Velay Dome (French Massif Central); melt generation and granite emplacement during orogenic evolution. *Tectonics*, **342**; pp. 207-237.

Leslie A. G. and Nutman A. P. (2003) Evidence for Neoproterozoic orogenesis and early high temperature Scandian deformation events in the southern East Greenland Caledonides. *Geological Magazine* **140**(3), 309-333.

Ludwig K. R. (1991) ISOPLOT; a plotting and regression program for radiogenic-isotope data; version 2.53, pp. 39. U. S. Geological Survey.

Lyberis N. and Manby G. (1999) Continental collision and lateral escape deformation in the lower and upper crust; an example from Caledonide Svalbard. *Tectonics* **18**(1), 40-63.

McCann A. J. (2000) Deformation of the Old Red Sandstone of NW Spitsbergen; links to the Ellesmerian and Caledonian orogenies. In *New perspectives on the Old Red Sandstone*. (ed. F. Friend Peter and P. J. Williams Brian). Geological Society of London. London, United Kingdom. 2000.

Miller C. F., McDowell S. M., and Mapes R. W. (2003) Hot and cold granites? Implications of zircon saturation temperatures and preservation of inheritance. *Geology* **31**(6), 529-532.

Mortensen J. K., Williams I. S., and Compston W. (1997) Ion microprobe and cathodeluminiscence investigations of unsupported Pb in zircon. *GAC/MAC Annual Meeting Abstract Volume, Ottawa, ON*, 105 pp.

Oberli F., Meier M., Berger A., Rosenberg C. L., and Giere R. (2004) U-Th-Pb and (super 230) Th/ (super 238) U disequilibrium isotope systematics; precise accessory mineral chronology and melt evolution tracing in the Alpine Bergell Intrusion. *Geochimica et Cosmochimica Acta* **68**(11), 2543-2560.

Ohta Y. (1974) Tectonic development and bulk chemistry of rocks from the Smeerenburgfjorden area, Spitsbergen. *Norsk Polarinstitutt Skrifter* **158,** Contribution to the geology of north western Spitsbergen, 69-107.

Ohta Y. (1982) Relationships between the Kapp Hansteen Formation and the Brennevinsfjorden Formation in Botniahalvøya, Nordaustlandet, Svalbard. *Norsk Polarinstitutt Skrifter* **178**, 1-18.

Ohta Y. (1985) Geochemistry of Precambrian basic igneous rocks between St. Jonsfjorden and Isfjorden, central western Spitsbergen, Svalbard. *Polar Research* **3**(1), 49-67.

Ohta Y., Dallmeyer R. D., and Peucat J. J. (1989) Caledonian terranes in Svalbard. . *Terranes in the Circum-Atlantic Paleozoic orogens. Boulder, CO, United States, Geological Society of America (GSA).* **230:** , 1-15.

Ohta Y., Hjelle A., and Dallmann W. K. e. (1996a) sheet A4G Vasahalvøya. Preliminary edition, update November 2002. *Geological map of Svalbard*.

Ohta Y., Hjelle A., and Dallmann W. K. e. (1996b) sheet A4G Vasahalvøya. Preliminary edition, update November 2002. *Geological map of Svalbard*.

Ohta Y. and Larionov A. N. (1998) Grenvillian single-grain zircon Pb age of a granitic rock from the southern island of Hesteskoholmen, Liefdefjorden, northwestern Spitsbergen, Svalbard. *Polar Research* **17**(2), 147-154.

Ohta Y., Larionov A. N., and Tebenkov A. M. (2003) Single-grain zircon dating of the metamorphic and granitic rocks from the Biscayarhalvoya-Holtedahlfonna zone, north-west Spitsbergen. *Polar Research* **22**(2), 247-265.

Ohta Y., Larionov A. N., Tebenkov A. M., Lepvrier C., Maluski H., Lange M., and Hellebrandt B. (2002) Single-zircon Pb-evaporation and (super 40) Ar/ (super 39) Ar dating of the metamorphic and granitic rocks in North-west Spitsbergen. *Polar Research* **21**(1), 73-89.

Parrish R. R. and Noble S. R. (2003) Zircon U-Th-Pb geochronology by isotope dilution; thermal ionization mass spectrometry (ID-TIMS). In *Zircon*, Vol. **53**;, pp. 183-213. Mineralogical Society of America and Geochemical Society.

Patino D. A. E. (1999) What do experiments tell us about relative contributions of crust and mantle to the origin of granitic magmas? In *Understanding granites; integrating new and classical techniques*, Vol. 168;, pp. 55-75. Geological Society of London.

Pedersen S. A. S., Craig L. E., Upton B. G. J., Ramo O. T., Jepsen H. F., and Kalsbeek F. (2002) Palaeoproterozoic (1740 Ma) rift-related volcanism in the Hekla Sund region, eastern North Greenland; field occurrence, geochemistry and tectonic setting. *Precambrian Research* **114**(3-4), 327-346.

Petford N., Cruden A. R., McCaffrey K. J. W., and Vigneresse J. L. (2000) Granite magma formation, transport and emplacement in the Earth's crust. *Nature (London)* **408** (6813), 669-673.

Peucat J. J., Ohta Y., Gee D. G., and Bernard G. J. (1989) U-Pb, Sr and N evidence for Grenvillian and latest Proterozoic tectonothermal activity in the Spitsbergen Caledonides, Arctic Ocean. *Lithos* **22**(4), 275-285.

Piepjohn K. (2000) The Svalbardian-Ellesmerian deformation of the Old Red Sandstone and the pre-Devonian basement in NW Spitsbergen (Svalbard). In *New perspectives on the Old Red Sandstone*, Vol. **180**; pp. 585-601. Geological Society of London.

Piepjohn K., Brinkmann L., Grewing A., and Kerp H. (2000) New data on the age of the uppermost ORS and the lowermost post-ORS strata in Dickson Land (Spitsbergen) and implications for the age of the Svalbardian deformation. In *New perspectives on the Old Red Sandstone*, Vol. **180**;, pp. 603-609. Geological Society of London.

Sandelin S., Tebenkov A. M., and Gee D. G. (2001) The stratigraphy of the lower part of the Neoproterozoic Murchisonfjorden Supergroup in Nordaustlandet, Svalbard. *Geologiska foreningen Stockholms forhandlingar* **123**(2), 113-127.

Schetelig J. (1912) Exploration du Norde-Ouest du Spitsberg (Mission Isachsen). Les Formations Primitives. *Res. des campagnes scient. du Prince de Monaco.* **XLIII (IV)**.

Schoene B., Crowley J. L., Condon D. J., Schmitz M. D., and Bowring S. A. (in press) Reassessing the uranium decay constants for geochronology using ID-TIMS U-Pb data. *Geochimica et Cosmochimica Acta* **In Press, Corrected Proof**.

Stacey J. S. and Kramers J. D. (1975) Approximation of terrestrial lead isotope evolution by a two-stage model. *Earth and Planetary Science Letters* **26**(2), 207-221.

Strachan R. A., Nutman A. P., and Friderichsen J. D. (1995) SHRIMP U-Pb geochronology and metamorphic history of the Smallefjord sequence, NE Greenland Caledonides. *Journal of the Geological Society of London*. Volume **152**,(5), pp. 779-784

Strachan, R.A., Martin, M.W. & Friderichsen J.D. 2001. Evidence for contemporaneous yet contrasting styles of granite magmatism during extensional collapse of the northeast Greenland Caledonides. *Tectonics*, **20**, 458-473.

Tebenkov A. M., Ohta Y., Balashov Y. A., and Sirotkin A. N. (1996) Newtontoppen granitoid rocks: their geology, chemistry and Rb-Sr age. *Polar research* **15**(67-80).

Tebenkov A. M., Sandelin S., Gee D. G., and Johansson A. (2002) Caledonian migmatization in central Nordaustlandet, Svalbard. *Norsk Geologisk Tidsskrift* **82**(2), 15-28.

Torsvik, T.H., Smethurst, M.A., Meert, J.G., Van der Voo, R., McKerrow, W.S., Brasier, M.D., Sturt, B.A. & Walderhaug, H.J. 1996. Continental break-up and collision in the Neoproterozoic and Paleozoic; a tale of Baltica and Laurentia. *Earth Science Reviews,* **40**, 229-258.

Trettin H. P., Parrish R., and Loveridge W. D. (1987) U-Pb age determinations on Proterozoic to Devonian rocks from northern Ellesmere Island, Arctic Canada. *Canadian Journal of Earth Sciences = Journal Canadien des Sciences de la Terre* **24**(2), 246-256.

Upton B. G. J., Ramo O. T., Heaman L. M., Blichert T. J., Kalsbeek F., Barry T. L., and Jepsen H. F. (2005) The Mesoproterozoic Zig-Zag Dal basalts and associated intrusions of eastern North Greenland; mantle plume-lithosphere interaction. *Contributions to Mineralogy and Petrology* **149**(1), 40-56.

Vogt T. (1938) The stratigraphy and tectonics of the Old Red formations of Spitsbergen. *Abstracts of the Proceedings of the Geological Society, London, 1936* **88**.

Watson E. B. and Harrison T. M. (1983) Zircon saturation revisited; temperature and composition effects in a variety of crustal magma types. *Earth and Planetary Science Letters* **64**(2), 295-304.

Watt G. R., Kinny P. D., and Friderichsen J. D. (2000) U-Pb geochronology of Neoproterozoic and Caledonian tectonothermal events in the East Greenland Caledonides. *Journal of the Geological Society of London*, **157**, 1031-1048

Watt G. R. and Thrane K. (2001) Early Neoproterozoic events in East Greenland. In *Assembly and breakup of Rodinia*, Vol. **110**; 1-4, pp. 165-184. Elsevier.

Welbon A. I. and Andresen A. (1992) The Pretender lineament- structural and stratigraphic significanse of a major lineament in western Spitsbergen. *Norsk Geologisk Tidsskrift* 72, 139.

Witt-Nilsson P. (1998) The West Ny Friesland Terrane: An Obliquely Convergent Orogen,. *Acta Universitatis Upsaliensis.* Comprehensive Summaries of Uppsala Dissertations from the Faculty of Science and Technology **415** 28 pp